ENVIRONMENTAL EFFECTS OFFICE

INTERNAL REPORT

BALLOON STRATOSPHERIC RESEARCH FLIGHTS

NOVEMBER 1974 TO JANUARY 1976

PREPARED BY

LOCKHEED ELECTRONICS CO., INC.

AEROSPACE SYSTEMS DIVISION

UNDER CONTRACT

NAS 9-15200

FOR

National Aeronautics and Space Administration

LYNDON B. JOHNSON SPACE CENTER

Houston, Texas

DECEMBER 1976

LEC-9904

ENVIRONMENTAL EFFECTS OFFICE

INTERNAL REPORT

BALLOON STRATOSPHERIC RESEARCH FLIGHTS

NOVEMBER 1974 TO JANUARY 1976

SUBMITTED BY:

Norman C. Allen/LEC

APPROVED BY:

John F. Stanley/TC411

Andrew E. Potter, Jr./TC411

LEC-9904

CONTENTS

Section Page

FIGURES

TABLES

APPENDIXES

Appendix

GENERAL SUMMARY

The NASA/JSC Environmental Effects Project Office (EEPO), in conjunction with several government and private agencies, conducted six balloon-parachute flights from the National Scientific Balloon Facility (NSBF) at Palestine, Texas, during the period from November 1974 through January 1976. These flights (see Table I) were designed to measure the vertical concentration profile of trace stratospheric species which form major links in the photochemical system of the upper atmosphere.

This document contains an overview of the scientific goals of the program, a statement of program management and support functions, a brief description of the instrumentation flown, pertinent engineering and payload operations data, and a summary of the scientific data obtained for each of the last five flights during this period. The first flight, a parachute test flight, is fully documented in JSC Internal Report JSC-10903 (High-Altitude Flight Performance of a 9.75-meter Diameter Guide Surface Parachute) dated January 1976.

TABLE I. BALLOON STRATOSPHERIC RESEARCH FLIGHTS
NOVEMBER 1974 to JANUARY 1976

Flight	NCAR Flight No.	Type of Experiment	Date Launch Time Landing Time	Participating Agencies
1	867-P	Parachute Test Flight	11-12-74 0657 CST 1039 CST	NASA/JSC-NCAR
2	868-P	1st Atomic Oxygen $O(^3P)$ Measurement	11-25-74 0735 CST 1110 CST	NASA/JSC - NCAR - University of Pittsburgh(1) - Wallops Flight Center(2)
3	872-P	2nd Atomic Oxygen $O(^3P)$ Measurement	2-7-75 0703 CST 1059 CST	NASA/JSC - NCAR - University of Pittsburgh(1) - Wallops Flight Center(2)
4	912-P	1st Hydroxyl $OH(X^2\pi)$ Measurement (OH/O_3-1)	7-18-75 1633 CDT 2032 CDT	NASA/JSC - NCAR - University of Michigan(1) - Wallops Flight Center(2) - Goddard Space Flight Center(3)
5	934-P	2nd Hydroxyl $OH(X^2\pi)$ Measurement (OH/O_3/Aerosol-2)	10-19-75 1343 CDT 1834 CDT	NASA/JSC - NCAR - University of Michigan(1) - Wallops Flight Center(2) - Goddard Space Flight Center(3) - Langley Research Center/ University of Pittsburgh(4)
6	940-P	3rd Hydroxyl $OH(X^2\pi)$ Measurement (OH/O_3/Aerosol-3)	1-12-76 1256 CST 1641 CST	NASA/JSC - NCAR - University of Michigan(1) - Goddard Space Flight Center(3) - Langley Research Center/ University of Pittsburgh(4)

(1) Resonance/fluorescence instrumentation
(2) Ozonesondes
(3) Ozone absorption photometer on loan from GSFC
(4) Aerosol instrumentation

SCIENTIFIC RATIONALE AND GOALS

Over the past decade, as our understanding of the delicate photochemical balance of the Earth's upper atmosphere has expanded, it has become clear that irreversible harm can be done to this region of the atmosphere by contaminants released at the Earth's surface or in the lower atmosphere. Of particular concern is the depletion of stratospheric ozone (O_3) - an important natural resource due to its unique capability of screening the Earth's surface from ultraviolet radiation. Attempts to quantitatively predict photochemical perturbations of the ozone layer (and thus variations in the ultraviolet dosage reaching the surface) resulting from the injection and diffusion of gases into the stratosphere, have demonstrated that insufficient empirical knowledge exists regarding the concentration of various atomic and diatomic radicals in the stratosphere. These minor species are thought to control ozone through catalytic reaction cycles.*

Although our appreciation for potential problems has grown, our understanding of the fundamental physical and chemical processes which control the stratosphere is incomplete and seriously lacking in observational verification. In particular, most of the major atomic and

* A description of ozone chemistry and ozone reduction by catalytic reaction cycles is given in JSC Internal Note JSC 09688 (Fundamentals of Stratospheric Ozone) dated June 1975.

diatomic species which are thought to couple the oxygen, hydrogen, nitrogen, and chlorine photochemical systems together have never been observed. Thus, it is difficult to defend theories which attempt to correlate the injection of a stable compound with, for example, the depletion of stratospheric ozone.

The complexity of stratospheric photochemistry is illustrated in figure 1. The major chemical source terms, indicated by upward-pointing arrows, are relatively stable polyatomic molecules released from the earth's surface and within the troposphere. These species have chemical lifetimes on the order of weeks to months so that their upward flow and global distribution is, in general, governed by transport processes. The linking radicals are formed directly (and irreversibly) from the chemical source terms either by photolysis (dissociation by ultraviolet solar radiation) or chemical reaction. The radicals, in contrast to the source terms, have chemical lifetimes on the order of minutes and they thus reflect the chemical conditions in their immediate vicinity. The reservior or sink terms, indicated by downward-pointing arrows, are formed by the recombination of the radicals. Like the source terms, they are rather stable chemically but may be recycled into the radical system by photolysis and chemical reaction or removed by downward and meridional transport.

The NASA/JSC Environmental Effects Project Office, in conjunction with several government and private agencies, is studying the vertical

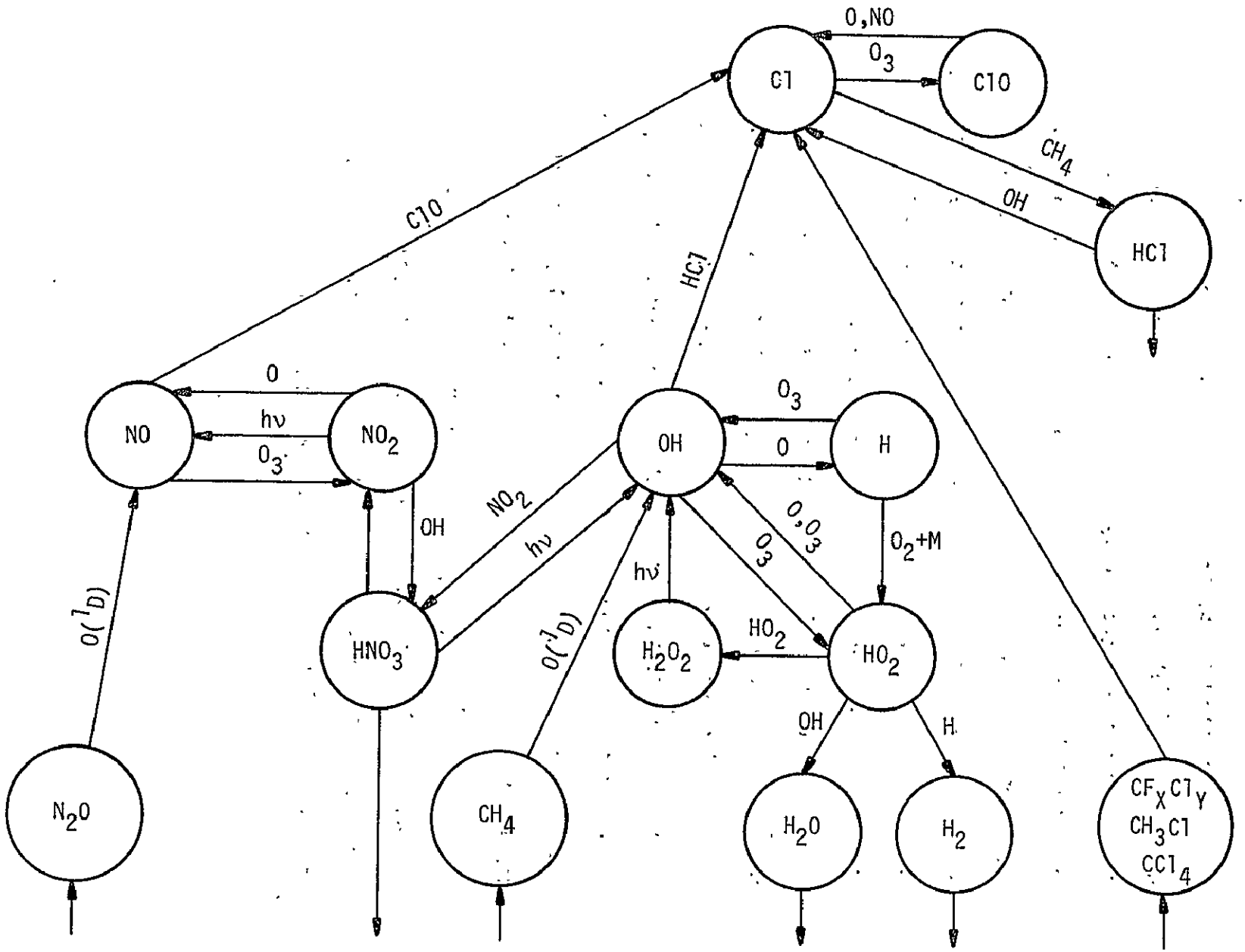

Figure 1.— Oxygen, hydrogen, nitrogen and chlorine photochemical systems.

concentration profiles of those radicals which form major links in the photochemical systems of the stratosphere. The goal of the research is to determine simultaneously the absolute concentration of one or more radicals in each of the major stratospheric systems. This will allow for empirical verification of calculated ozone depletion resulting from the presence of hydrogen, nitrogen, and chlorine source gases in the stratosphere. The data gathered are indicative of the current state of the stratosphere and will establish an invaluable basis for measurement of future changes in the concentration of the critical trace species. Among the most important constituents are atomic oxygen, ozone, hydrogen, chlorine, and the oxides of hydrogen, nitrogen, and chlorine - all of which are under study at the present time. This report documents five balloon-parachute flights conducted to measure the concentration of atomic oxygen (O) and hydroxyl (OH) at various levels in the stratosphere. Reference measurements of stratospheric ozone (conducted either in situ or via radiosonde) and an ancillary measurement of stratospheric aerosols are also documented. Figures 2 through 8 are scenes typical of the launch operations at the National Scientific Balloon Facility and payload recovery.

NASA
S- 74- 33979

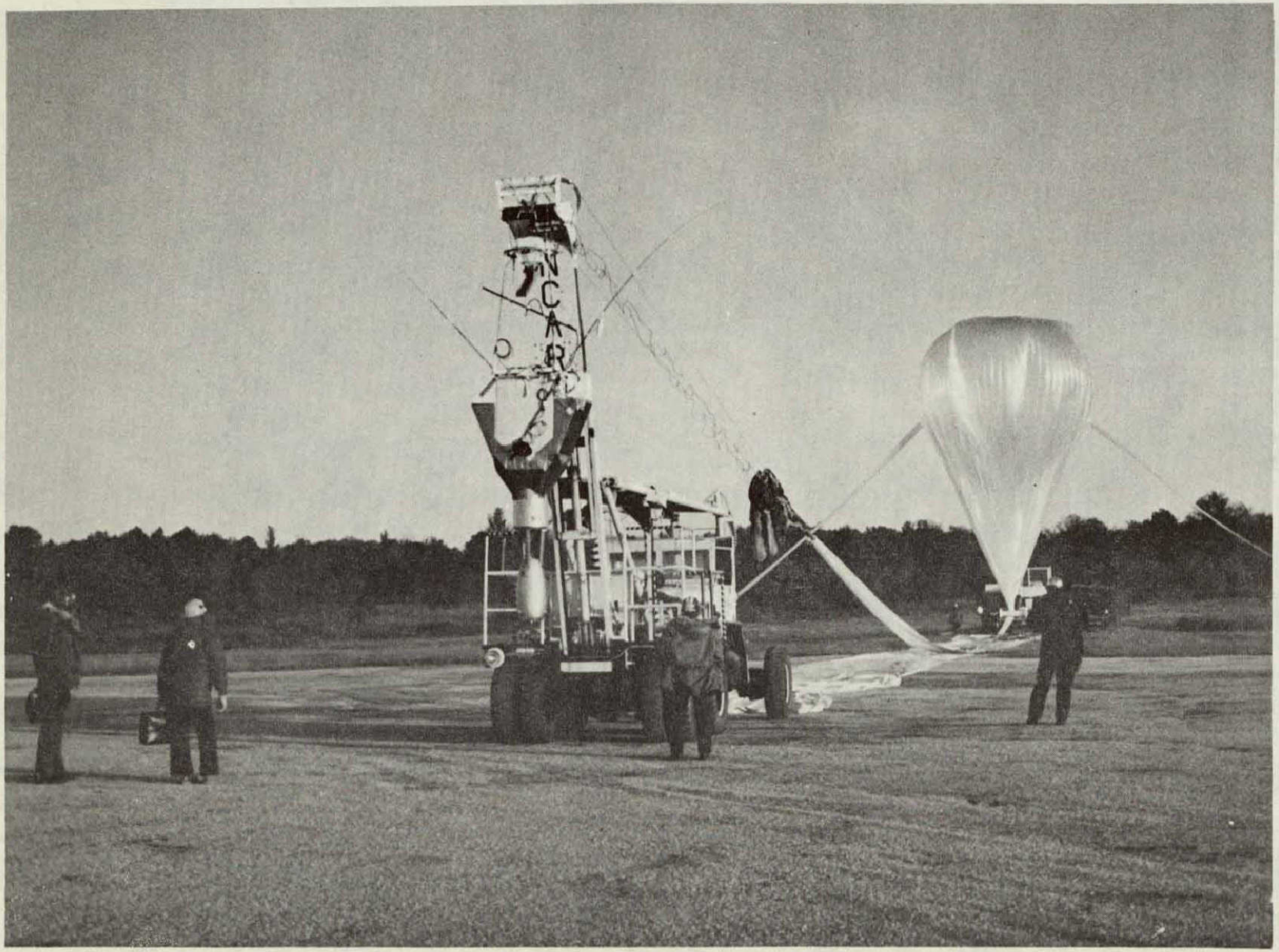

Figure 2. - Payload ready for flight with balloon being inflated in the background

NASA
S- 74- 33810

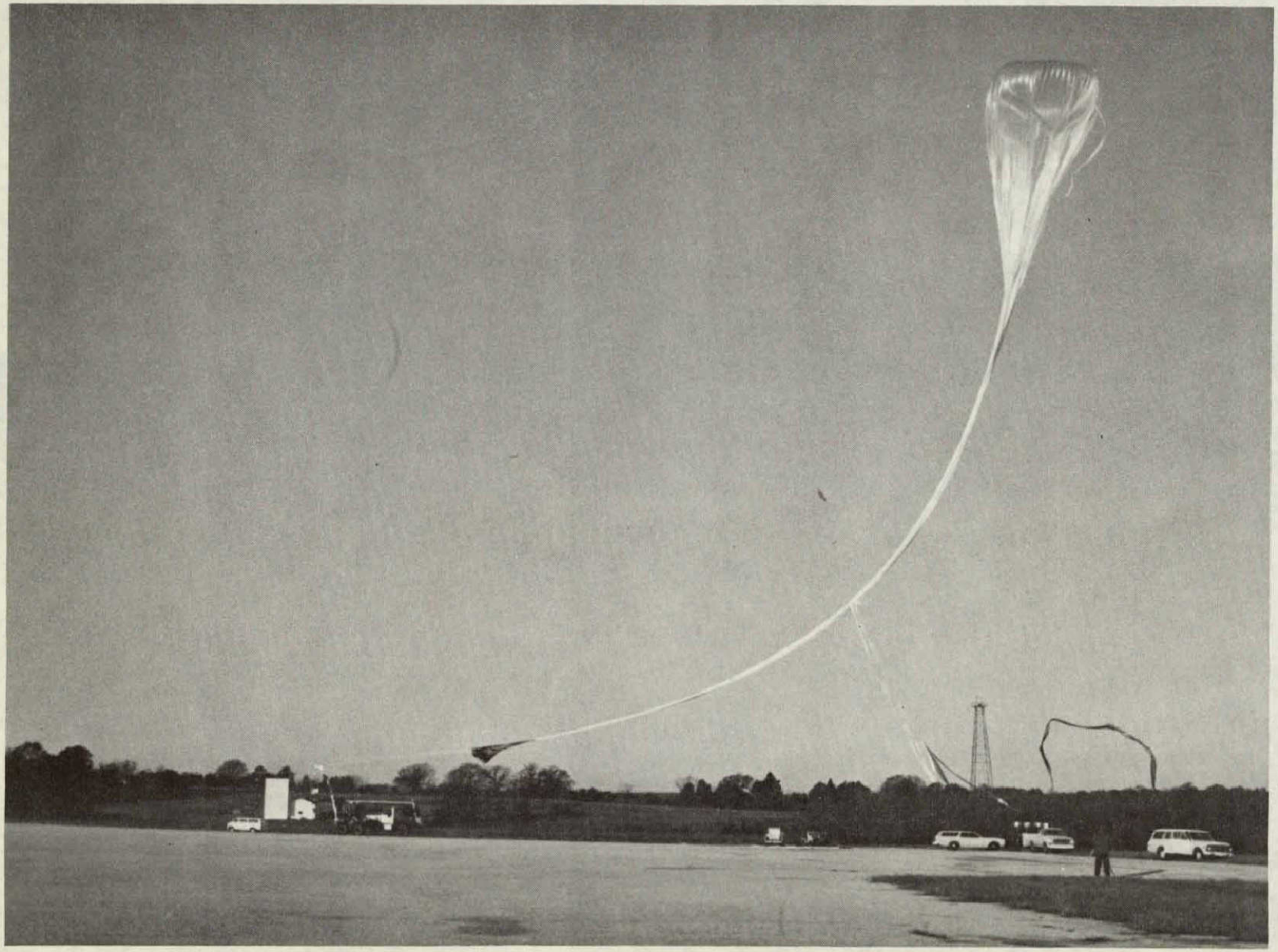

Figure 3. - Immediately after balloon release

NASA
S- 74- 33811

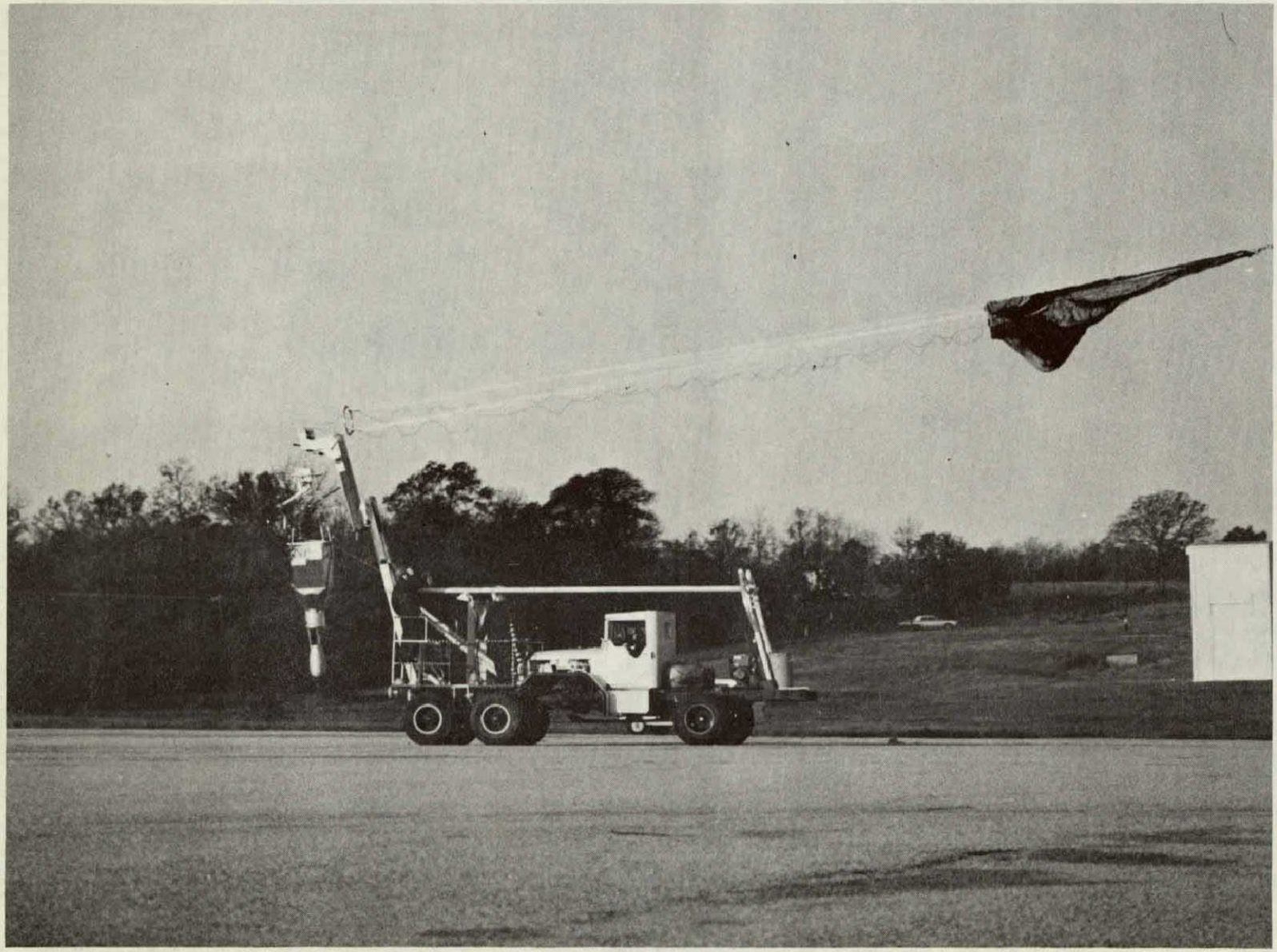

Figure 4. - Launch vehicle maneuvering to align balloon and payload

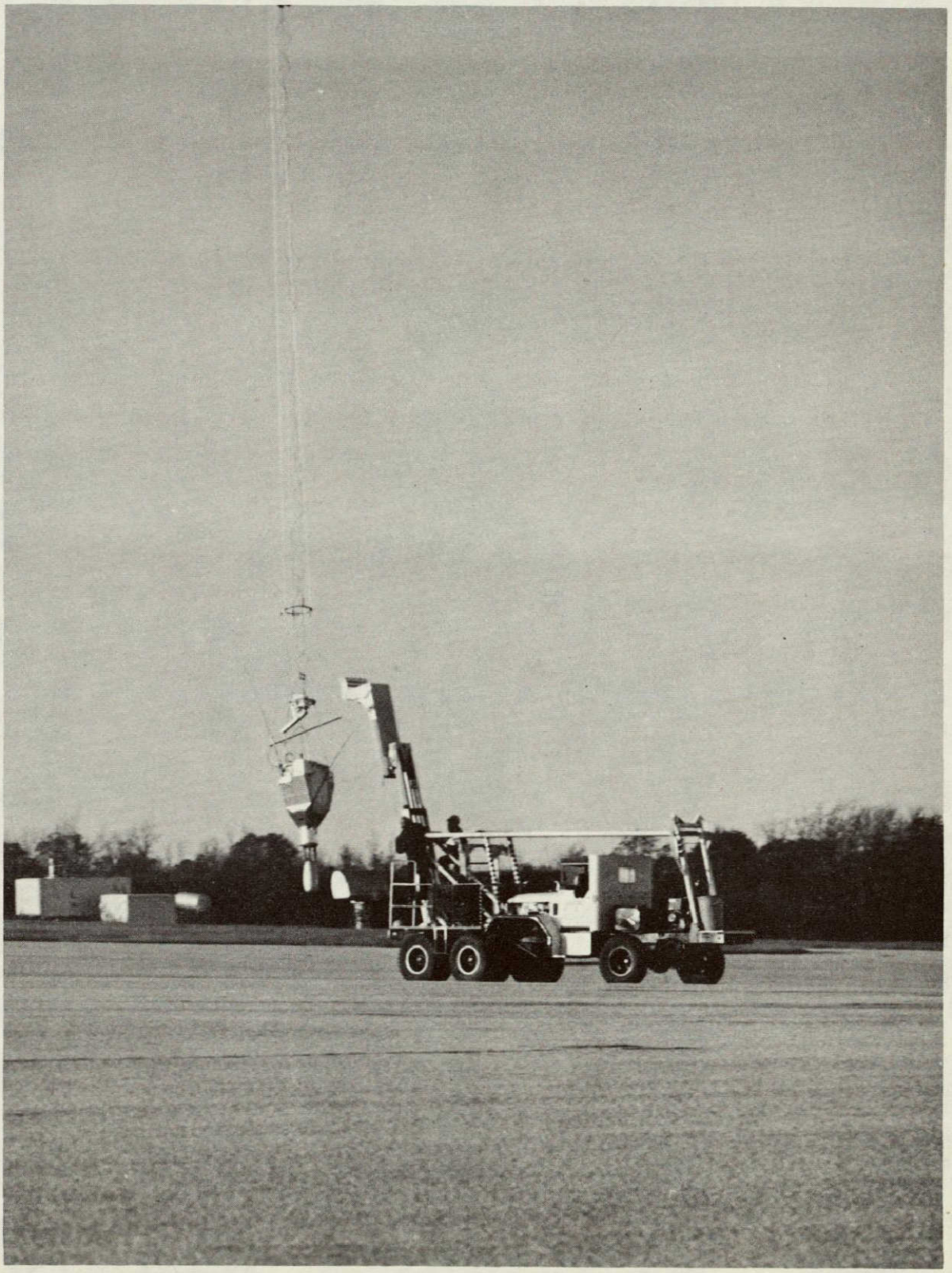

NASA
S- 74- 33808

Figure 5. - Immediately after release of payload

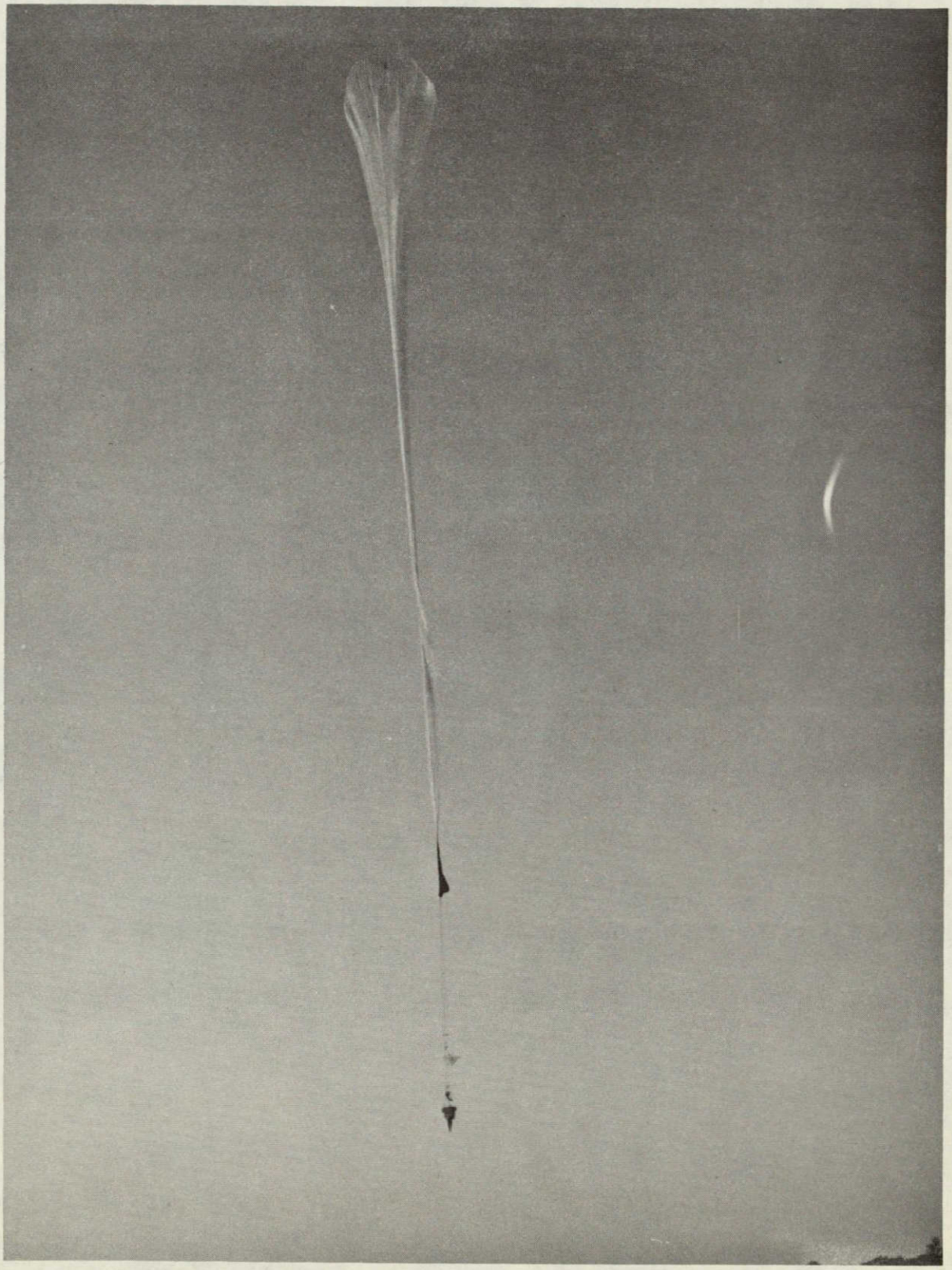

NASA
S- 74- 12953

Figure 6. - Off into the wild blue stratosphere

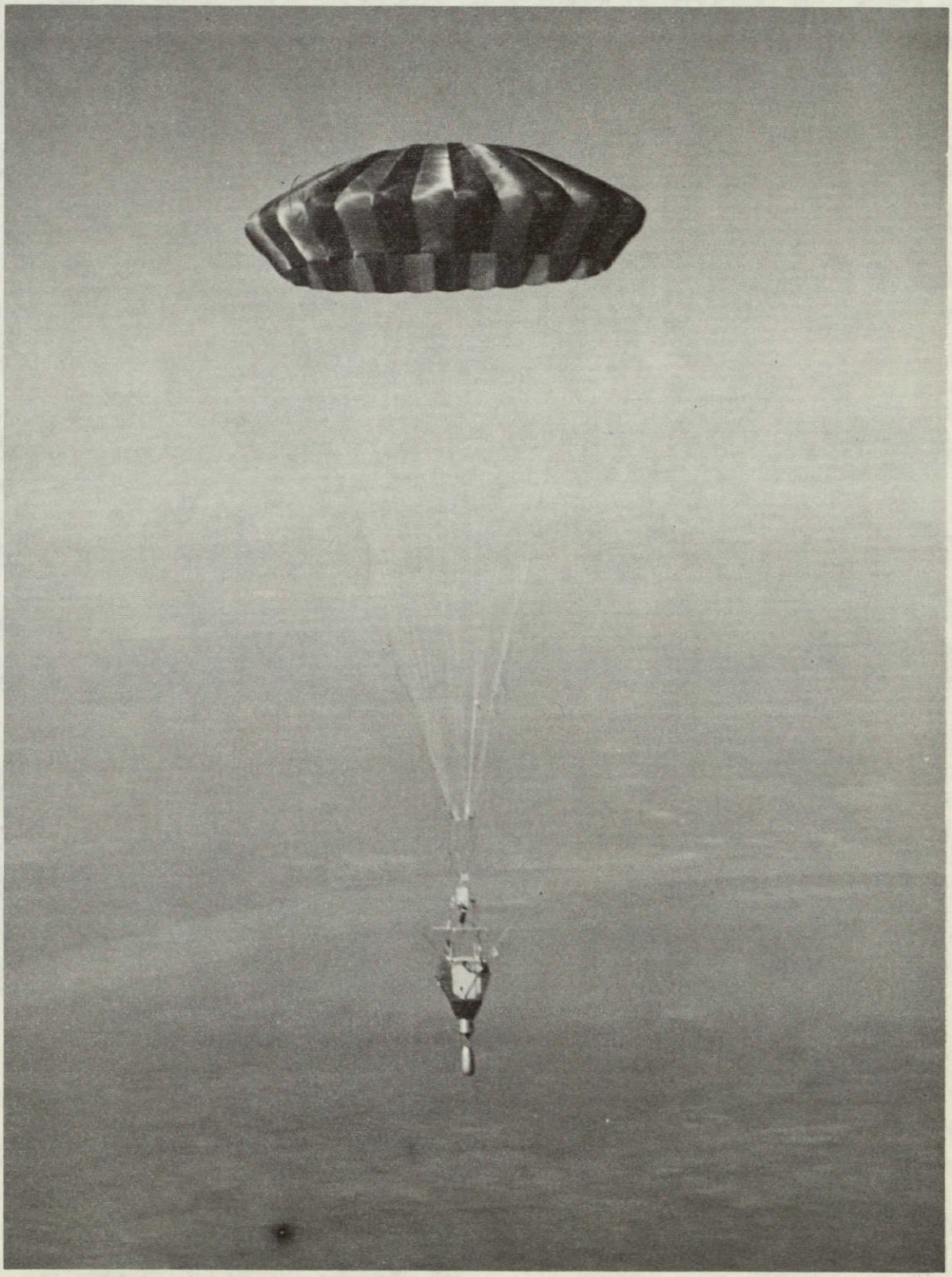

NASA
S- 75- 21490

Figure 7. - Payload/parachute configuration during descent measurement

NASA
S- 74- 33976

Figure 8. - Some complications encountered in recovering the payload

PROGRAM MANAGEMENT

The JSC Science and Applications Directorate is responsible for the overall direction and evaluation of the balloon-parachute stratospheric measurements program.

PROGRAM SUPPORT

The JSC/Environmental Effects Project Office (EEPO) conducts the balloon-parachute flight operations. Prime overall technical and operational support of the payload is provided by Lockheed Electronics Company, Inc. (LEC), the custodian of the JSC payload components and ground station equipment. The National Center for Atmospheric Research (NCAR) provides prime operational support such as launch operations, payload tracking, recovery operations, range safety, facilities, and meteorological data.

The University of Pittsburgh (atomic oxygen $O(^3P)$ flights) and the University of Michigan (hydroxyl $OH(X^2\pi)$ flights) working under contract to the EEPO have responsibility for the resonance fluorescence instrumentation and shares data reduction and analysis responsibility with the EEPO for $O(^3P)$ and $OH(X^2\pi)$ measurements. LEC has prime responsibility for the operation of the ozone photometer (on loan from Goddard Space Flight Center) flown on the $OH(X^2\pi)$ flights and for data reduction and analysis of the *in situ* ozone measurements. The University of Pittsburgh under the sponsorship of Langley Research Center is responsible for

ancillary aerosol particle counter instrumentation flown on the second and third hydroxyl OH($X^2\pi$) flights and also for reduction and analysis of the aerosol data. Wallops Flight Center is responsible for operation of the reference ozone (radiosonde) instrumentation and for data reduction of the resulting ozone measurements.

In addition to scientific and managerial administration of the program, NASA/JSC also provides logistics and technical support for the flights. The JSC/Logistics Division is responsible for transportation of payload, support equipment and instrumentation vans to the NCAR facility. The JSC/Space Environment Test Division assists in demonstrating the capability of the instrumentation to withstand the thermal and vacuum conditions encountered during balloon flights. The JSC/Space Vehicle Battery Facility is responsible for preparation and delivery of the flight and spare battery. The JSC/Photographic Division provides documentary photography for launch, flight, and recovery.

FIRST ATOMIC OXYGEN $O(^3P)$ MEASUREMENT

(NCAR FLIGHT NO. 868-P)

25 November 1974

SUMMARY

This balloon-parachute flight was the first flight of the laminar flow through/resonance fluorescence instrument (principal investigator: Dr. James Anderson, University of Pittsburgh) and was successfully accomplished on 25 November 1974. The purposes of the flight were to measure the vertical concentration profile of atomic oxygen in the stratosphere and to test modified parachute rigging for improved attitude stability.

The flight was launched at 0735 CST from the NSBF at Palestine, Texas. Hardware consisted of a 1.3×10^5 cubic meter balloon, 9.75-meter diameter guide surface parachute, NCAR telemetry system, JSC flight support module, and the resonance fluorescence instrument tuned to the ^3P-^3S transition of atomic oxygen at 130.4 nm. The payload reached a float altitude of 39 km (129 k ft) at 0940 CST. The payload was separated from the balloon (descent data gathering phase began) at 1031 CST; its performance was excellent. The scientific data from the flight were used to produce the first vertical profile of atomic oxygen concentration in the 26 to 39 km region.[1] The parachute/payload landed in the Cane River 3 nm southeast of Cloutierville, Louisiana at 1110:21 CST and was recovered in fair condition.

1. Anderson, J. G., "The Absolute Concentration of $O(^3P)$ in the Earth's Stratosphere", Geophysical Research Letters, Vol. 2, No. 6, June 1975.

A single ozone radiosonde was launched at 1133 CST to provide reference data on the concentration of stratospheric ozone. It reached a terminal altitude of 33 km (110 k ft) at 1321 CST.

INTRODUCTION

In order to verify and study the various catalytic reaction cycles thought to control the generation and, in some cases, the depletion of stratospheric ozone, a series of balloon-parachute flights is being performed to determine the vertical concentration profile of trace species believed to be important for the photochemical balance of the upper atmosphere. The data gathered is indicative of the current state of the stratosphere and will represent an invaluable comparative legacy for future studies as mankind continues to perturb his environment.

The presence of atomic oxygen is required for the completion of several of the catalytic reaction cycles responsible for the production of ozone. But atomic oxygen is also believed to participate in the destruction of ozone. It is thus intimately tied to ozone photochemistry. The first scientific flight of the current series was instrumented to measure the concentration of atomic oxygen in the stratosphere.

Payload

The payload weighed approximately 200 kg, and consisted of telemetry, balloon control, descent-observation, and scientific instrumentation.

Instrumentation

Instrumentation carried as part of the payload included NCAR and JSC telemetry instrumentation, NCAR balloon control instrumentation, NCAR and JSC pressure transducers to measure the altitude of the payload, two vertical reference gyros and a three-axis magnetometer to measure payload attitude, x-, y-, and z-axis accelerometers to determine the loading forces when the parachute is deployed, two up-looking motion picture cameras to observe parachute opening and descent characteristics, and the laminar flow through/resonance fluorescence instrument to measure the concentration of atomic oxygen. Ozone reference instrumentation consisted of a potassium iodide ozonesonde.

Function, manufacturer, model, and serial numbers for support instrumentation are itemized in Appendix A. Pertinent electrical and mechanical drawings are listed in Appendix B. A description of the telemetry systems and channel allocations is given in Appendix C. Photographic documentation for the flight is itemized in Appendix D.

The major scientific instrument flown on this flight was the resonance fluorescence instrument (see fig. 9) developed by Dr. James Anderson of the University of Pittsburgh (now with the University of Michigan). The basis of the technique, which is adaptable for measuring the concentrations of a variety of radicals (both atomic and molecular), is depicted in figure 10. A flowing

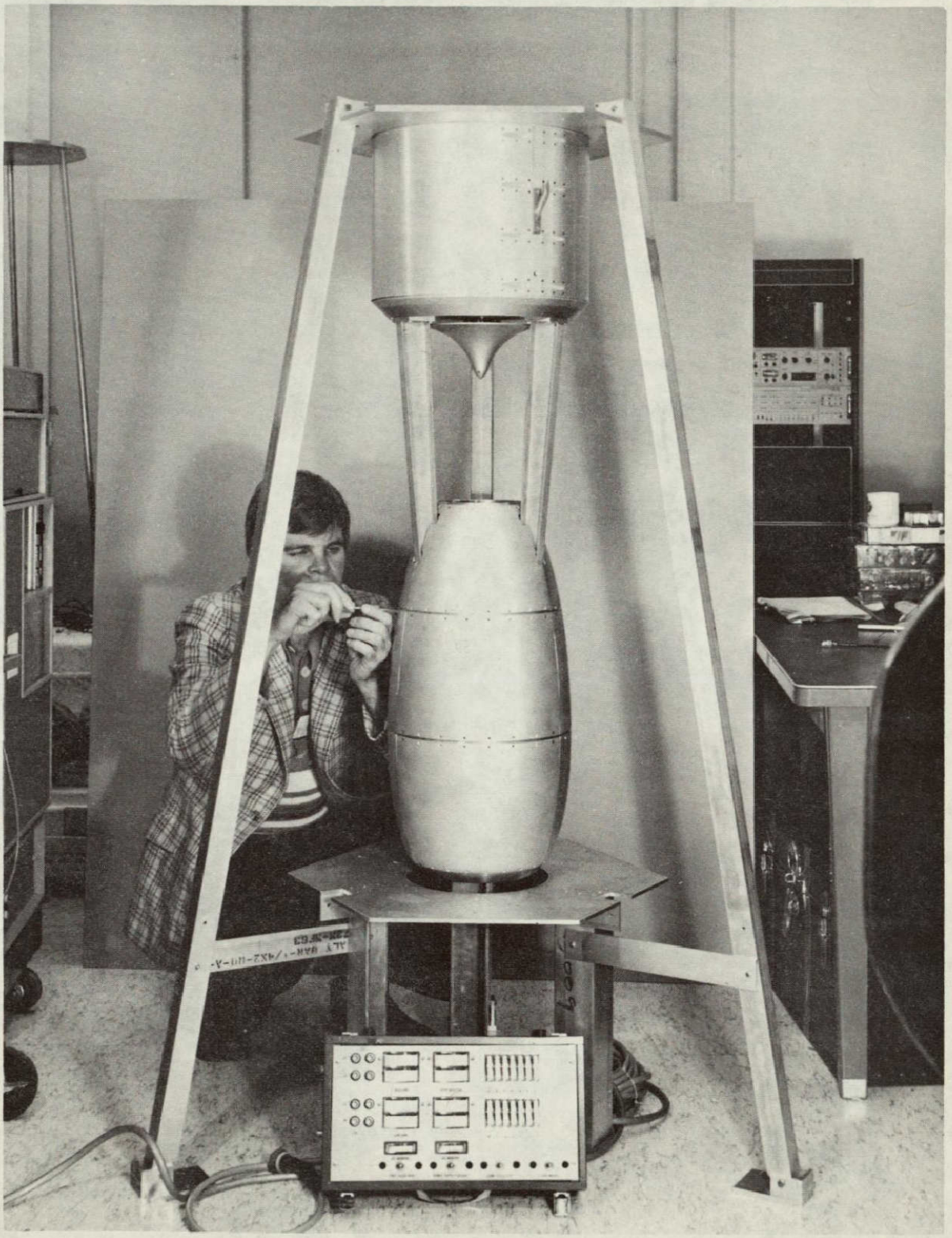

NASA
S-74-29386

Figure 9. - Laminar flow through/resonance fluorescence instrument

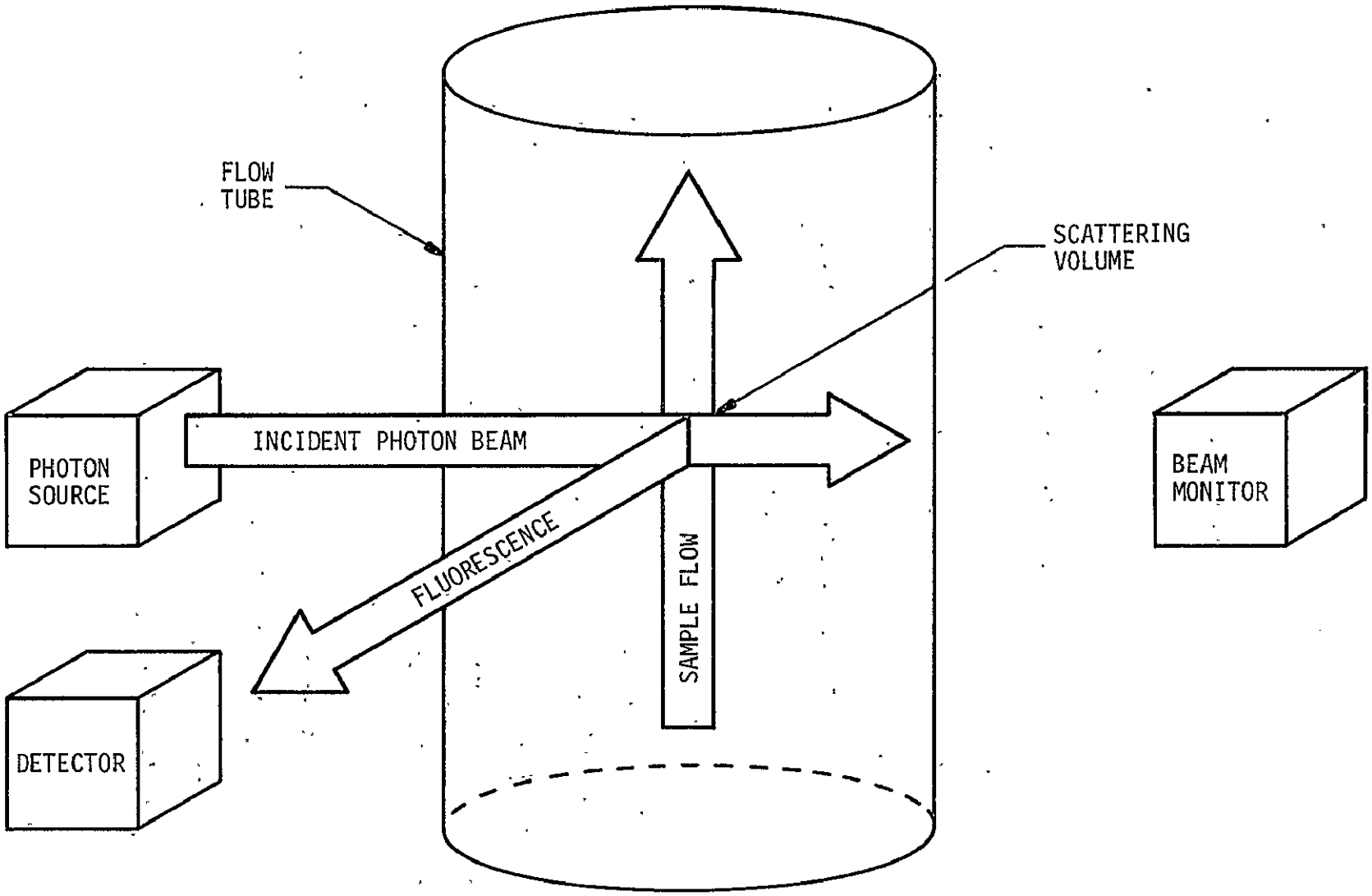

Figure 10. — Schematic depiction of the flow through/resonance fluorescence technique.

gas sample is probed with a collimated beam of light resonant in energy with a preselected electronic transition of the radical under study. The absorption and subsequent reemission of resonant photons results in the isotropic redistribution (scattering) of energy from the incident beam. The number of photons scattered per unit time, in the absence of reabsorption of the scattered photons, is proportional to the number of radicals per unit volume which have transitions out of the ground state to an upper bound electronic state with an energy difference equal to the energy of the incident resonant photons. Hence the count rate is a measure of the concentration of the radical under study. Concentrations as low as one part in 10^{12} can be measured by the technique.

In practice, the beam of photons is generated by a low pressure lamp (a plasma discharge resonance lamp) containing a small amount (0.1 to 1 percent) of gas either the same as or related to the atomic or molecular transition of interest. The beam is collimated by a lens-baffle system and directed into a detection chamber as shown in figure 11 (a schematic of the flight instrument along a plane perpendicular to the flow axis). In the present experiment, the source lamp contained a small amount of O_2 gas which was dissociated and excited by an RF oscillator operating at approximately 100 MHz to yield a virtually pure spectrum of the $^3P - {}^3S$ transition of atomic oxygen (a triplet at 130.2, 130.4 and 130.6 nm). The intensity

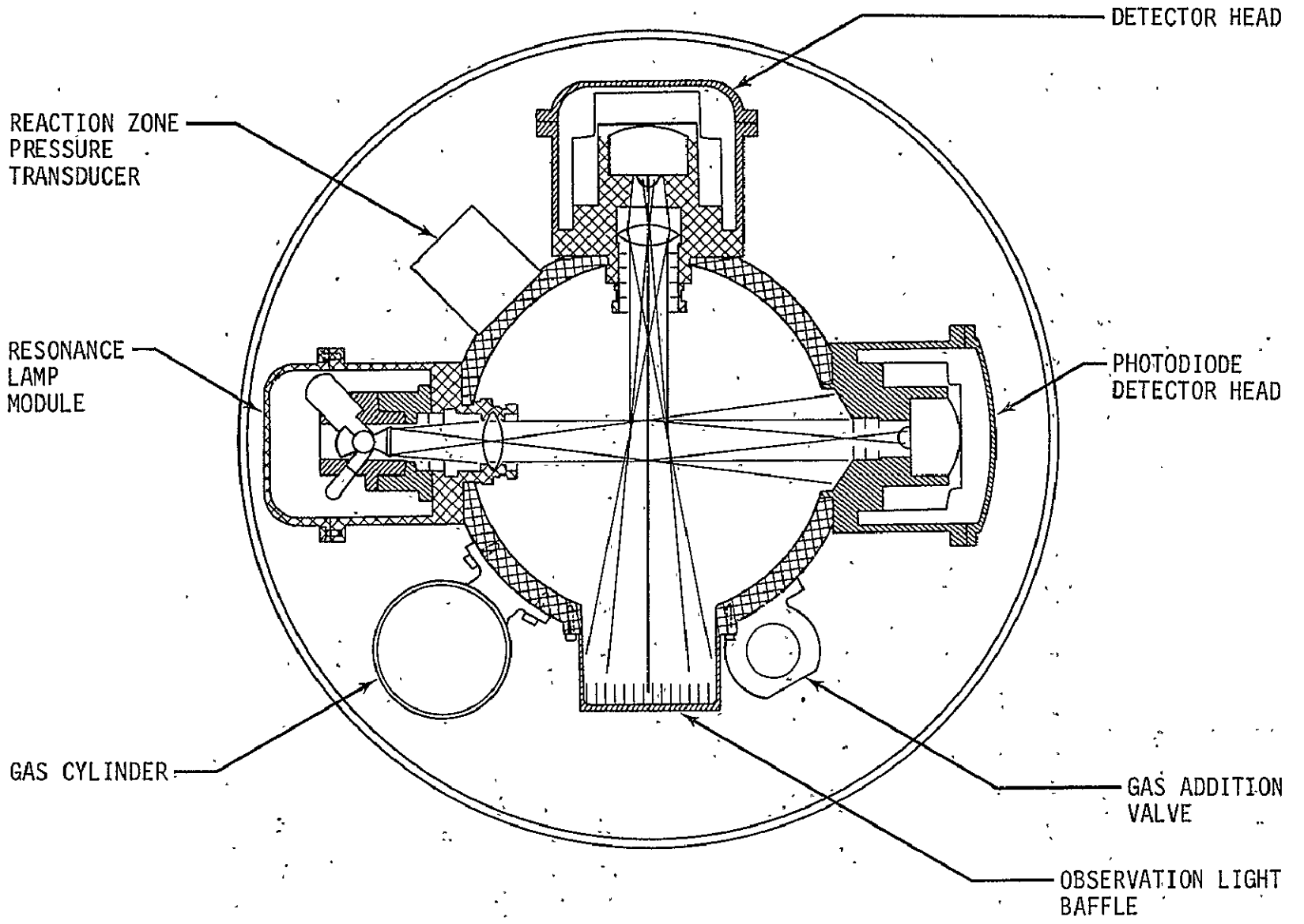

Figure 4.— Resonance fluorescence instrument (schematic along a plane perpendicular to flow axis).

of the source beam is monitored continuously by a photomultiplier-interference filter combination mounted in the collimated beam. Photons resonantly scattered out of the beam are counted photoelectrically by a detector observing in a direction perpendicular to the source after passing through a collimating baffle, magnesium fluoride lens and far ultraviolet interference filter. The count rate, after various instrumental corrections and calibrations are applied, is a measure of the concentration of the fluorescing species (in this case $O(^3P)$) within the volume defined by the intersection of the source beam and the field of view of the photomultiplier detector tube (the scattering volume).

In addition to detecting the atom or radical, it is essential that the measured sample remain unaltered by the presence of the detection equipment (most of the species of interest recombine with unit efficiency at any wall with which they collide). This problem is circumvented by flowing the sample gas at high velocity in a direction perpendicular to both the incident beam and the direction of observation of the detector (in the present case the instrument is lowered at high velocity through the stratosphere on a parachute). Figure 12 presents a schematic of the flight instrument in a plane containing the flow axis.

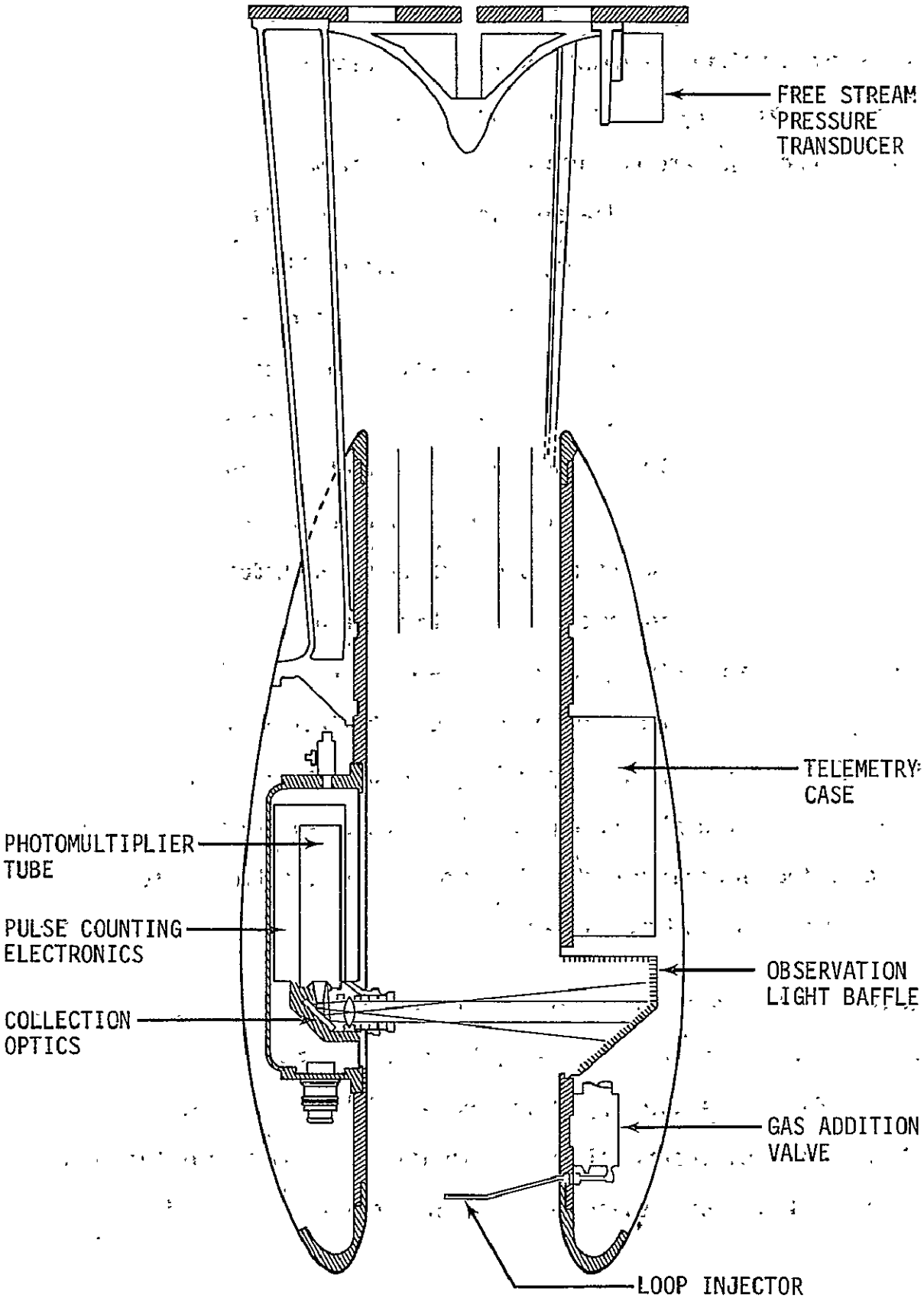

Figure 5.— Resonance fluorescence instrument (schematic along a plane containing flow axis).

Under the conditions encountered during in situ measurements, an aerodynamically shaped shell or nacelle insures a laminar flow of stratospheric gas around and through the instrument. The dimensions and geometry of the nacelle are such that at the particular velocity and pressure regime under consideration, the residence time of the sample within the instrument is two to three orders of magnitude less than the diffusion time from the scattering volume to the inner wall of the detection nacelle. Thus, corrections for depletion of atomic species by collision with the instrument are negligible (at high altitude) or very small (at lower altitudes). In addition, the parachute is of "guide surface" design which successfully damps oscillations of the descent system so that the angle between the flow axis and the velocity vector is held typically to less than 10 degrees. Measurements are made within the instrument throat in order to provide optical discrimination against atmospheric scatter and to contain the flow so that species within the flow can be converted chemically either for purposes of detection or for determination of background count rates.

In general for this experiment, the photon count rate is the sum of contributions from (1) photomultiplier dark current, (2) atmospheric (solar) Rayleigh scattering incompletely baffled by the instrument, (3) internal reflections of the source lamp beam within the detection chamber, (4) Rayleigh scattering of lamp radiation by N_2 and O_2

within the scattering volume, and (5) resonance/fluorescence from atoms within the scattering volume. The first four contributions are considered background and the difference between their sum and the total count rate is the net resonance fluorescence signal. This difference was measured during the flight by the periodic addition of cis-2-butene (C_4H_8) gas through the loop injector at the entrance of the instrument. Cis-2-butene effectively removes oxygen atoms by chemical reaction (thus terminating resonance/fluorescence) without affecting the count rate due to other contributions. Additional corrections to the data are required below 28 kilometers to account for attenuation of the source beam by O_2 absorption at 130.4 nm (monitored during descent) and to account for the generation of ozone by the rapid recombination of atomic and molecular oxygen upon termination of solar ultraviolet radiation as the sample enters the instrument throat.

DATA RESULTS

Payload Stability and Descent Characteristics

The flight profile for the First Atomic Oxygen $O(^3P)$ Flight is illustrated in figure 13. Launch occurred at 0735 CST, 25 November 1974, and was accomplished using the dynamic launch technique. The balloon system ascended at an average rate of 5.20 meters per second to a float altitude of 39 km. The balloon was allowed to

Figure 6.— Flight profile for the first atomic oxygen $O(^3P)$ flight.

float at altitude for 51 minutes before the payload was released on command from the tracking aircraft at 1031 CST and the data gathering phase of the mission began. Onboard motion picture cameras and accelerometers observed parachute deployment and measured the loading forces while gyros and magnetometers monitored the descent attitude of the system. The velocity/altitude profile of the descending payload and the loading force as a function of time after parachute deployment are illustrated in figures 14 and 15, respectively.

One of the goals of the present flight was to verify that modifications made to parachute rigging after the 12 November 1974 parachute test flight (NCAR Flight No. 867-P) resulted in improved attitude stability. A stable payload is required to ensure a laminar flow through the detection nacelle and to minimize the depletion of atomic oxygen by collision with the wall of the instrument. In order to obtain a numerical representation of the attitude stability of the system, the percentage of time the payload attitude was within certain limits was determined as a function of altitude. Figure 16 shows the probability that the attitude was within 5, 10, and 15 degrees of vertical for the flight. A detailed comparison of the stability and descent characteristics of the parachute/payload system for the first three flights in the stratospheric measurement program is made in JSC Internal Report JSC-10903. The minor redesign of parachute rigging first tested during the First Atomic Oxygen $O(^3P)$ Flight significantly

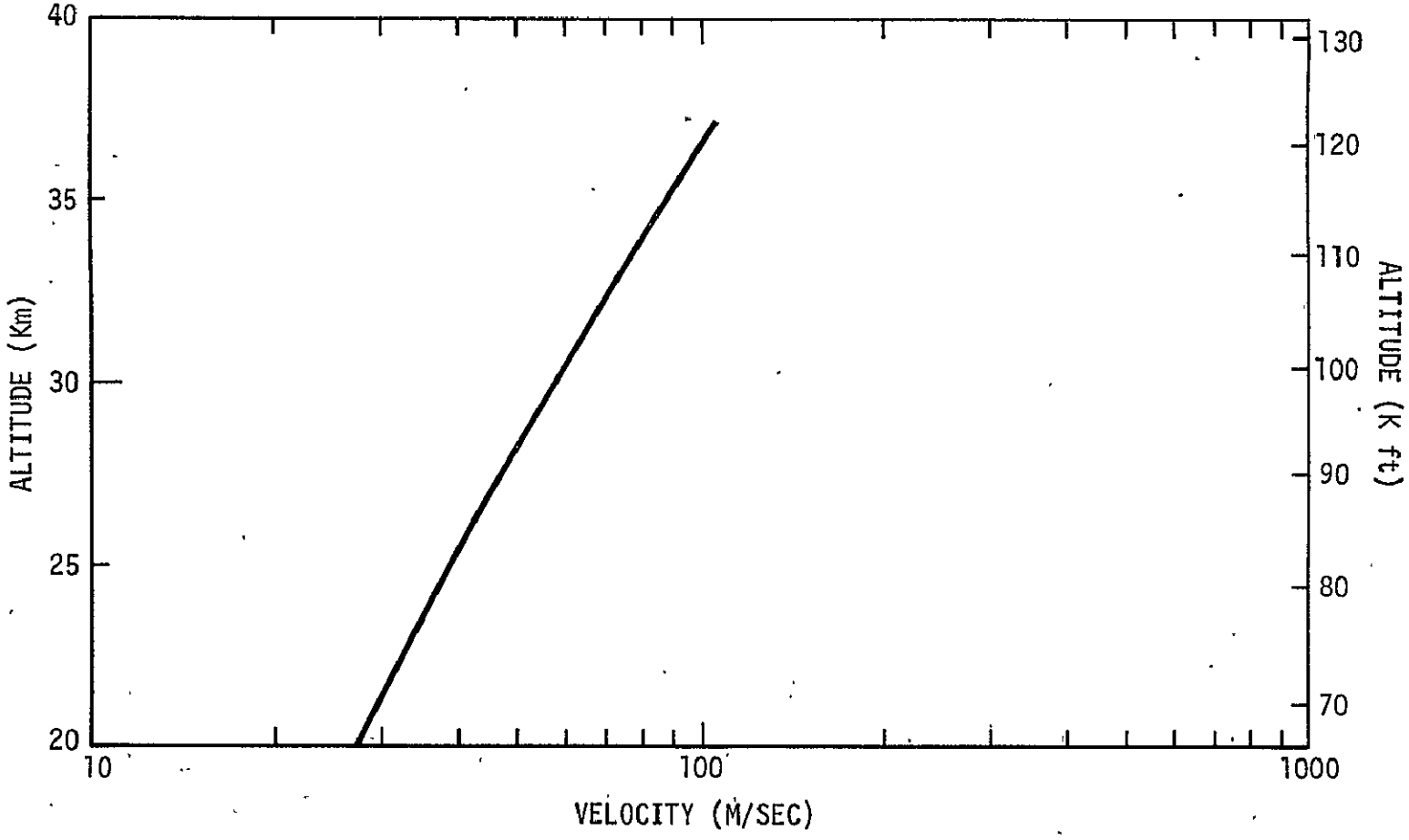

Figure 7.— Velocity/altitude profile of descending payload for the first atomic oxygen $O(^3P)$ flight.

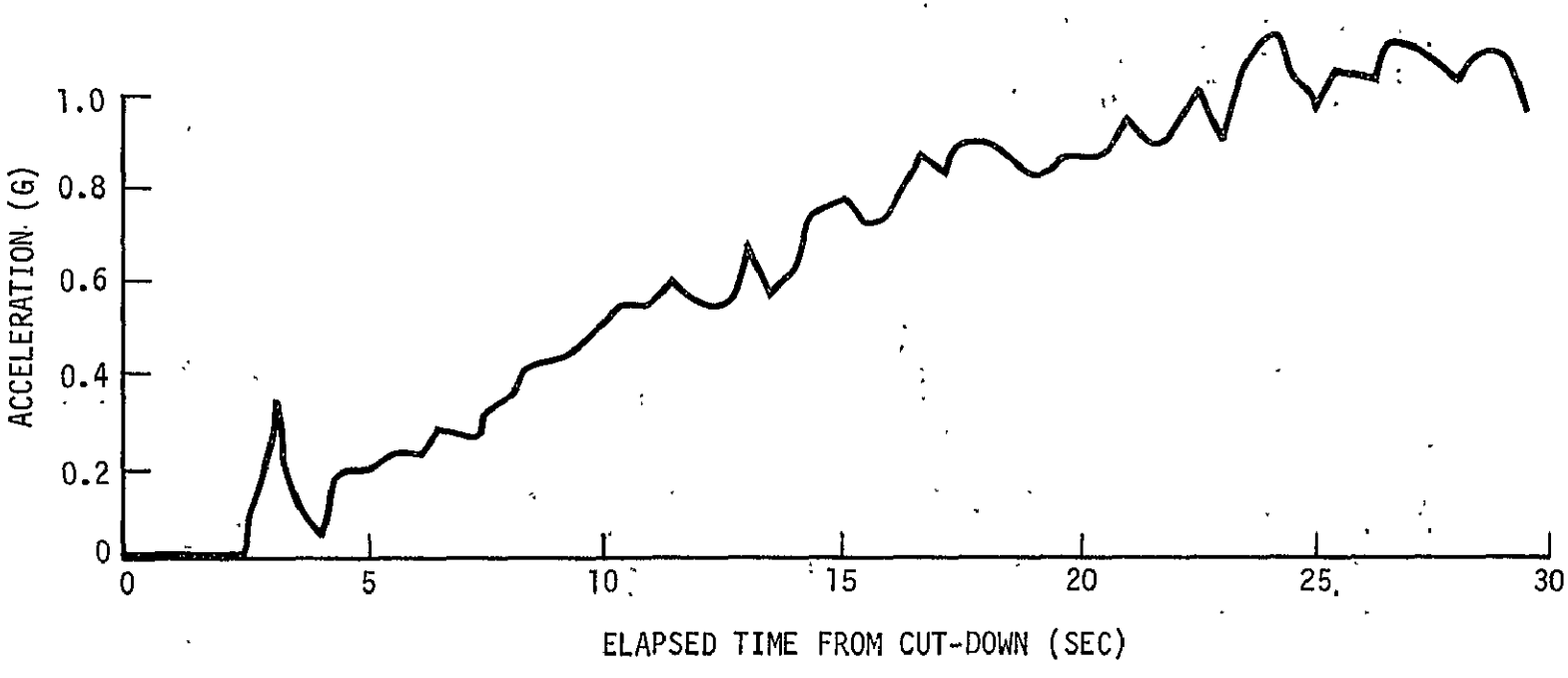

Figure 8.— Vertical force on payload after parachute deployment for the first atomic oxygen $O(^3P)$ flight.

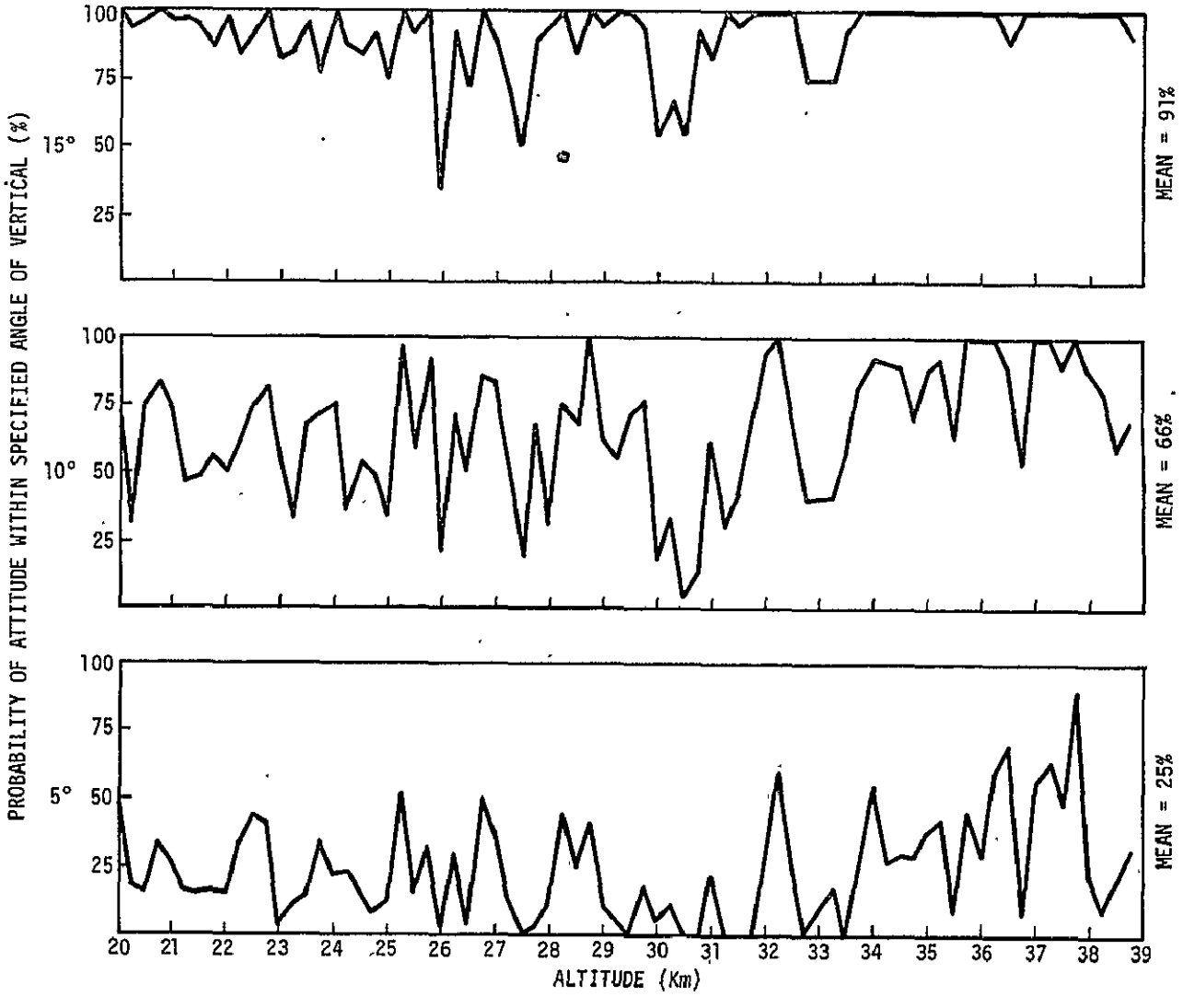

Figure 9.— Payload attitude probabilities as a function of altitude for the first atomic oxygen $O(^3P)$ flight.

improved stability and provided a descent satisfactory to the measurement of various stratospheric species. In fact, a post-flight comparison between the photon count rate and the angle between the descent velocity vector and the instrument flow axis (typically between 7 and 12 degrees) demonstrated the insensitivity of the measured concentration of atomic oxygen to the angle of attack. Similarly, the insignificance of the depletion of atomic oxygen due to collision with the wall of the instrument was empirically verified by correlating the time development of the resonance/fluorescence signal with the descent velocity of the parachute package as it accelerated from rest to its terminal velocity.

Atomic Oxygen $O(^3P)$ Measurement

The measured profile of the concentration of atomic oxygen $O(^3P)$ between 39 and 26 km (integrated over 500 meter intervals above 30 km and 1 km intervals below 30 km) is presented in figure 17. Also plotted in figure 17 is the range of uncertainty based on a realistic appraisal of 1) the quality of the raw data and laboratory calibration and 2) the degree to which the raw data can be accurately adjusted to correct for instrumental effects*, photolysis of O_2 in the lamp beam, and recombination of atomic and molecular oxygen within the detection nacelle.

---

*including extraneous light (solar radiation scattered by Earth's atmosphere and internal reflection of the source lamp beam), Rayleigh scatter of lamp radiation by N_2 and O_2, and photomultiplier dark current.

The data plotted were secured during the 3.2 minute drop time from 39 to 26 km commensing at 1031 CST 25 November 1974 (solar zenith angle of 56 degrees and latitude of 31.6 degrees North).

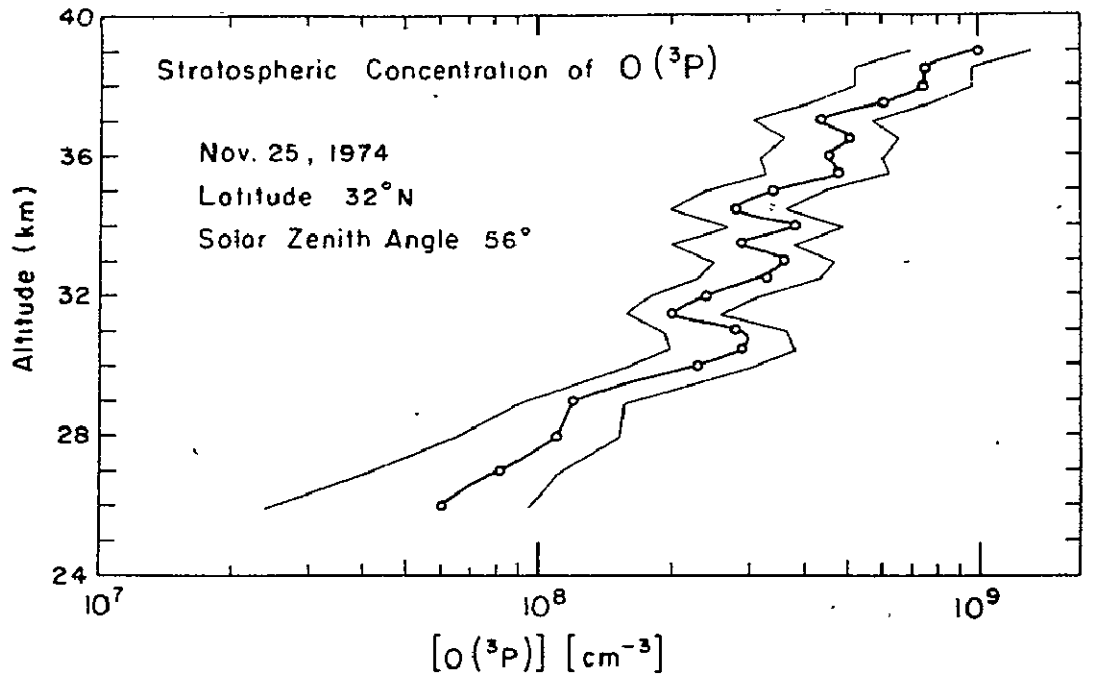

Figure 17. — Stratospheric Concentration of Atomic Oxygen Measured on the First Atomic Oxygen $O(^3P)$ Flight

Ozone Measurement

Because it is hypothesized that atomic oxygen and ozone are in mutual photochemical equilibrium, measurements of the concentration profiles of atomic oxygen and stratospheric ozone is important. A direct verification of the hypothesis is afforded by the simultaneous

measurement of species within the same, localized region of the stratosphere (a capability which was first added on flight number 4 - the First Hydroxyl OH($X^2\pi$) Measurement). A preliminary step was taken by launching radiosondes to obtain reference data on the concentration of stratospheric ozone. Ozone data was scheduled to be collected at the time the atomic oxygen measurement was being made. Two ozonesondes were launched on schedule but a power failure caused loss of data from the first. The balloon failed on the second. A third ozonesonde was launched at 1133 CST and collected good data. The radiosonde instrumentation measured the progress of an electrochemical reaction between ozone and an aqueous solution of potassium iodide. The third ozonesonde reached a terminal altitude of 33 km at 1321 CST. The ozone concentration profile is presented in figure 18. The ozone mixing ratio by mass was 11 µg/g between 26 and 29 km and 15 µg/g between 30 and 33 km, typical stratospheric values.

POSTFLIGHT

Landing

The parachute/payload landed in the Cane River 3 nm southeast of Cloutierville, Louisiana at 1110:21 CST.

The ground crew recovered the payload in fair condition three hours after splashdown and returned it to Palestine, Texas, on 25 November 1974.

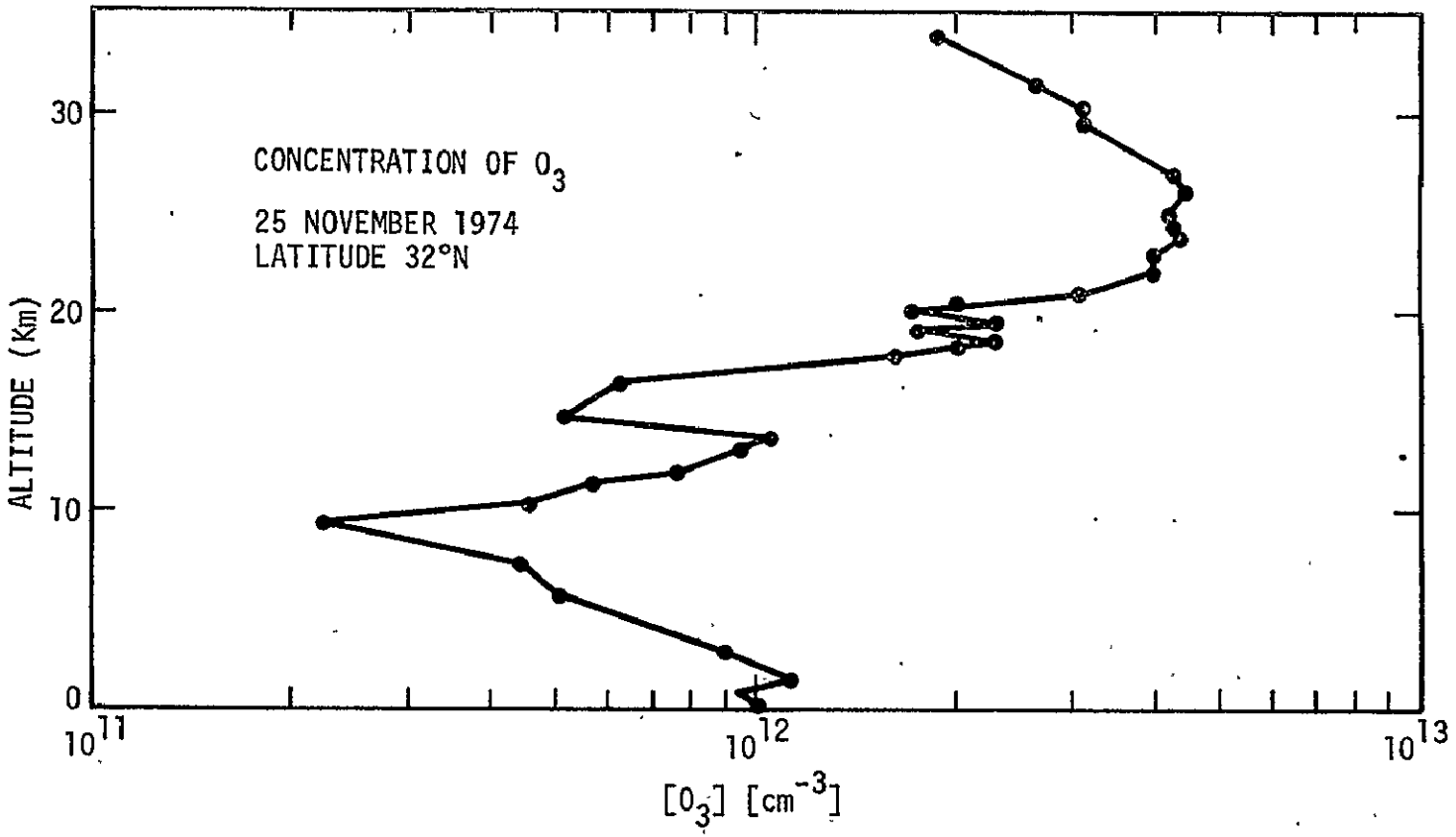

Figure 11.— Concentration of ozone determined by radiosonde subsequent to the first atomic oxygen $O(^3P)$ flight.

Inspection

Post flight inspection revealed that the 3-hour period of partial submersion caused extensive galvanic corrosion at numerous locations throughout the payload (terminal points, solder terminals, relay boxes, connectors, and pins). Power was on at impact (splashdown) and both gyros were running when the package was retrieved. The command to power down at lower altitude was not received by the payload - presumably due to the combined effects of signal strength and antenna pattern. The battery plug showed evidence of burn due to shorting. The package was left overnight at ambient conditions to dry with the panels off after return to the NSBF.

The resonance fluorescence instrument was taken back to the University of Pittsburgh for laboratory checks and analysis and the JSC components were returned to JSC for refurbishment.

CONCLUSIONS

The laminar flow through/resonance fluorescence technique provides a simple and direct means of measuring concentrations of trace atmospheric species at stratospheric altitudes accessible to zero pressure balloons.

The minor redesign of parachute rigging significantly improved payload attitude stability and resulted in a descent satisfactory to the measurement of the concentration of atomic oxygen in the stratosphere.

The results of this observational experiment agree reasonably well with theory regarding the $O(^3P)$ to O_3 ratio throughout much of the 26 to 39 km region. However, the importance must be emphasized of measuring the highly reactive species, which are not controlled by transport, simultaneously within the same volume element in order to accurately test models of stratospheric photochemistry. In addition, in order to establish a basis for prediction, several balloon-parachute flights are required to investigate diurnal, seasonal, and latitudinal dependencies.

SECOND ATOMIC OXYGEN $O(^3P)$ MEASUREMENT

(NCAR FLIGHT NO. 872-P)

7 February 1975

SUMMARY

This balloon-parachute flight was the second flight of the laminar flow through/resonance fluorescence instrument (principal investigator: Dr. James Anderson, University of Pittsburgh) and was successfully accomplished on 7 February 1975. The purpose of the flight was to measure the vertical concentration profile of atomic oxygen in the stratosphere and to corroborate the scientific results from the previous flight (First Atomic Oxygen $O(^3P)$ Measurement, NCAR flight no. 868-P).

The flight was launched at 0703:30 CST from the NSBF at Palestine, Texas. Hardware consisted of a 4.3×10^5 cubic meter balloon, 9.75-meter diameter guide surface parachute, NCAR telemetry system, JSC flight support module, and the resonance fluorescence instrument tuned to the ^3P-^3S transition of atomic oxygen at 130.4 nm. The payload reached a float altitude of 44 km (144.5 k ft) at 1003 CST and was released from the balloon (descent data gathering phase began) at 1020:00 CST. The scientific data from the flight were of excellent quality and were used to produce a profile of atomic oxygen concentration in the 27 to 44 km region of the stratosphere. The atomic oxygen data, to within the errors of measurement, showed the same overall density and structuring as the previous flight. The parachute/payload landed in a wooded area 20 nm southeast of Natchez, Mississippi at 1059 CST and was recovered in good condition.

Three ozone radiosondes were launched in conjunction with the flight to provide reference data on the concentration of stratospheric ozone. They were launched at 0810, 0857, and 1134 CST and reached terminal altitudes of 37.6, 40.2, and 27.9 km (123, 132, 92 k ft), respectively.

INTRODUCTION

In order to establish a basis for prediction, a series of balloon-parachute flights is being performed to verify and study stratospheric catalytic reaction cycles and to investigate diurnal, seasonal, and latitudinal dependencies of the vertical concentration profiles of trace species believed to be important for the photochemical balance of the upper atmosphere. The purpose of this flight was to repeat, in the same season and under conditions of comparable solar illumination, the measurements made on the previous flight of this series so that a comparison, and hopefully a corroboration, of the scientific results could be made.

Payload

The payload weighed approximately 200 kg, and consisted of telemetry, balloon control, descent-observation, and scientific instrumentation. A sketch of the payload is shown in figure 19.

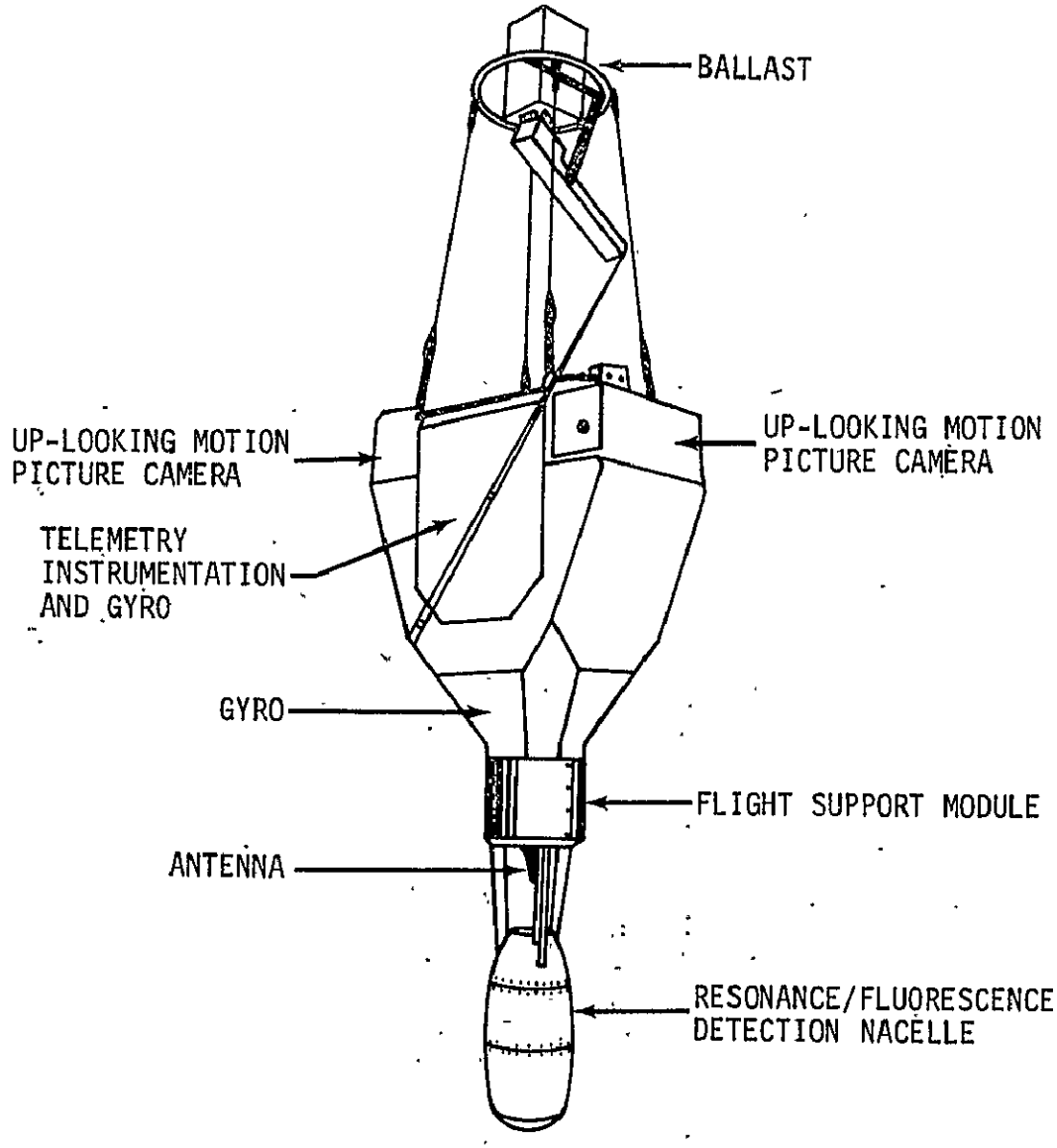

Figure 19.— Sketch of payload for the second atomic oxygen $O(^3P)$ flight.

Instrumentation

Instrumentation carried as part of the payload included NCAR and JSC telemetry instrumentation, NCAR balloon control instrumentation, NCAR and JSC pressure transducers to measure the altitude of the payload, two vertical reference gyros to measure payload attitude, a z-axis accelerometer to determine the loading forces when the parachute is deployed, two up-looking motion picture cameras to observe parachute opening and descent characteristics, and the laminar flow through/resonance fluorescence instrument to measure the concentration of atomic oxygen. The three-axis magnetometer and the x- and y-axis accelerometers, flown on the previous flight, were deleted due to the more operational role of the payload. In addition, a set of pressure transducers were flown to evaluate their ability to improve the altitude data and the motion picture cameras were geared for two different film speeds (16 and 64 frames per second). Ozone reference instrumentation consisted of three potassium iodide ozonesondes.

Function, manufacturer, model, and serial numbers for support instrumentation are itemized in Appendix A. Pertinent electrical and mechanical drawings are listed in Appendix B. A description of the telemetry systems and channel allocations is given in Appendix C. Photographic documentation for the flight is itemized in Appendix D.

Balloon

A larger balloon (4.3×10^5 as compared to 1.3×10^5 cubic meter for the previous flight) was used to attain a higher altitude and extend the range over which measurements were taken.

DATA RESULTS

Payload Stability and Descent Characteristics

The flight profile for the Second Atomic Oxygen $O(^3P)$ flight is illustrated in figure 20. Launch occurred at 0703:30 CST, 7 February 1975, and was accomplished using the dynamic launch technique. The balloon system ascended at an average rate of 4.12 meters per second to a float altitude of 44 km and was allowed to float at altitude for 17 minutes before the payload was released on command from the tracking aircraft at 1020:00 CST, beginning the data gathering phase of the mission.

The descent system was not changed from the previous flight, except a new guide surface parachute was used. Solar zenith angle at the time of cutdown was 51 degrees (approximating the 56 degree solar zenith angle for the previous flight). Onboard motion picture cameras and accelerometers observed parachute deployment and measured the loading forces while two vertical reference gyros monitored the descent attitude of the system. Due to the higher altitude of the payload at cutdown, the velocity/altitude profile of the descending payload (fig. 21) is somewhat steeper and the loading force as a function of time after parachute deployment (fig. 22) is somewhat gentler than on the previous flight. Also, because of the higher altitude, the time taken to reach terminal velocity (when the acceleration approached a value of 1.0 g) was somewhat longer than for the previous flight.

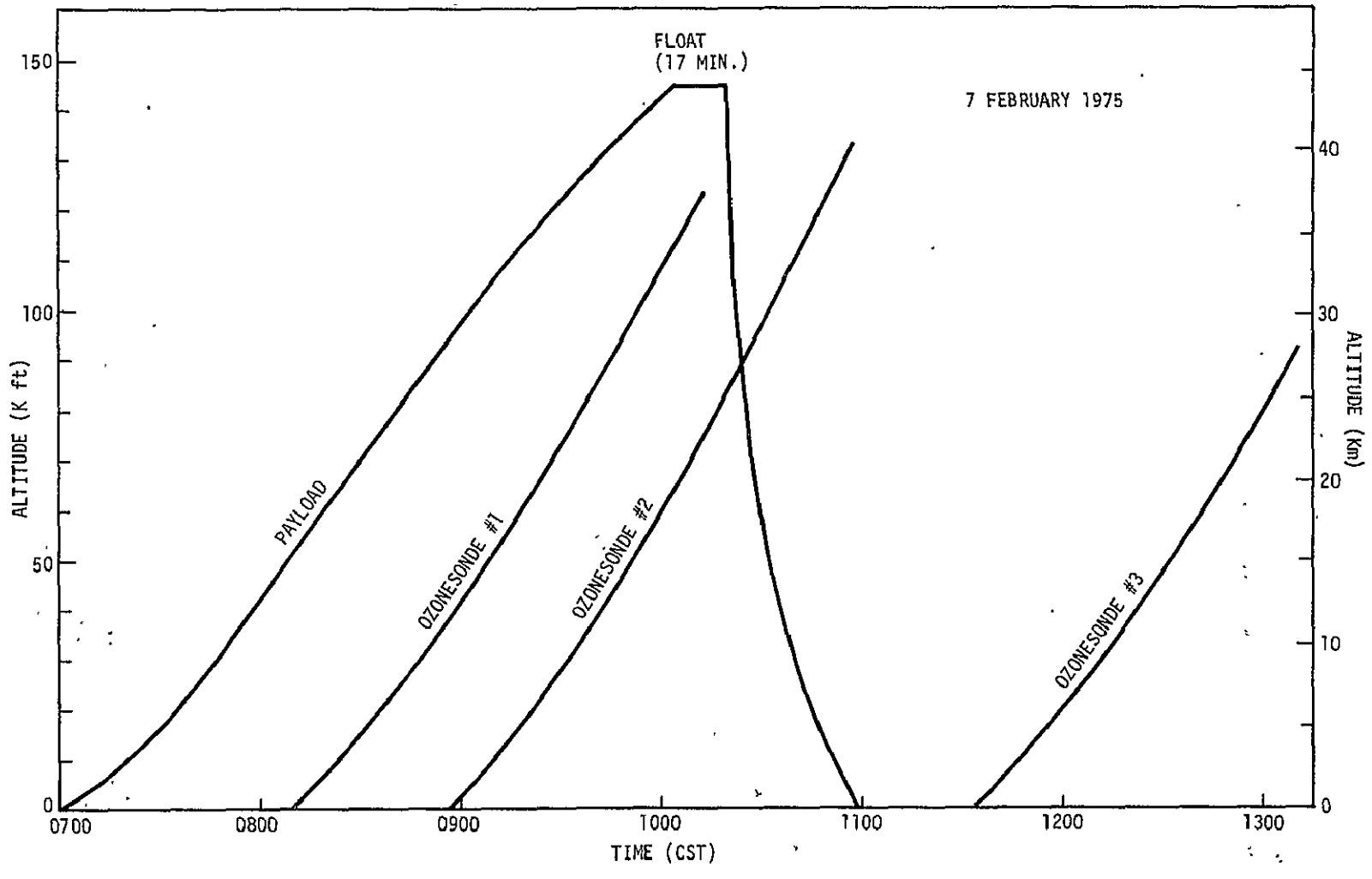

Figure 20.— Flight profile for the second atomic oxygen $O(^3P)$ flight.

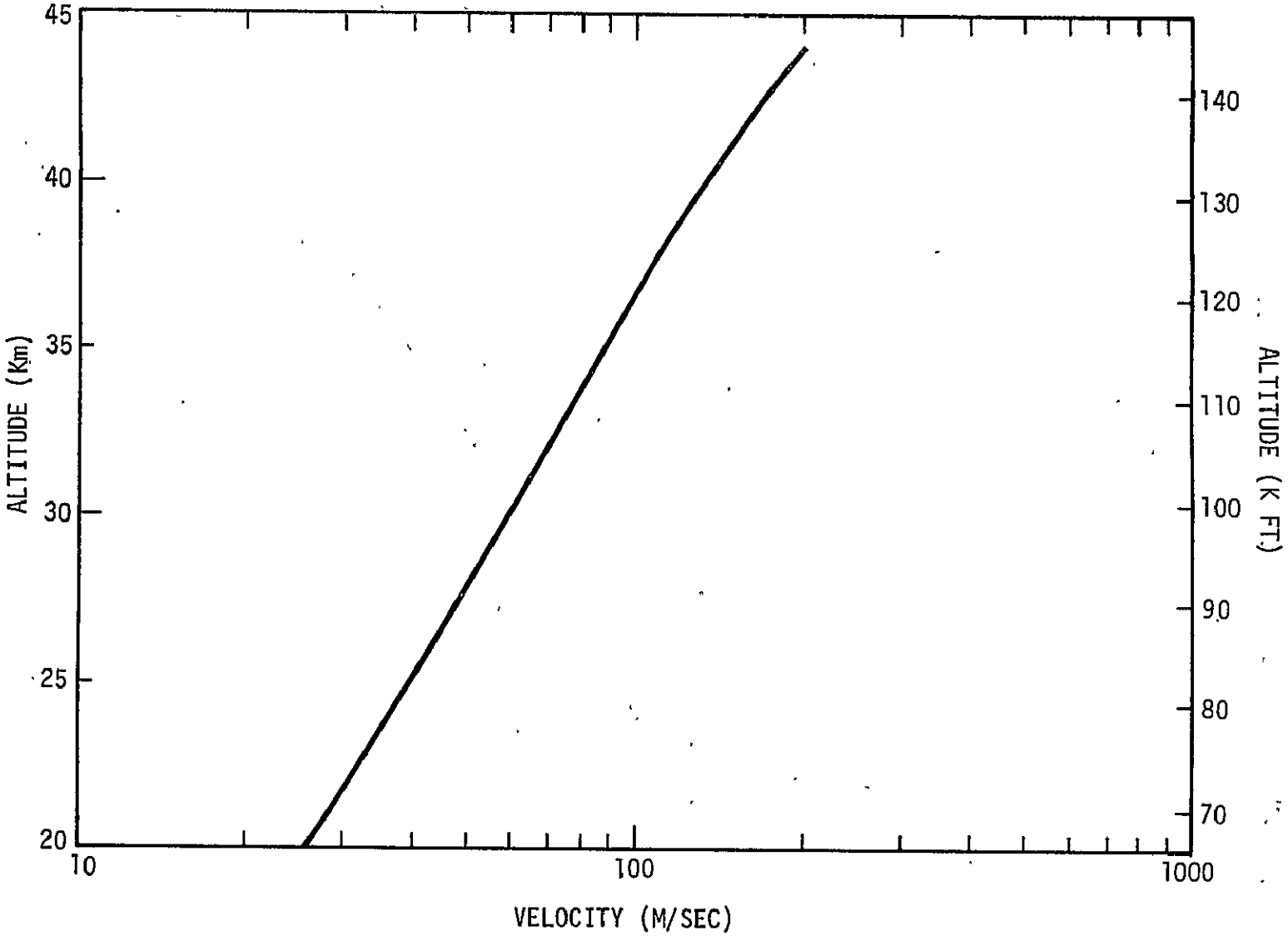

Figure 21.— Velocity/altitude profile of descending payload for the second atomic oxygen $O(^3P)$ flight.

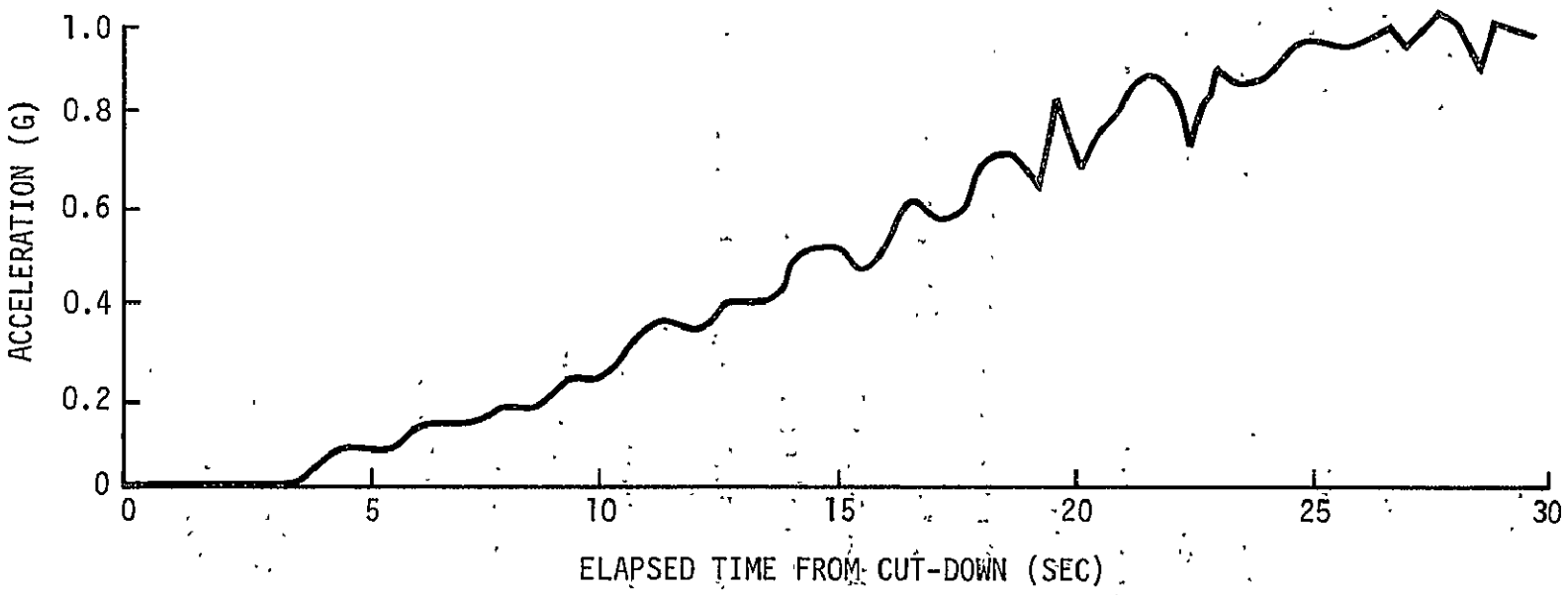

Figure 22.— Vertical force on payload after parachute deployment for the second atomic oxygen $O(^3P)$ flight.

As with all flights of this series, a stable payload during descent is important to ensure a laminar flow through the detection nacelle to minimize the depletion of straotspheric species by collision with the wall of the instrument. Figure 23 shows the probability as a function of altitude that the attitude was within 5, 10, and 15 degrees of vertical for the data gathering phase of the flight. A comparison of figure 23 with figure 16 (the corresponding diagram for the previous flight) shows a further improvement in attitude stability for the present flight. The percentage of time spent within 10 degrees of vertical was 84 percent for the present flight as compared to 53 and 66 percent for the first and second flights of the present series, respectively. Thus the attitude stability was superior to that achieved on the previous two flights and the velocities encountered during descent were again satisfactory for the measurement of atomic oxygen.

High altitude photographic coverage of the descending payload was obtained using a T-38 (JSC) as a chase plane which tracked the payload on descent from 12 km (40 k ft) down to 3 km (10 k ft). The aircraft made numerous passes using both still and motion picture cameras. Figure 7 is one of the photographs obtained.

Good telemetry signals were received at both JSC and the NSBF until the payload was below 12 km (40 k ft) in altitude at a distance of 250 to 275 nm.

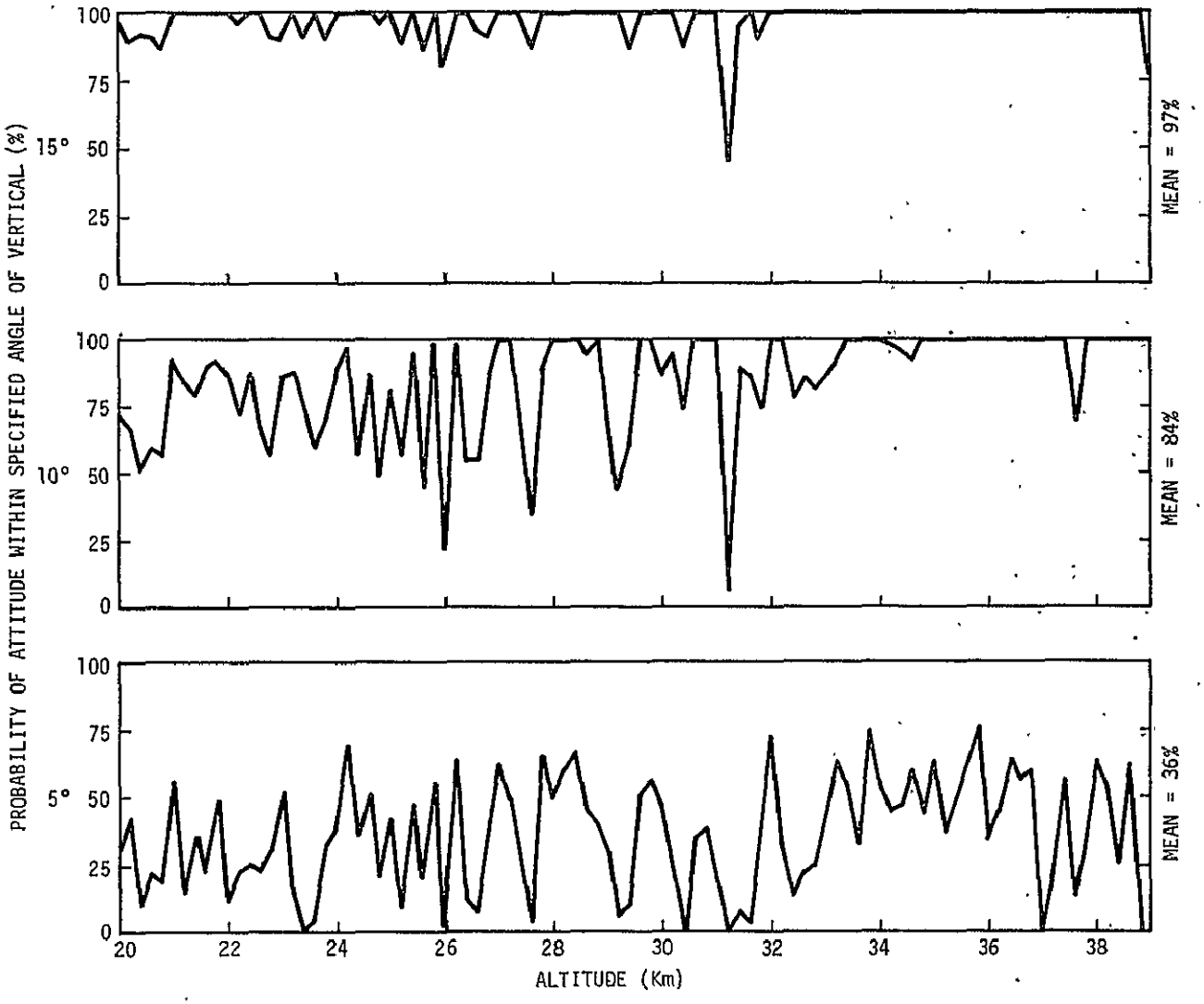

Figure 23.— Payload attitude probabilities as a function of altitude for the second atomic oxygen $O(^3P)$ flight.

Flight Anomaly

One unusual incident involving the instrument, or telemetry system, occurred during this flight. At 0828 CST when the payload was at an altitude of 21 km (70 k ft) the 10^{-9} atomic oxygen concentration channel went dead. Ground checks determined that the problem was in the airborne instrument, and that the other three data channels were unaffected. At 0910 CST when the payload was at an altitude of 30 km (100 k ft) the 10^{-9} channel began working again and worked well for the remainder of the flight.

Atomic Oxygen $O(^3P)$ Measurement

The profile of the concentration of atomic oxygen $O(^3P)$ between 44 and 27 km (integrated over 500 meter intervals above 30 km and 1 km intervals below 30 km) measured on this flight is presented in figure 19. The data plotted were secured during the 3.8 minute drop time from 44 to 27 km commencing at 1020:00 CST 7 February 1975 (solar zenith angle of 51 degrees and latitude of 31.4 degrees North). For comparison purposes, the stratospheric concentration of $O(^3P)$ measured on the 25 November 1974 flight is also plotted in figure 24. The overall concentration levels observed in the two flights are quite similar with a considerable amount of local structure apparent below an altitude of 35 km. This structure is real since the statistics of the measurement are sufficiently high that it cannot be attributed to noise in the data.

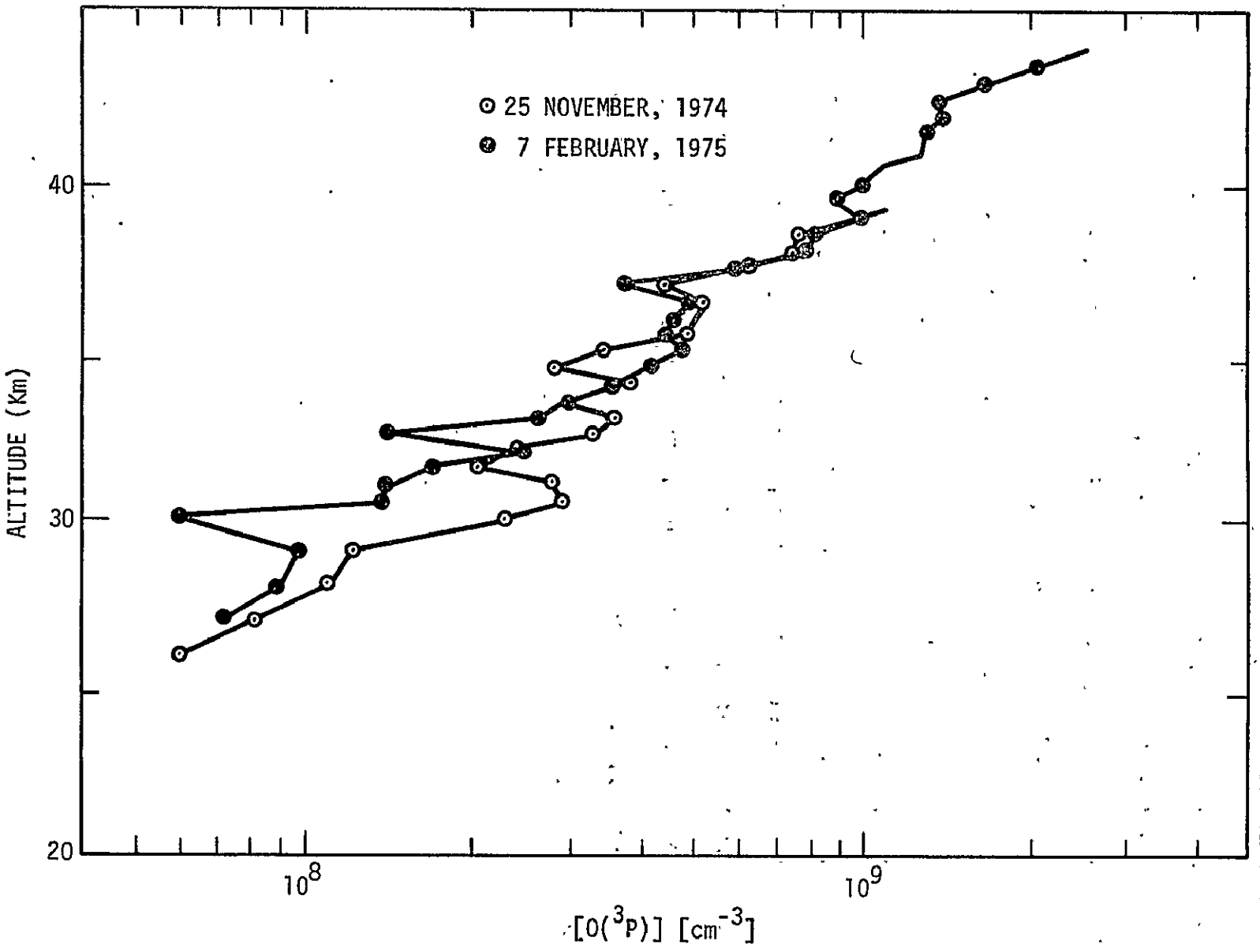

Figure 24.— Stratospheric concentration of atomic oxygen measured on the first and second atomic oxygen $O(^3P)$ flights.

Ozone Measurement

As for the previous flight, three radiosondes were released in conjunction with the atomic oxygen measurement to measure the concentration of stratospheric ozone. Their purpose was to establish the normal ozone level for the day according to accepted precepts. The planned flight profile called for a time difference between launching of the radiosondes of 30-45 minutes. Due to the high winds aloft (drift rate), the NCAR operations group chose to keep the tracking sonde on the oxygen instrument ON until the down range tracking station (Laurel, Mississippi) acquired the payload signal on their telemetry. Therefore the tracking equipment for the second ozonesonde was not available until 0855 CST. The ozonesondes were launched at 0810, 0857, and 1134 CST and reached terminal altitudes of 37.6, 40.2, and 27.9 km (123, 132, 92 k ft), respectively. The ozone concentration profiles (which are typical for winter conditions at the latitude of 32 degrees North) derived from the three successful radiosondes are presented in figure 25.

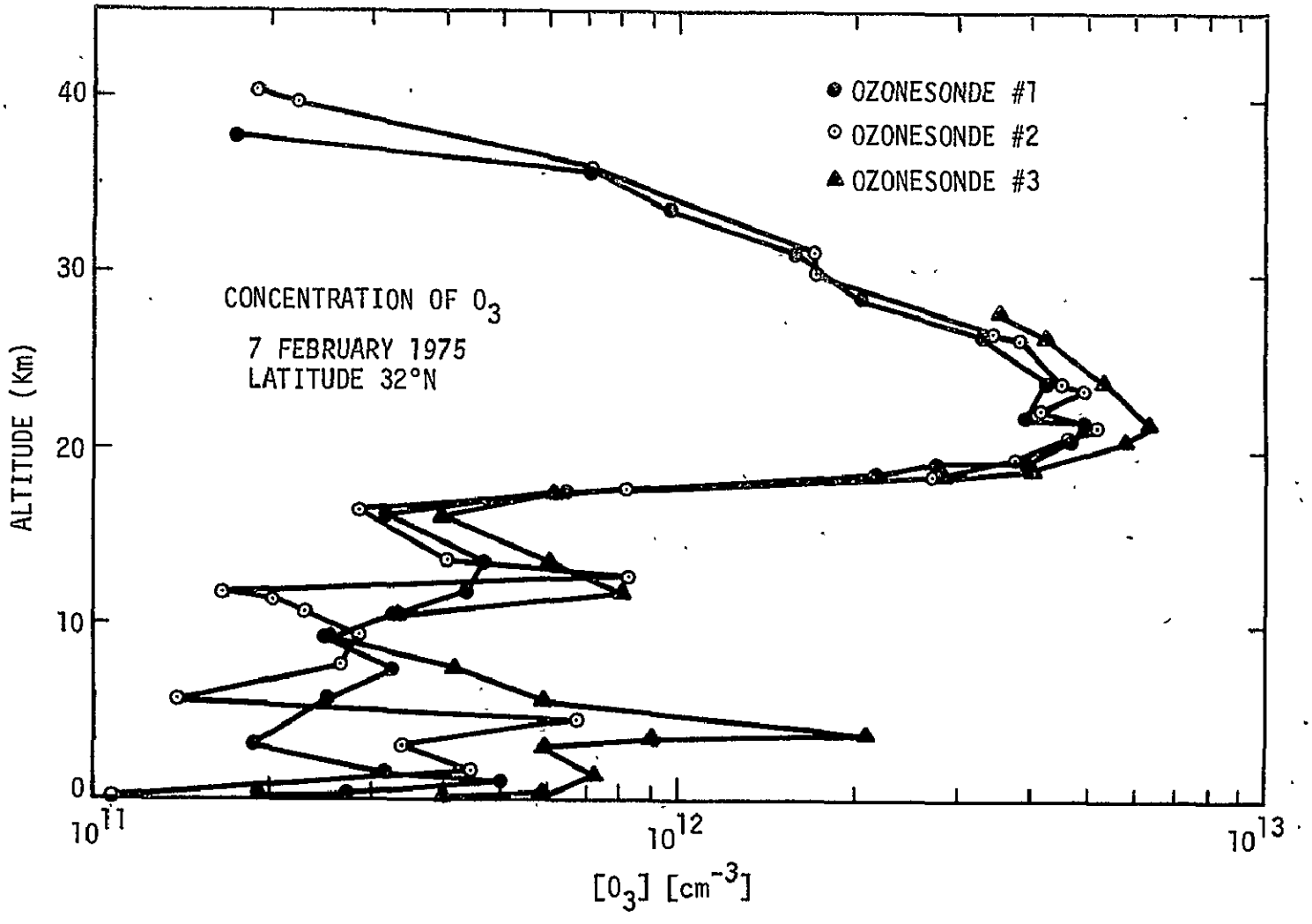

Figure 25.— Concentration of ozone determined by radiosondes released in conjunction with the second atomic oxygen $O(^3P)$ flight.

POSTFLIGHT

Landing

The parachute/payload landed in a wooded area 20 nm southeast of Natchez, Mississippi at 1059:00 CST. The recovery crew found the payload in good condition the morning of 8 February 1975 and returned it to Palestine, Texas, on 9 February 1975.

Inspection

The telemetry package was inspected and was operated. There was no evidence of mechanical or electrical damage. RF transmitted telemetry appeared normal. Both vertical reference gyros were started to verify operational status.

The flight and spare battery packs checked good and were returned to the JSC/Space Vehicle Battery Facility for preparation for reflight.

Inspection of the resonance fluorescence instrument was performed at JSC. Several wires were found to be broken. Inspection of the broken ends revealed evidence of wire damage during stripping. The anomaly in the 10^{-9} atomic oxygen concentration channel, which occurred during ascent, was caused by a separation of the data line in the umbilical at the back of the connector. This occurred during the coldest part of the flight (allowing for thermal lag of the instrument). As the

instrument warmed up, the wire (which was in a potted connector) reconnected. The connector had been inspected after arrival at the NSBF and no broken connections were found.

CONCLUSIONS

The scientific data obtained on this flight corroborated the results of the previous flight. The same overall profile for atomic oxygen concentration was obtained with statistically significant structuring below 35 km. The flight performance of the instruments during the second atomic oxygen measurement was excellent.

FIRST HYDROXYL OH($X^2\pi$) MEASUREMENT

(NCAR FLIGHT NO. 912-P)

18 July 1975

SUMMARY

This balloon-parachute flight was the third flight of the laminar flow through/resonance fluorescence instrument (principal investigator: Dr. James Anderson, University of Michigan) and took place on 18 July 1975. The purposes of the flight were to measure the vertical concentration profiles of the hydroxyl radical (OH) and ozone (O_3) from 20 to 45 km and to evaluate the impact of Rayleigh-scattered solar radiation on the OH measurements.

The flight was launched at 1633:05 CDT from the NSBF at Palestine, Texas. The late afternoon launch represented a change in flight operations and was required to minimize background noise (originating from solar radiation scattered from the lower atmosphere) while retaining a nominal OH density profile. Hardware consisted of a 4.3×10^5 cubic meter balloon, 9.75-meter diameter guide surface parachute, NCAR telemetry system, JSC flight support module, the resonance fluorescence instrument (of modified design) tuned to the (0-0) band of the $A^2\Sigma$-$X^2\pi$ electronic transition of OH (bandhead at 306.4 nm), and an ozone monitor on loan from GSFC for *in situ* measurement of ozone using the ultraviolet (UV) absorption method. Good data on the concentration of ozone were obtained during the ascent phase of the flight from 14 km (46 k ft) to 32 km (105 k ft). The payload reached a float altitude of 43.3 km (142 k ft) at approximately 1906 CDT. The background count rate for the resonance fluorescent instrument was monitored during the ascent and float

phases of the flight by operating the experiment with the source lamp OFF. The decision to delay the release of the payload from the balloon until 2000:00 CDT (to begin the OH data gathering phase of the mission) was made in real time on the basis of the background level. Useful scientific data were obtained from the OH resonance fluorescence instrument only between 41 km (135 k ft) and 39 km (128 k ft) because the instrument did not discriminate adequately against Rayleigh scatter from the lower atmosphere which entered the fluorescence chamber along the flow axis of the instrument at lower altitudes. Nevertheless the measured concentration ($2.0 \, ^{+1.5}_{-1.0} \times 10^7$ cm^{-3} at 40 km) of OH is of significant scientific value since this is the first time that the absolute concentration of this species has been measured in the stratosphere at an altitude lower than 45 km. Good data (with the exception of 6 data points between 27 and 25 km) on the concentration of ozone were also obtained during the descent phase of the flight from 32 km (105 k ft) to 12 km (39 k ft). The parachute/payload landed 7 nm SSW of Comanche, Texas at 2032:30 CDT and was recovered in good condition.

A total of four ozone radiosondes (two being optional) were scheduled for launch in conjunction with the flight to provide reference data on the concentration of stratospheric ozone according to accepted precepts and to allow for a comparison with the in situ measurements made aboard the payload. Unfortunately, due to a failure in the NCAR GMD-1A (a general meteorological ground station) no ozonesonde data was received.

INTRODUCTION

In order to verify and study the various catalytic reaction cycles thought to control the generation and, in some cases, the depletion of stratospheric ozone, a series of balloon-parachute flights is being performed to determine the vertical concentration profile of trace species believed to be important for the photochemical balance of the upper atmosphere. Hydroxyl (OH) was chosen as the second species to be studied in the stratospheric measurements program because it is the major linking radical in the oxygen, hydrogen, nitrogen and chlorine systems and since no data existed on the concentration of the radical in the middle and lower stratosphere below 45 km.

Although the existence of the hydroxyl radical in the region of maximum stratospheric ozone production and concentration has been assumed for years, its presence had never been measured. At the levels predicted for this region, OH plays a key role in controlling the chemistry and concentrations of many minor stratospheric species which are critical to the maintenance of the ozone layer. For example, OH has a direct destructive catalytic effect on ozone reactions. It also combines with the nitrogen oxides (primarily NO and NO_2 which destroy ozone) to form nitric acid (HNO_3). In addition, the reaction between OH and gaseous hydrochloric acid (HCl)

controls the rate of converting HCl to atomic chlorine (Cl) and thus the Cl to HCl ratio. It has been recently shown that atomic chlorine (like the oxides of nitrogen) can act as a catalyst to destroy stratospheric ozone. Measurements of the chlorofluoromethanes used as refrigerants and propellants demonstrate that they diffuse into the stratosphere and directly deposit Cl by the photolysis of solar ultraviolet radiation. Because of this, the determination of concentrations for the chlorine compounds and those species such as OH which chemically control them has taken on great importance. Thus, within the coupled stratospheric photochemical system which includes oxygen, hydrogen, nitrogen and chlorine, the hydroxyl radical is now recognized as a key constituent with three important effects:

(1) The presence of the oxides of hydrogen (OH included) dominates the catalytic conversion of atomic oxygen and ozone to molecular oxygen between the tropopause and approximately 23 km and in the region above approximately 50 km.

(2) The ratio of the odd nitrogen oxides (NO and NO_2) to nitric acid is thought to be governed throughout the stratosphere by catalytic recombination with OH so that the fraction of the total nitrogen oxides which exist in a form capable of destroying ozone is inversely proportional to the OH concentration.

(3) The partitioning between the oxides of chlorine (ClO_x) and hydrochloric acid is dependent upon the concentration of hydroxyl since atomic chlorine is recycled from HCl principally by reaction with hydroxyl. Thus the fraction of Cl and ClO (which are capable of catalytically destroying ozone) is directly proportional to the OH concentration in the stratosphere.

Because the hydroxyl radical is a highly reactive species not controlled by transport processes, it is important that measurements of its concentration and the concentration of ozone be made in the same, localized region of the stratosphere. For this reason, the third scientific flight of the current series was instrumented to measure the concentration levels of both species concurrently. Ozone reference data, scheduled to be obtained according to accepted precepts using potassium iodide radiosondes, would allow for a comparison of the two techniques by an appropriate correlation of the data.

Payload

The payload weighed approximately 280 kg, and consisted of telemetry, balloon control, descent-observation, and scientific instrumentation. A sketch of the payload and flight configuration is shown in figure 26.

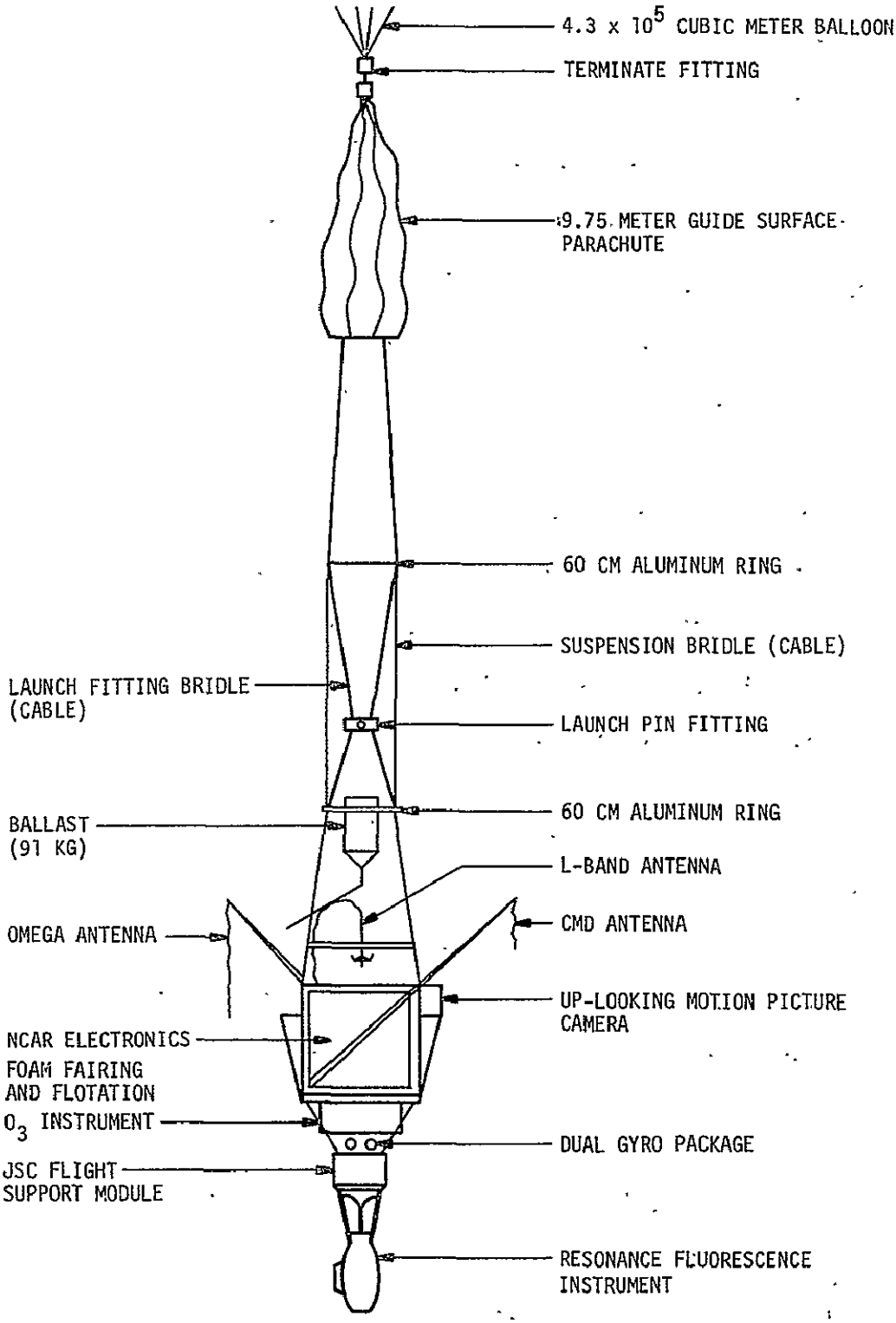

Figure 26.— Flight configuration for first hydroxyl OH($X^2\pi$) measurement.

Instrumentation

Instrumentation carried as part of the payload included NCAR and JSC telemetry instrumentation, NCAR balloon control instrumentation, NCAR and JSC pressure transducers to measure the altitude of the payload, two vertical reference gyros to measure payload attitude, a z-axis accelerometer to determine the loading forces when the parachute is deployed, a single up-looking motion picture camera (64 frames/sec using a 10 mm lens) to observe parachute opening and descent characteristics, an ozone monitor (on loan from GSFC) to measure in situ the concentration of stratospheric ozone, and the laminar flow through/resonance fluorescence instrument to measure the concentration of the hydroxyl radical. Ozone reference instrumentation consisted of up to four potassium iodide ozonesondes.

Function, manufacturer, model, and serial numbers for support instrumentation are itemized in Appendix A. Pertinent electrical and mechanical drawings are listed in Appendix B. A description of the telemetry systems and channel allocations is given in Appendix C. Photographic documentation for the flight is itemized in Appendix D.

The major scientific instrument flown on this flight was the resonance fluorescence instrument developed by Dr. James Anderson of the University of Michigan tuned to the (0-0) band of the $A^2\Sigma$- $X^2\pi$ electronic transition of the OH radical (bandhead at 306.4 nm, peak intensity at 309.0 nm).

Conceptually, molecular resonance fluorescence is identical to atomic resonance fluorescence. However, it represents a rather different problem from the experimental point of view. First, the resonance cross sections for molecules are lower by three to four orders of magnitude than for atoms. Thus the ratio of scattered photons to resonance fluorescence photons is higher for the case of molecules. But the smaller resonance cross section is not entirely unfavorable. Photons within the lamp plasma are not trapped by self absorption so that it is possible to increase the lamp flux by a large factor. The diminished optical depth within the plasma also allows for the advantageous use of a spherical mirror behind the plasma to increase the net beam flux.

The second major difference between molecular and atomic resonance fluorescence is that the ground state transitions of molecular species and their radicals typically take place in the near ultraviolet, not in the vacuum ultraviolet as is the case for the ground state transitions of atoms. The optical depth of the Earth's atmosphere is quite different in these two spectral regions. Solar radiation in the vacuum ultraviolet is totally absorbed by molecular oxygen and nitrogen and by atomic oxygen at altitudes above the stratosphere while in the 309.0 nm region appropriate to hydroxyl, the atmosphere is virtually transparent. Thus the fluorescence chamber must be isolated both from the direct rays of the sun and

from solar radiation backscattered from the lower atmosphere. This, coupled with the fact that surface reflectivities are higher in the near ultraviolet than in the vacuum ultraviolet, makes the optical problem of descriminating the resonance fluorescence photons from the unwanted scattered and reflected photons more difficult. One favorable effect of operating in the near ultraviolet is that the transmission of optical components is considerably higher than in the vacuum ultraviolet.

A third problem which must be dealt with for molecular fluorescence in the 10^{-12} mixing ratio range is Rayleigh scatter from the lamp beam by molecular nitrogen and oxygen. In fact, if the atmospheric concentration of N_2 and O_2 are sufficiently high, Rayleigh scatter from the lamp beam becomes competative with the resonance fluorescence signal from OH. This is true, however, only in the case of an unpolarized detector. Resonance fluorescence results in unpolarized light while Rayleigh scattering is strongly polarizing. Hence by placing a polarizing filter in the appropriate orientation between the scattering volume and the detector, Rayleigh scattering may be discriminated against. While the polarizing filter rejects both resonance fluorescence and Rayleigh scattered photons, the net effect is a significant gain in the signal to noise ratio.

The overall geometry of the resonance fluorescence flight instrument (shown in figs. 4 and 5) was identical to that used on the previous two flights with the exception of the observation light baffle. The baffle was enlarged (to such an extent that it protruded from the side of the detection nacelle) in an attempt to minimize internal reflections. The only other major differences in the flight instrument were those resulting from its use in the near ultraviolet. The photon source consisted of a low pressure (about 2 torr) microwave discharge (2.4 GHz) of helium mixed with a trace amount of water vapor and contained in a quartz tube. A spherical mirror and quartz lens combination maximized the optical collection efficiency from the discharge region and served to initially collimate the source beam. The photon detector consisted of a narrow bandpass interference filter centered at 309.0 nm, a polarizing filter which rejected radiation with a plane of polarization perpendicular to the plane defined by the lamp beam and observation direction in order to discriminate against Rayleigh scatter by O_2 and N_2 from the lamp beam, and a quartz lens which optically condensed the image of the scattering volume on the cathode of the photomultiplier tube operated in the pulse counting mode. During the descent phase of the flight, the background count rate in the absence of OH was periodically determined by adding cis-2-butene (C_4H_8) gas at the entry throat of the instrument with the loop injector (see fig. 5). C_4H_8 was chosen

because it reacts rapidly with OH to chemically eliminate it from the flow, yet it does not react with any other known atom or radical to produce OH within the time scale of the conversion.

Collisional deactivation ("quenching") of the $A^2\Sigma$ state of OH was treated by calculating the fraction of A state molecules that radiate before being deactivated through some other channel. For the case considered here, the only important deactivation channels are radiation and quenching by N_2 and O_2. The fraction is calculated using well known values for 1) the bimolecular quenching rate constants of the A state of OH by molecular nitrogen and oxygen, 2) the A to X radiative rate and 3) the concentration of nitrogen and oxygen at the point of measurement.

The concentration profile of stratospheric ozone was measured with an ozone monitor modified for use at stratospheric altitude on loan from Dr. E. Hilsenrath of GSFC. This instrument, which was flown as an integral part of the scientific payload with the resonance fluorescence experiment, made <u>in situ</u> measurements of ozone using the ultraviolet absorption method. A detailed description of the ozone instrument and its performance on this (and the two subsequent flights in this series) may be found in JSC Internal Report JSC-11380 (Application of Dasibi Ultra-Violet Ozone Monitor to Stratospheric Measurements) dated June 1976. The source of UV radiation for the

instrument's absorption chamber is a stable, low pressure mercury vapor lamp. The principal output line in the lamp's spectrum is at 253.7 nm (near the ozone UV absorption maximum). The lamp output is directed to two photomultiplier tube detectors with similar responses. One of the detectors serves as a reference detector to monitor the lamp stability while the other measures the absorption of UV radiation by ozone within an absorption chamber. The measurement cycle is divided into two phases. In the reference phase, stratospheric gas is passed through a selective gas filter which removes only ozone from the sample. In the sample phase, unfiltered stratospheric gas enters the chamber. The attenuation of the lamp beam by UV absorption of ozone within the chamber is then a measure of the concentration of ozone.

DATA RESULTS

Payload Ascent, Descent and Stability Characteristics

The flight profile for the First Hydroxyl OH($X^2\pi$) Flight is illustrated in figure 27. Launch occurred at 1633:05 CDT, 18 July 1975, and was accomplished using the dynamic launch technique. The balloon system ascended at an average rate of 4.62 meters per second to a float altitude of 43.4 km. The ozone monitor was operated during both the ascent and descent phases of the flight. The resonance fluorescence instrument was operated during the ascent and float

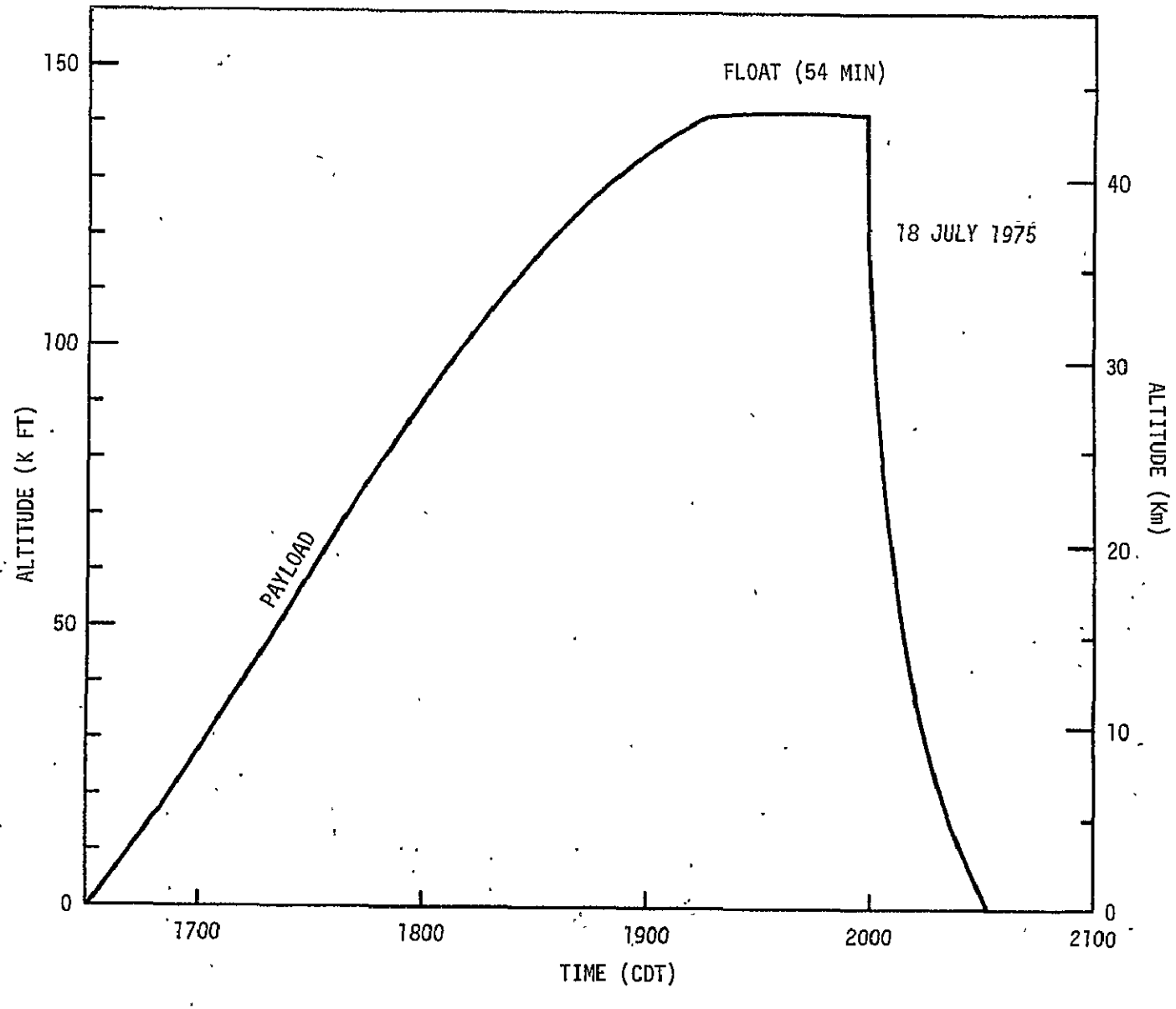

Figure 27.— Flight profile for the first hydroxyl OH($X^2\pi$) flight.

phases of the flight (source lamp OFF) to monitor the background from Rayleigh scattering of solar radiation entering the measurement chamber from the lower atmosphere (see fig. 28). A real time decision (anticipated in the original flight plan) was made to slip the time of payload release from 1930 to 2000 CDT to minimize the background count rate. The balloon was allowed to float at altitude for approximately 54 minutes. The payload was released on command from the tracking aircraft at 2000:00 CDT and the OH data gathering phase of the mission began. Solar zenith angle at the time of cut down was 80 degrees and the payload latitude was 31.7 degrees North. An onboard motion picture camera and accelerometers observed parachute deployment and measured the loading forces while two vertical reference gyros monitored the descent attitude of the system. Payload altitude as a function of time around the time of cut down is illustrated in figure 29. The velocity/altitude profile of the descending payload is shown in figure 30. The velocities encountered at a given altitude are about 10 percent greater than on the previous flight due to the increased payload weight. Terminal velocity (when the acceleration approached a value of 1.0g) was reached 30 seconds after cut down. Figure 31 shows the probability as a function of time since cut down and altitude that the payload attitude was within 5, 10, 15 and 20 degrees of vertical.

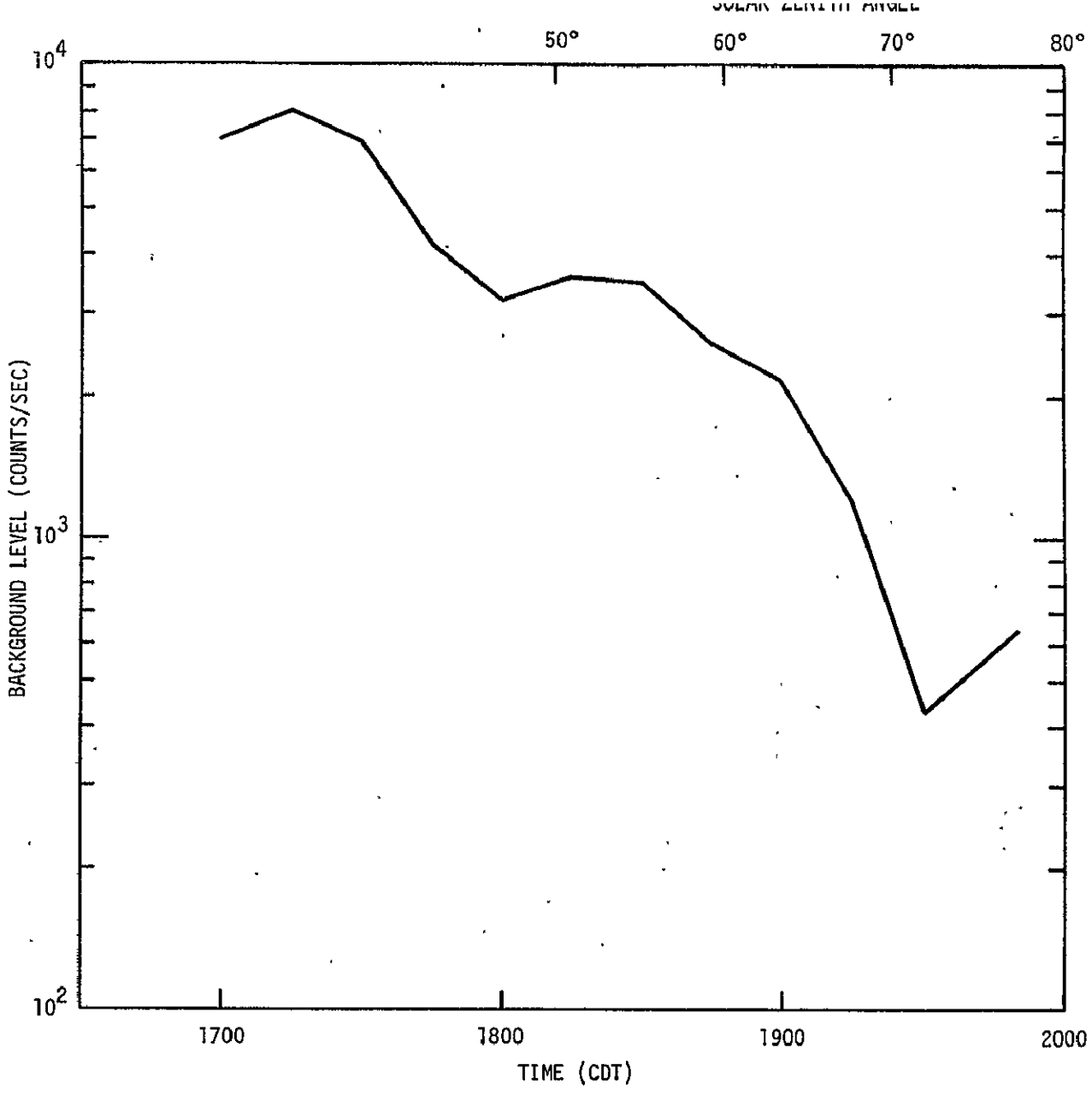

Figure 28.— Background count rate monitored during ascent and float phases of the first hydroxyl OH($X^2\pi$) flight.

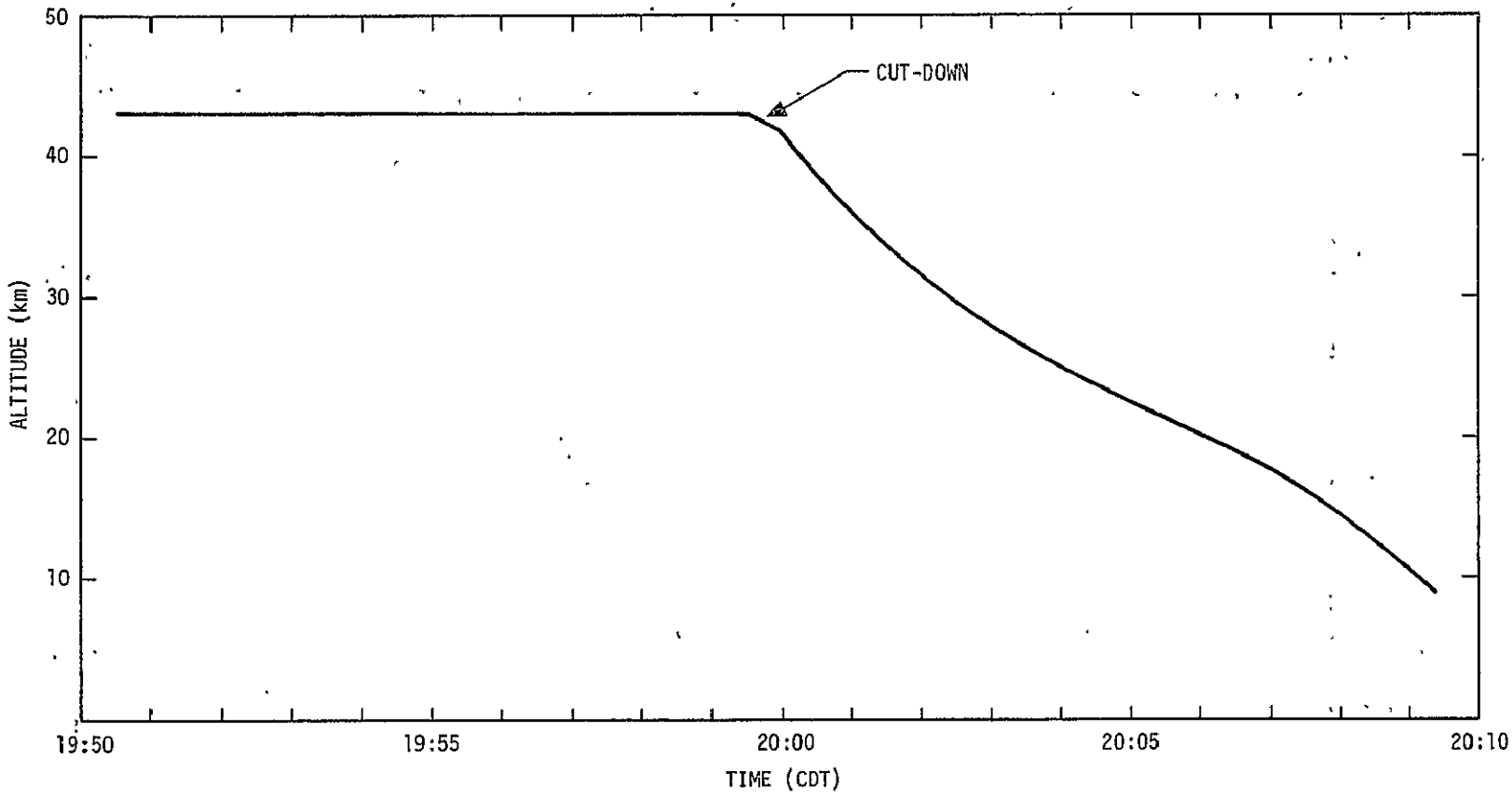

Figure 29.— Altitude/time profile for the first hydroxyl OH($X^2\pi$) flight around the time of cut-down.

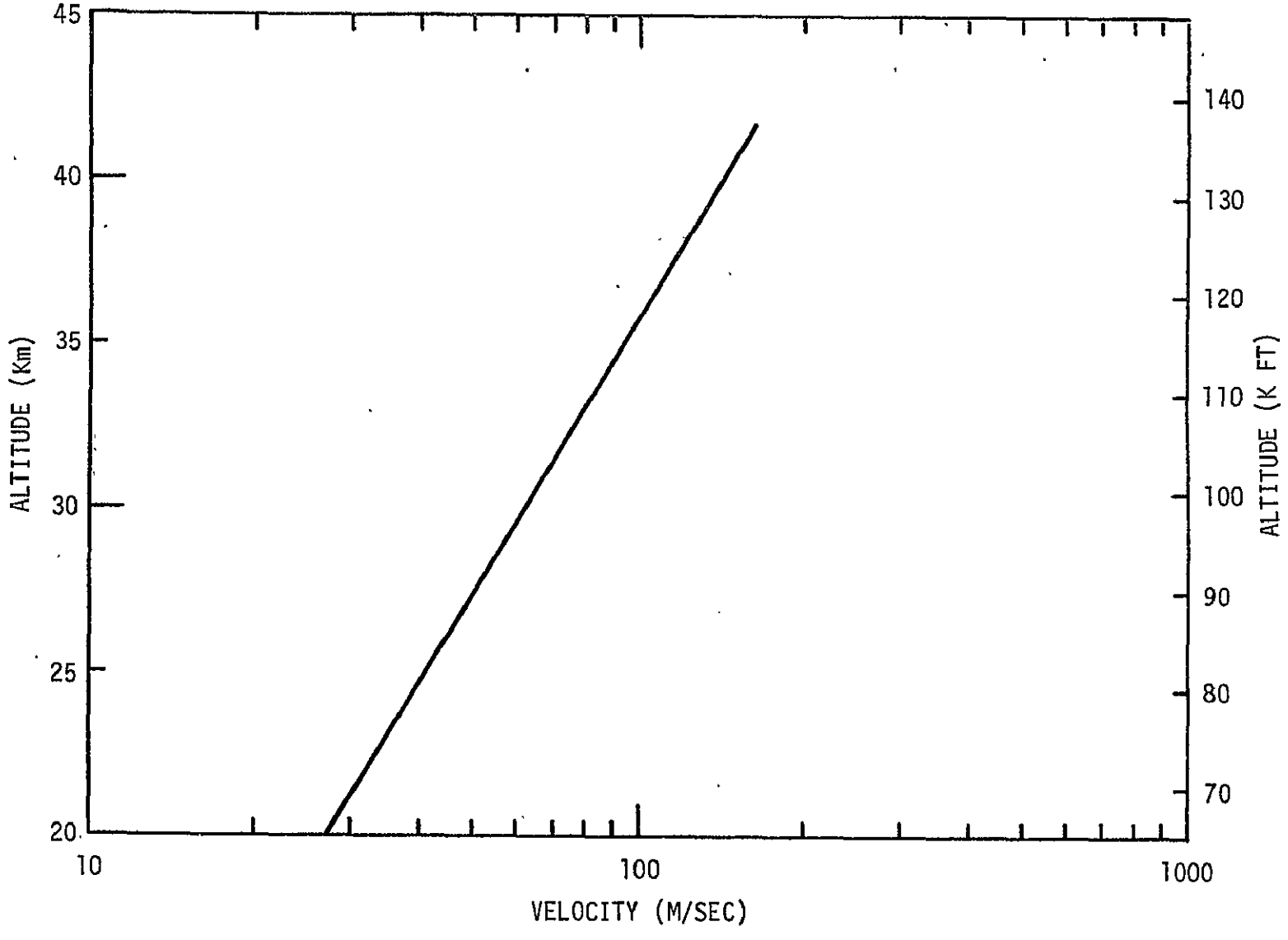

Figure 30.— Velocity/altitude profile for first hydroxyl OH($X^2\pi$) flight.

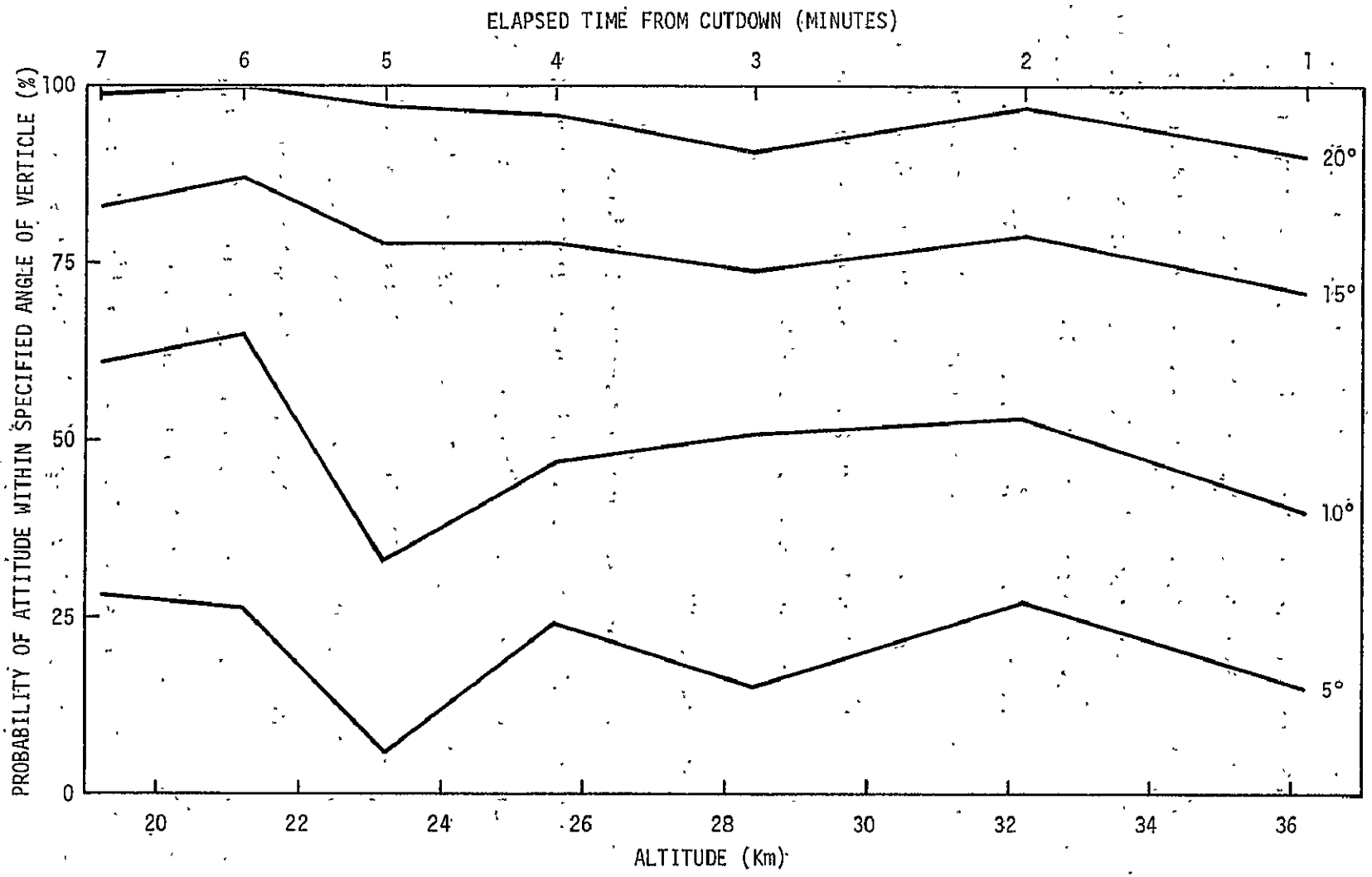

Figure 31.— Payload attitude probabilities as a function of time since cut-down and altitude for the first hydroxyl OH($X^2\pi$) flight.

The source lamp filament was turned on eight minutes before cut down and high voltage was supplied to the magnetron (the microwave frequency oscillator for the source lamp) six minutes later. A thermal history of the source lamp cavity and magnetron tube around the time of cut down is plotted in figure 32. Figure 33 is similar plot showing the resonance fluorescence experiment current levels. Thermal histories were also obtained at three locations on the frame of the payload (near the cis-2-butene tank, the photomultiplier tube which measured the resonance fluorescence signal, and the source lamp). These "frame temperatures" are plotted in figure 34 for the ascent phase of the flight and in figure 35 near the time of cut down.

Hydroxyl OH($X^2\pi$) Measurement

One of the purposes of the flight was to evaluate the impact of Rayleigh-scattered solar radiation from the lower atmosphere on the OH measurements. Despite the precautions of a late afternoon launch and the slip in the time of payload cut down, excessive background resulted in a poor signal to noise ratio at altitudes below 39 km. The flight confirmed the suspicion that the instrument was insufficiently baffled and had internal reflectivities too high to discriminate adequately against this source of background. Nevertheless the measured concentration ($2.0 \, ^{+1.5}_{-1.0} \times 10^7$ cm^{-3} at 40 km) of OH is of significant scientific value since this is the first time that the absolute concentration of this species has been measured in the stratosphere at an altitude lower than 45 km.

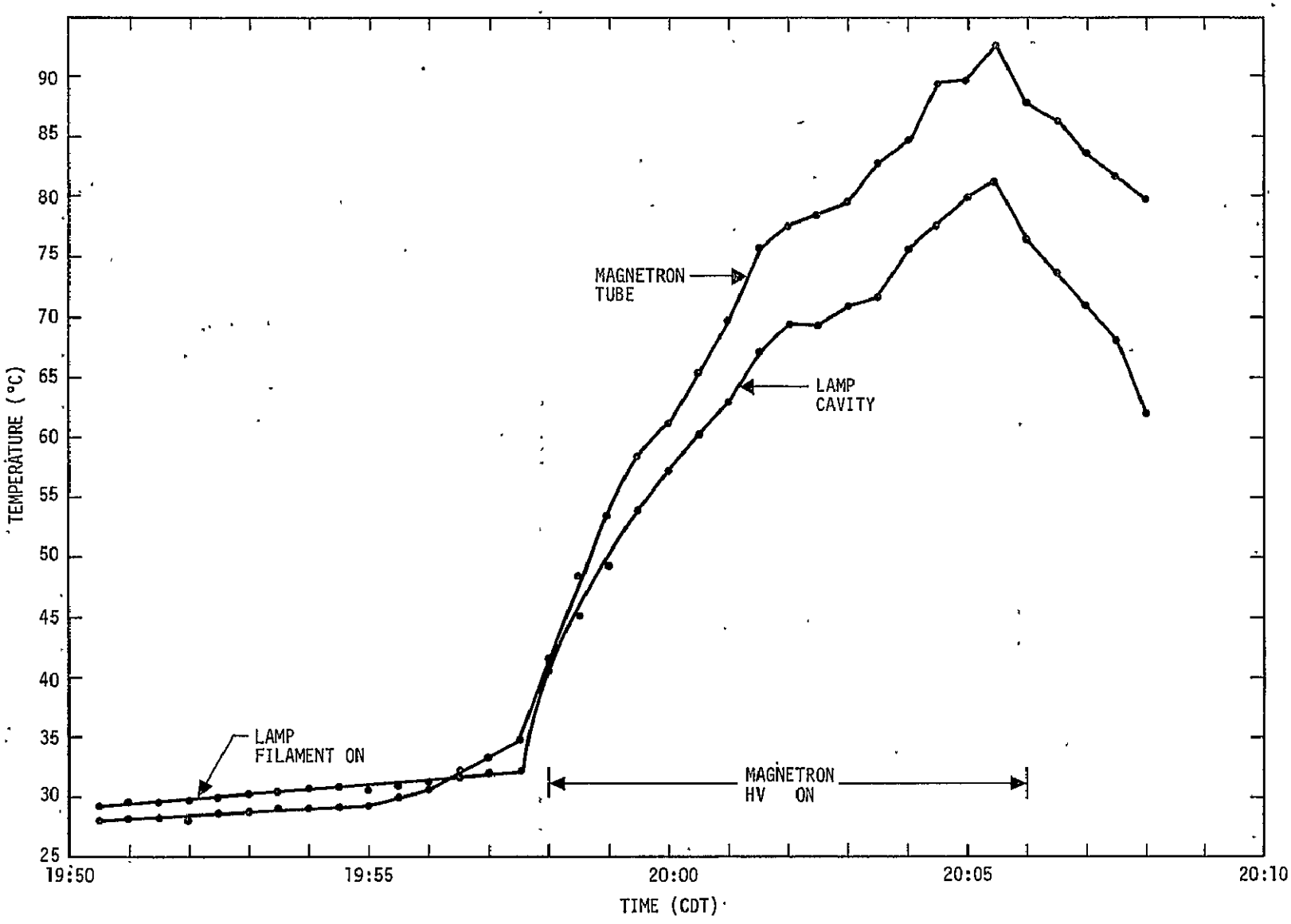

Figure 32.— Thermal history of source lamp cavity and magnetron tube for the first hydroxyl OH($X^2\pi$) flight.

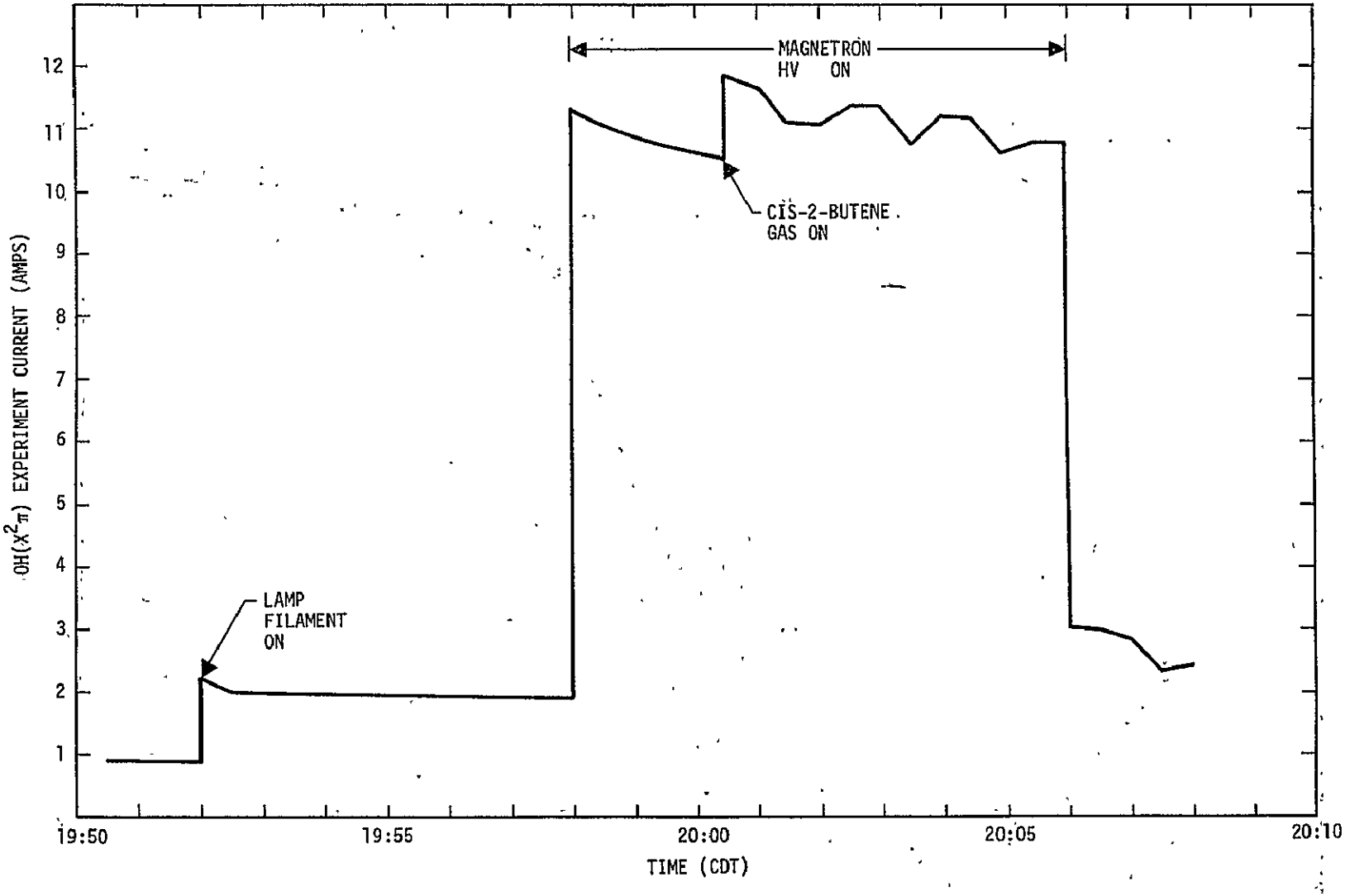

Figure 33.— Resonance fluorescence experiment current levels for the first hydroxyl OH($X^2\pi$) flight.

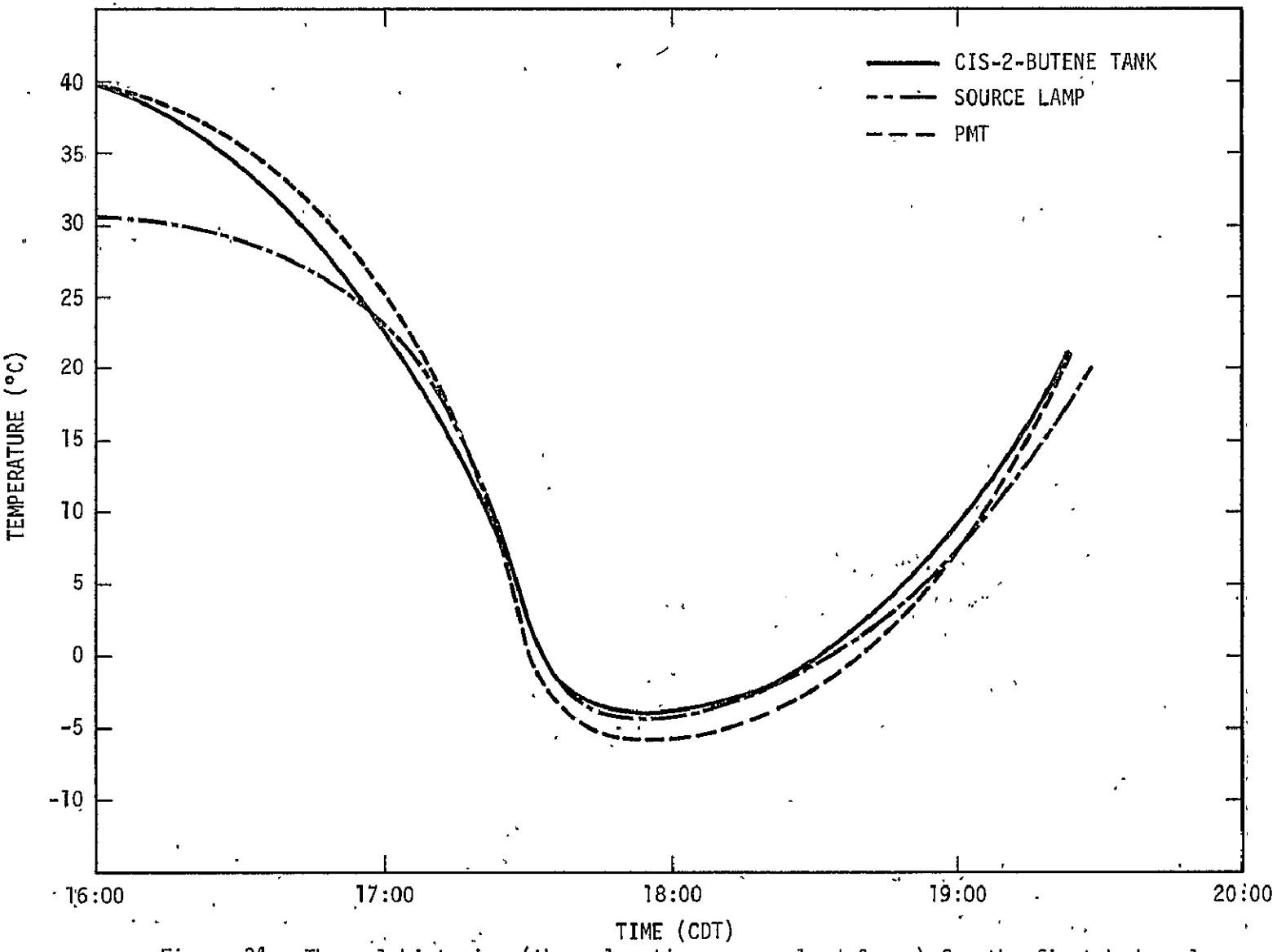

Figure 34.— Thermal histories (three locations on payload frame) for the first hydroxyl $OH(X^2\pi)$ flight during ascent.

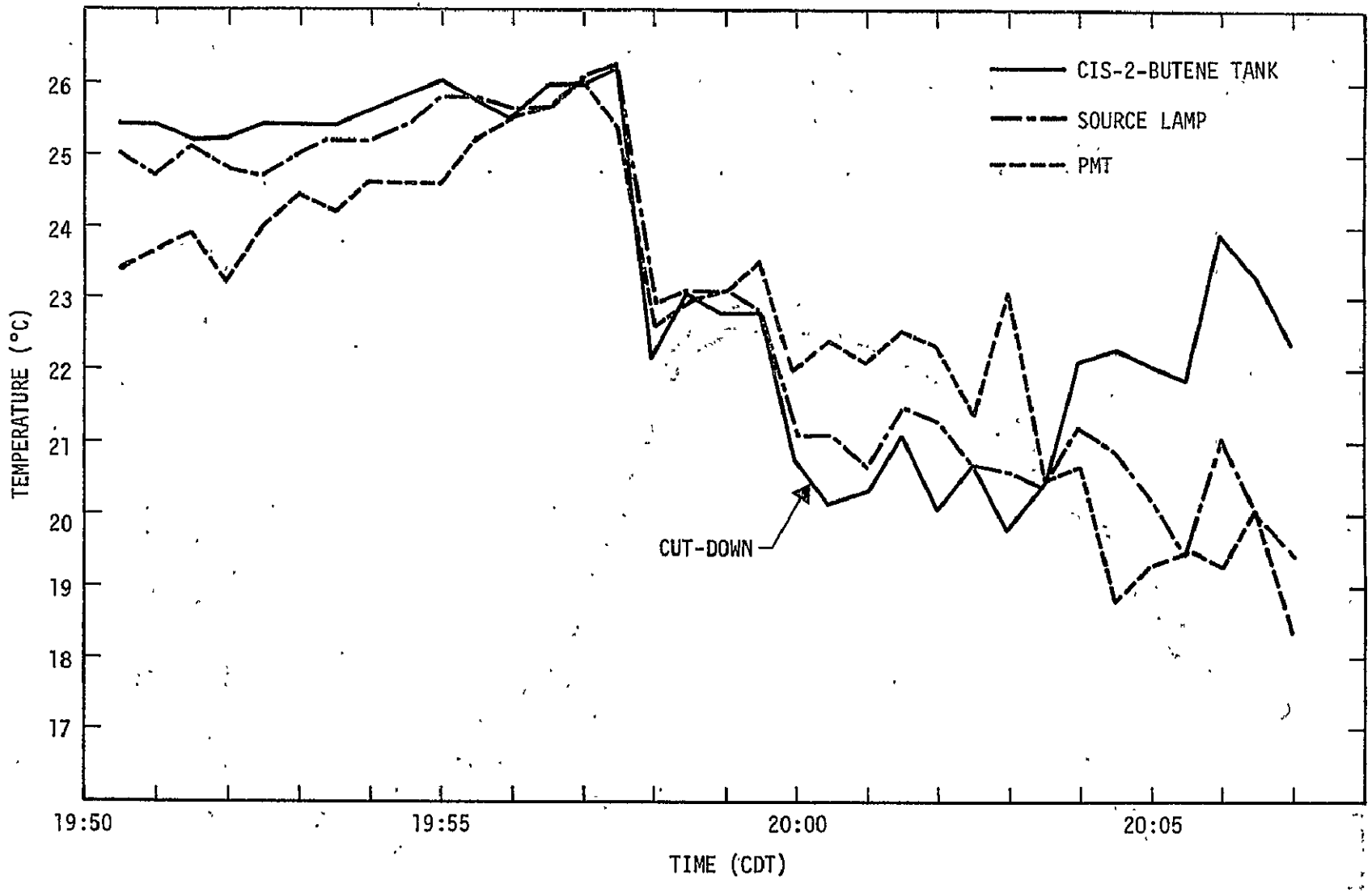

Figure 35.— Thermal histories (three locations on payload frame) for the first hydorxyl OH($X^2\pi$) flight ground time of cut-down.

Ozone Measurement

The first *in situ* measurement of the concentration profile of stratospheric ozone made in conjunction with a resonance fluorescent measurement was accomplished on this flight and a preliminary analysis of the ozone data has been made. Figure 36 shows the ozone concentration measured by the UV absorption ozone monitor as a function of altitude for the ascent phase of the flight. There are four blank regions in the profile. During these periods, ballast was being dropped and the exhaust pump was turned off to avoid contamination of the inlet tube of the monitor. Figure 37 shows the ozone concentration profile for the descent phase of the flight. These data are about 10 percent lower than the ascent data shown in figure 36. The ozone strata (seen as dips at 17, 19 and 22 km) are reproduced in the descent phase.

The only anomalous behavior of the instrument occurred during descent between the altitudes of 27 and 25 km when the monitor gave a series of six readings which were about 30 percent lower than the others of the profile. After these six low readings, the instrument recovered and produced reasonable data for the remainder of the flight. One possible explanation for the malfunction is that the exhaust pump may not have operated properly during this period of time.

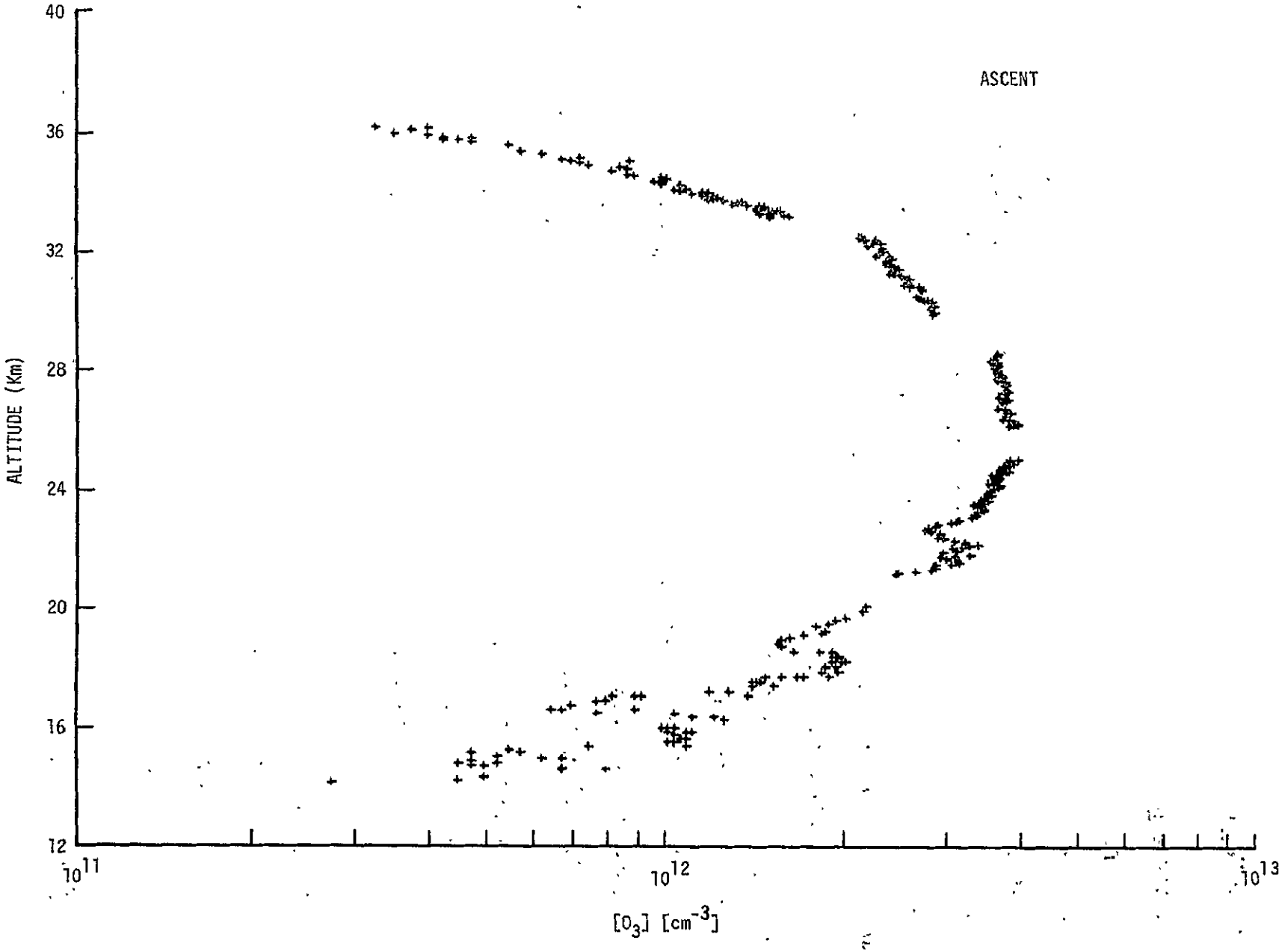

Figure 36. — Concentration of O_3 measured during ascent phase of the first hydroxyl $OH(X^2\pi)$ flight.

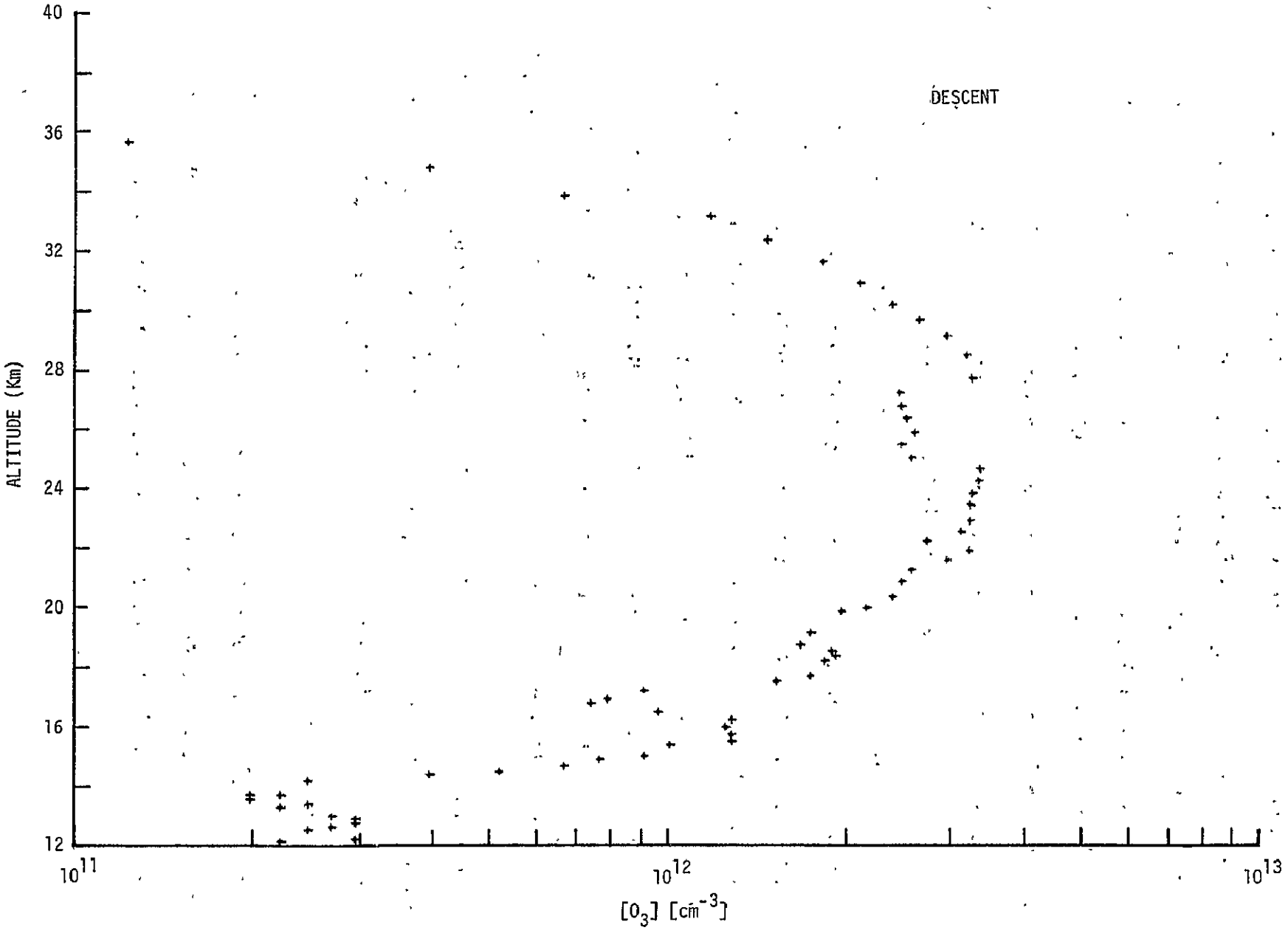

Figure 37. — Concentration of O_3 measured during descent phase of the first hydroxyl $OH(X^2\pi)$ flight.

The preliminary concentration data shown in figures 36 and 37 was obtained using the National Bureau of Standards calibration for the instrument performed in March 1975. In order to arrive at the actual concentrations, a correction must be applied to the preliminary data on both the ascent and descent phases of the flight. Namely, each concentration value must be increased by about 6 percent to account for the difference between the ambient pressure and the pressure inside the absorption chamber. Concentrations above 32 km must be considered invalid due to reduced flow through the chamber at the low ambient pressures which resulted in inadequate flushing before each measurement cycle was made. An additional correction must be made to the descent phase data. This correction involves the change in altitude which occurred between the times when the reference and sample phases of the measurement cycle were being made. This correction will tend to move the high altitude points to higher altitudes and leave the lower altitude data points unchanged.

Figure 38 is a thermal history of the ozone monitor during the flight. No temperature outside of acceptable values occurred, although the power inverter did reach a temperature of 69 degrees C (maximum value of 100 degrees C).

Unfortunately, although considerable effort was expended by WFC and NSBF personnel, no ozonesonde profiles for comparison with the measurements made in situ with the ozone monitor were obtained. The

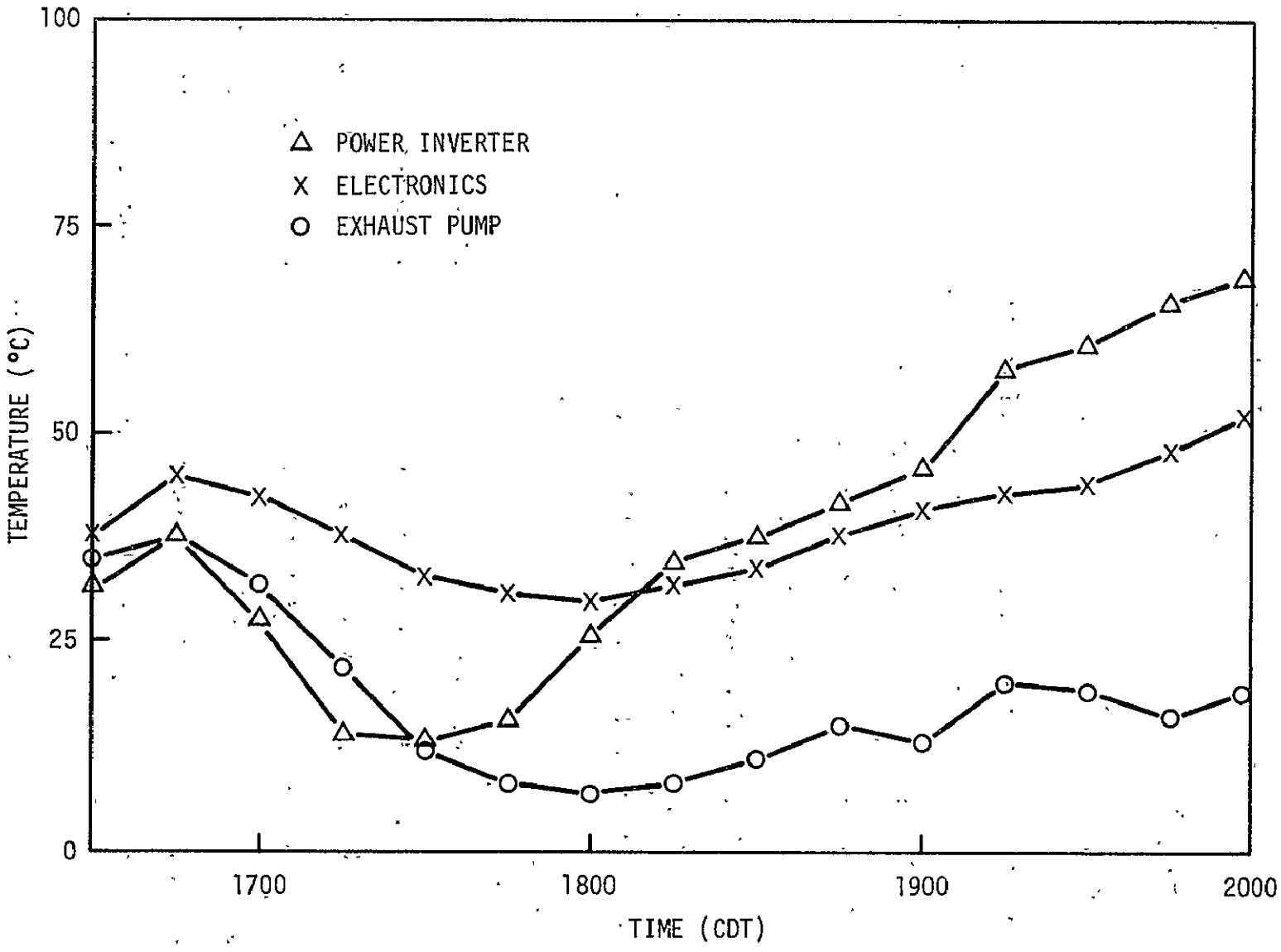

Figure 38.— Thermal history of ozone monitor for the first hydroxyl OH($X^2\pi$) flight.

difficulty was located in the NCAR GMD-1A meteorological ground station which is used to receive the ozonesonde data.

POSTFLIGHT

Landing

The parachute/payload landed 7 nm SSW of Comanche, Texas at 2032:30 CDT. Vertical speed at impact was approximately 7.9 meters/second. The recovery crew reached the landing site at approximately 2130 CDT and powered down the payload. Because of darkness, no attempt was made to retrieve the payload that evening; however, the payload openings were covered to protect against possible rain. Recovery was completed the following morning and the payload was returned to the NSBF on 19 July 1975 for shipment to JSC.

Inspection

Mechanical inspection of the payload revealed a 1-inch inward deflection of the bottom plate of the housing of the ozone monitor and a slight inward deflection of the top plate of the flight support module. These plates are above and below the honeycomb crush pad which was completely flattened at impact. The deflection of the top plate of the support module prevented removal of the JSC battery pack at the recovery site. No other mechanical damage was detected.

CONCLUSIONS

The effect of solar radiation backscattered from the lower atmosphere on the OH concentration measurement was evaluated during the ascent and float phases of the flight. Due to insufficient baffling and high internal reflectivities, useful scientific data were obtained from the resonance fluorescence instrument only between 41 and 39 km since the instrument did not discriminate adequately against this source of background. Nevertheless a concentration measurement was made and is of significant scientific value since it was the first time that this species had been detected at an altitude lower than 45 km in the upper stratosphere. The flight demonstrated the necessity of redesigning the baffling and reducing internal reflections to improve the signal to noise ratio on subsequent flights.

Good quality data on the concentration of ozone was obtained using the ultraviolet absorption ozone monitor during ascent and descent phases of the flight below 32 km. The flush time (approximately 2.2 seconds) was adequate to completely flush the chamber at altitudes up to 32 km. An increase in flush time will be required on subsequent flights to accomplish ozone measurements at higher altitudes. A differential pressure transducer will be installed for future flights in order to monitor the flow of gas through the system and detect any malfunction of the exhaust pump which may have given rise to the six low readings which occurred during descent.

SECOND HYDROXYL OH($X^2\pi$) MEASUREMENT

(NCAR FLIGHT NO. 934-P)

19 October 1975

SUMMARY

This balloon-parachute flight was the fourth flight of the laminar flow through/resonance fluorescence instrument (principal investigator: Dr. James Anderson, University of Michigan) and took place on 19 October 1975. The purposes of the flight were to measure the vertical concentration profiles of the hydroxyl radical (OH) and ozone (O_3) and to again evaluate the impact of Rayleigh-scattered solar radiation on the OH measurements. An ancillary experiment was flown as part of the payload to perform counting measurements (as a function of altitude) of stratospheric aerosols. This experiment was designed to count particles containing surface-ionizable constituents and would determine the signal levels required for the design of more advanced flight instruments.

The flight was launched at 1343:11 CDT from the NSBF at Palestine, Texas. Launch was scheduled to occur at 1400 CDT. The decision to launch early was based on the potential for launch area ground winds to increase and had no impact on the scientific experiment. The mid-afternoon launch was required to minimize background noise (originating from solar radiation scattered from the lower atmosphere) while retaining a nominal OH density profile. Hardware consisted of a 4.3×10^5 cubic meter balloon, 9.75-meter diameter guide surface parachute, NCAR telemetry system, JSC flight support module, the resonance fluorescence instrument (of modified design) tuned to the (0-0) band of the $A^2\Sigma$-$X^2\pi$ electronic transition of OH (bandhead at 306.4 nm), an ozone monitor on loan from GSFC for *in situ* measurement of ozone using the ultraviolet (UV) absorption method, and an aerosol particle counter to monitor the presence of particles larger and/or richer in surface ionizable constituents than a pre-set discrimination level. The University

of Pittsburgh, under the sponsorship of Langley Research Center, was responsible for the aerosol particle counter instrumentation and for reduction and analysis of the aerosol data.

Good data on the concentration of ozone were obtained during the ascent phase of the flight from 14 km (47 k ft) to 36 km (118 k ft). The payload reached a float altitude of 41.7 km (137 k ft) at approximately 1600 CDT. The background count rate for the resonance fluorescence instrument was monitored during the ascent and float phases of the flight by operating the experiment with the source lamp OFF. The aerosol experiment was operated at float altitude for about 30 minutes before cut-down.

The payload was released from the balloon at 1800:20.5 CDT to begin the OH data gathering phase of the mission. However, both NCAR and JSC (Houston) ground stations received a severely degraded telemetry signal within 700 milliseconds of the time of payload release. Good telemetry data was acquired 89 seconds later by retuning the NCAR receiver to a backup telemetry transmitter frequency and good data were obtained for approximately 4.5 minutes until the payload disappeared over the horizon, terminating all communications. This brief loss of telemetered data occurred at the most critical portion of the flight. As a consequence, the primary objective of this balloon-parachute flight (to measure the vertical concentration profile of hydroxyl) was not met. However, an evaluation of the instrumental background as a function of varying solar zenith angle could be obtained during the two hours at float altitude. Also the altitude depencence of instrumental background could be determined during that

portion of the descent for which data was secured (from 32 to about 19.8 km). Data from the UV absorption instrument and from the aerosol instrument was also received in this altitude range.

The parachute/payload landed in soft dry soil approximately 150 yards from the Mississippi River, 5 nm SW of Vicksburg, Mississippi, at 1834 CDT and was recovered the following day in good condition.

An Independent Anomaly Review Board determined that the most probable cause for the severe drop in telemetry signal strength was failure of the center conductor socket in the coaxial connector on the primary NCAR telemetry antenna.

INTRODUCTION

The primary objective of this balloon-parachute flight was to extend the altitude range of the hydroxyl concentration measurement made on the previous flight and to improve the signal to noise ratio of the measurement by using a resonance fluorescence instrument of modified design. The modified instrument was expected to improve the rejection of Rayleigh-scattered radiation from the lower atmosphere as a result of changes in the baffling and reduction of internal surface reflectivities. As in the previous flight, the payload was instrumented to measure the concentration level of O_3 and OH concurrently. An ancillary experiment to perform counting measurements of stratospheric aerosols was flown for the first time on this flight.

Payload

The payload weighed approximately 263 kg, and consisted of telemetry, balloon control, descent-observation, and scientific instrumentation. A sketch of the payload and flight configuration is shown in figure 39.

Instrumentation

Instrumentation carried as part of the payload included NCAR and JSC telemetry instrumentation, NCAR balloon control instrumentation, NCAR and JSC pressure transducers to measure the altitude of the payload, two vertical reference gyros to measure payload attitude, a z-axis accelerometer to determine the loading forces when the parachute is deployed, a single

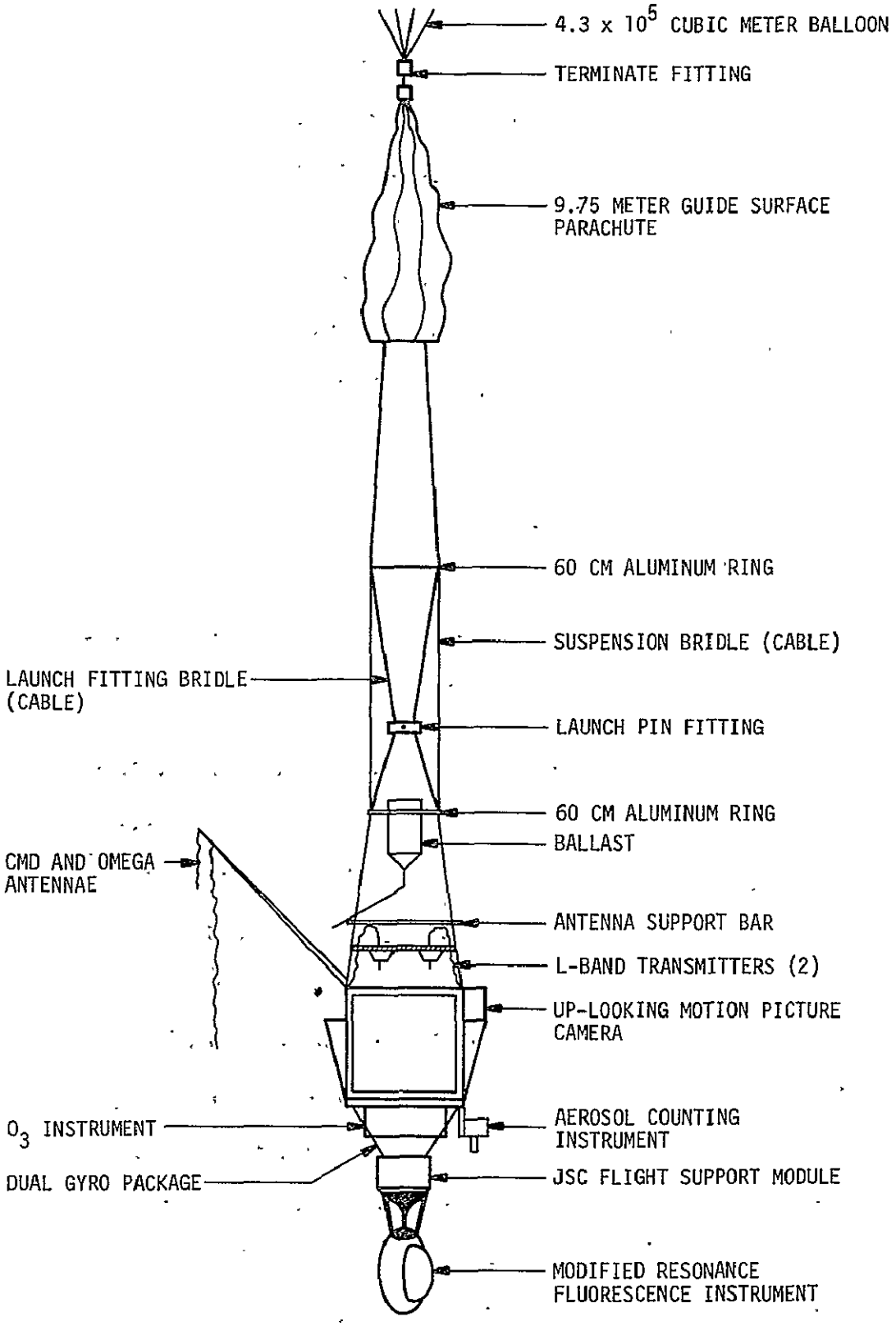

Figure 39.— Flight configuration for the second hydroxyl OH($X^2\pi$) measurement.

up-looking motion picture camera (64 frames/sec using a 10 mm lens) to observe parachute opening and descent characteristics, an ozone monitor (on loan from GSFC) to measure in situ the concentration of stratospheric ozone, an aerosol particle counter to monitor the presence of particulates, and the laminar flow through/resonance fluorescence instrument to measure the concentration of the hydroxyl radical. Ozone reference instrumentation consisted of four potassium iodide ozonesondes.

Function, manufacturer, model, and serial numbers for support instrumentation are itemized in Appendix A. Pertinent electrical and mechanical drawings are listed in Appendix B. A description of the telemetry systems and channel allocations is given in Appendix C. Photographic documentation for the flight is itemized in Appendix D.

The major scientific instrument flown on this flight was a modified version of the resonance fluorescence instrument developed by Dr. James Anderson of the University of Michigan tuned to the (0-0) band of the $A^2\Sigma$-$X^2\pi$ electronic transition of the OH radical (bandhead at 306.4 nm, peak intensity at 309.0 nm). As demonstrated on the previous flight, inadequate baffling and excessively high reflectivities of the internal surfaces of the instrument resulted in a background count rate which was too high to allow the accurate measurement of the concentration of hydroxyl at altitudes below 40 km. Modifications to the geometry of the instrument are shown in figures 40 and 41 (schematic representations of the resonance fluorescence instrument along a plane containing the flow axis and along a plane perpendicular to the flow axis, respectively). In order to improve the

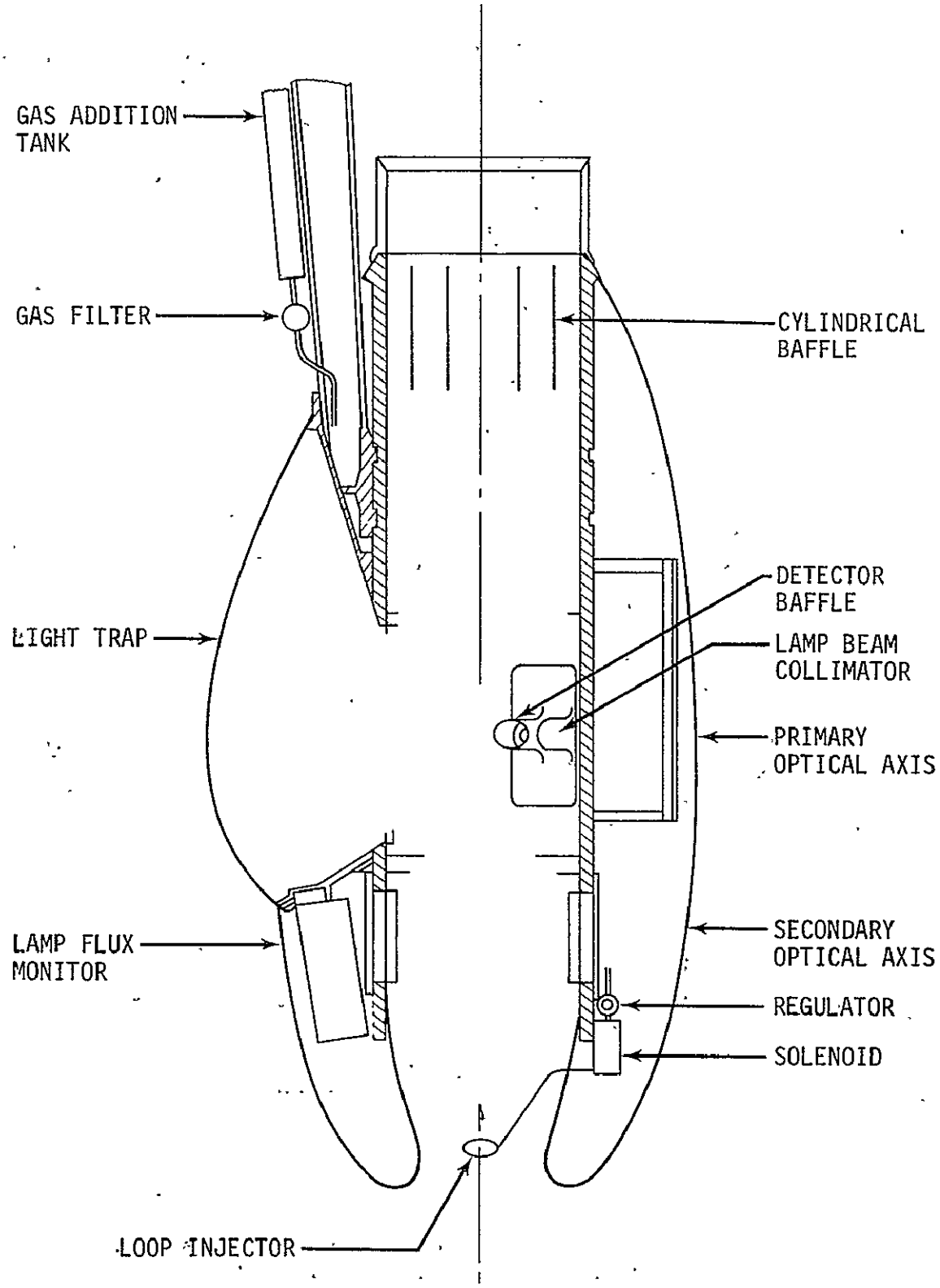

Figure 40.— Modified resonance fluorescence instrument (schematic along a plane containing flow axis).

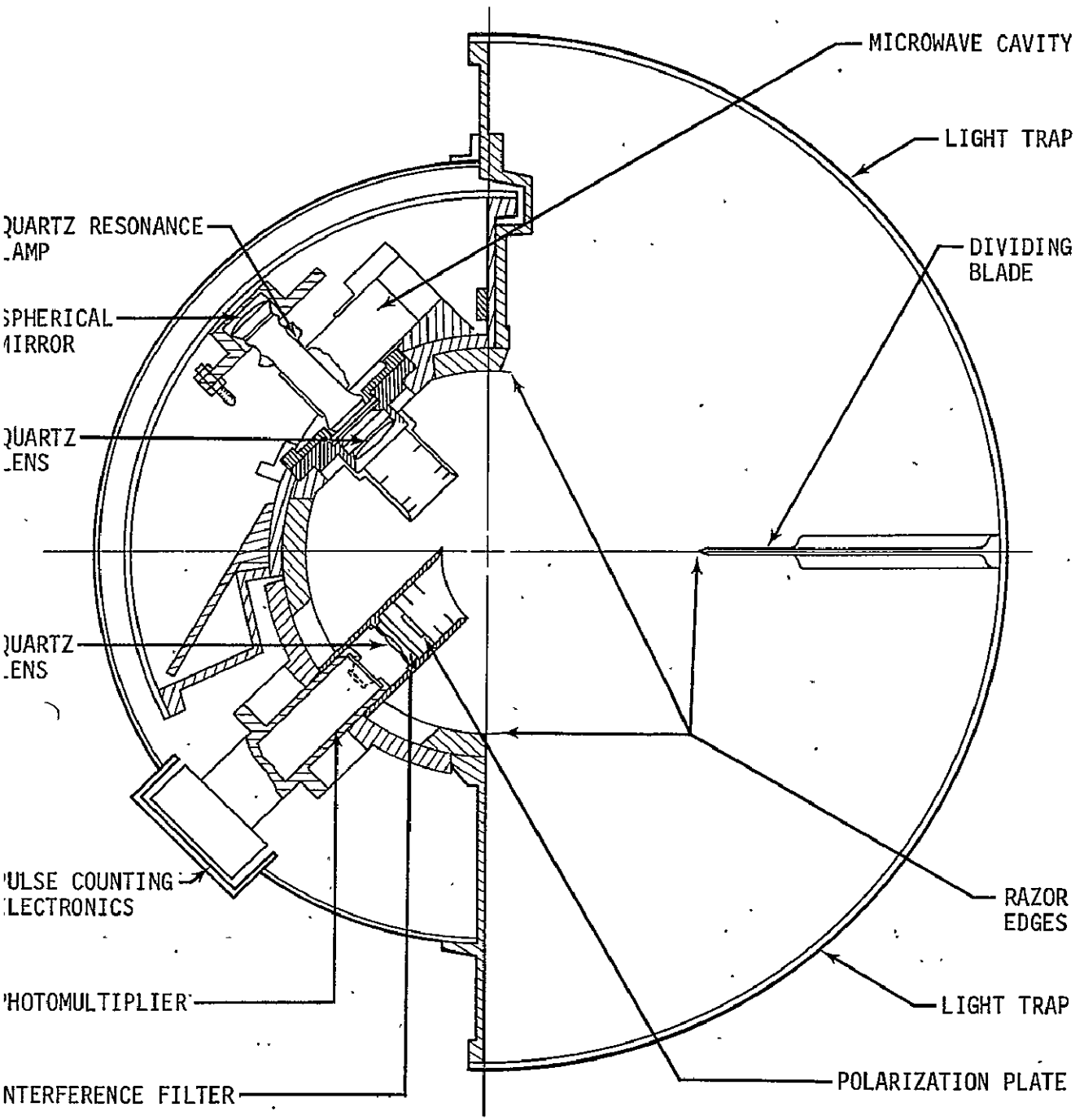

Figure 41.— Modified resonance fluorescence instrument (schematic along a plane perpendicular to flow axis).

isolation of the fluorescence chamber from the direct rays of the sun, the trailing end of the flow tube was extended approximately 10 cm. In addition, the airflow deflection plate (shown in fig. 12 for the previous configuration) and the inward facing surfaces of the three struts which support the detection nacelle were black anodized by a special process (Martin Marietta black) to minimize surface reflectivities. Rayleigh scattered photons, backscattered by the lower atmosphere, were eliminated by using a convex airfoil at the leading edge of the flow tube in conjunction with a razor edge in front of the fluorescence chamber. This configuration forms an effective light trap between the leading edge of the instrument and the optical axis and does not sacrifice in any significant way the unperturbed flow of stratospheric gas through the instrument. The detector light trap was enlarged and baffled in such a way that photons are captured whether they enter the trap in the plane of the optical axis or perpendicular to the optical axis. Thus, not only stray photons from the lamp but also photons which may have entered the fluorescence chamber from the leading or trailing edge of the flow tube are eliminated. All internal surfaces of the instrument were Martin Marietta black anodized to minimize internal reflections.

Due to the difficulty of maintaining tank pressure to provide an adequate flow of cis-2-butene gas, HCl gas was used to determine the background count rate. Like cis-2-butene, HCl reacts rapidly with OH to chemically eliminate it from the flow, yet it does not react with any other known atom or radical to produce OH within the time scale of the conversion.

Two changes in the ultraviolet absorption ozone monitor were made on this flight. The flush time of the absorption chamber was increased to 3.2 seconds to allow accurate ozone measurements up to 36 km. Also a differential pressure transducer was installed in order to monitor the flow of gas through the system and to detect any malfunction which might occur in the exhaust pump.

A surface ionization particle detector was flown for the first time on this flight to measure the presence of stratospheric aerosols. The detector operates by allowing a particle to strike a heated (about 1200 degrees C) metal surface where it decomposes and transfers a portion of its atomic and molecular constituents to the hot surface. Those atoms and molecules with ionization potentials comparable to, or less than the work function of the surface, are surface-ionized and boil off as a burst of positive ions, with a pulse duration of 10 to 50 microseconds. Both the detection of individual pulses and the total dc ion current, as a function of time, make up the information received. The former indicates the arrival of particles sufficiently large or sufficiently rich in surface ionizable constituents to trigger the pre-set pulse height discriminator, and the latter indicates total surface-ionizable species contributed by particles too small to produce counts above the pre-set pulse height discrimination level and surface-ionizable vapors. Surface ionization detectors using platinum filaments, as did the flight package, do not respond to water, sulfuric acid, or other aerosols without surface ionizable constituents. Platinum is an efficient surface ionizer for

the alkali metals. Thus the instrument was expected to detect mostly particles originating from sea spray or soil weathering. A schematic diagram of the aerosol particle counter is illustrated in figure 42.

As shown in figure 39, the aerosol instrument was mounted above and to one side of the resonance fluorescent instrument and at the same height as the ozone monitor. The hot filament and an adjacent ion collection electrode were mounted outside of a vacuum tight box, which held the power supplies and measurement circuitry, and in a vertical hollow tube through which stratospheric gas flowed during descent. Because of both the change of pressure and the change in payload velocity during descent, the impaction efficiency varies with altitude and corrections to the raw data are required. At high altitude, particles of all sizes impact with high efficiency; but at lower altitudes, lighter particles are carried around the hot wire detector by the air stream.

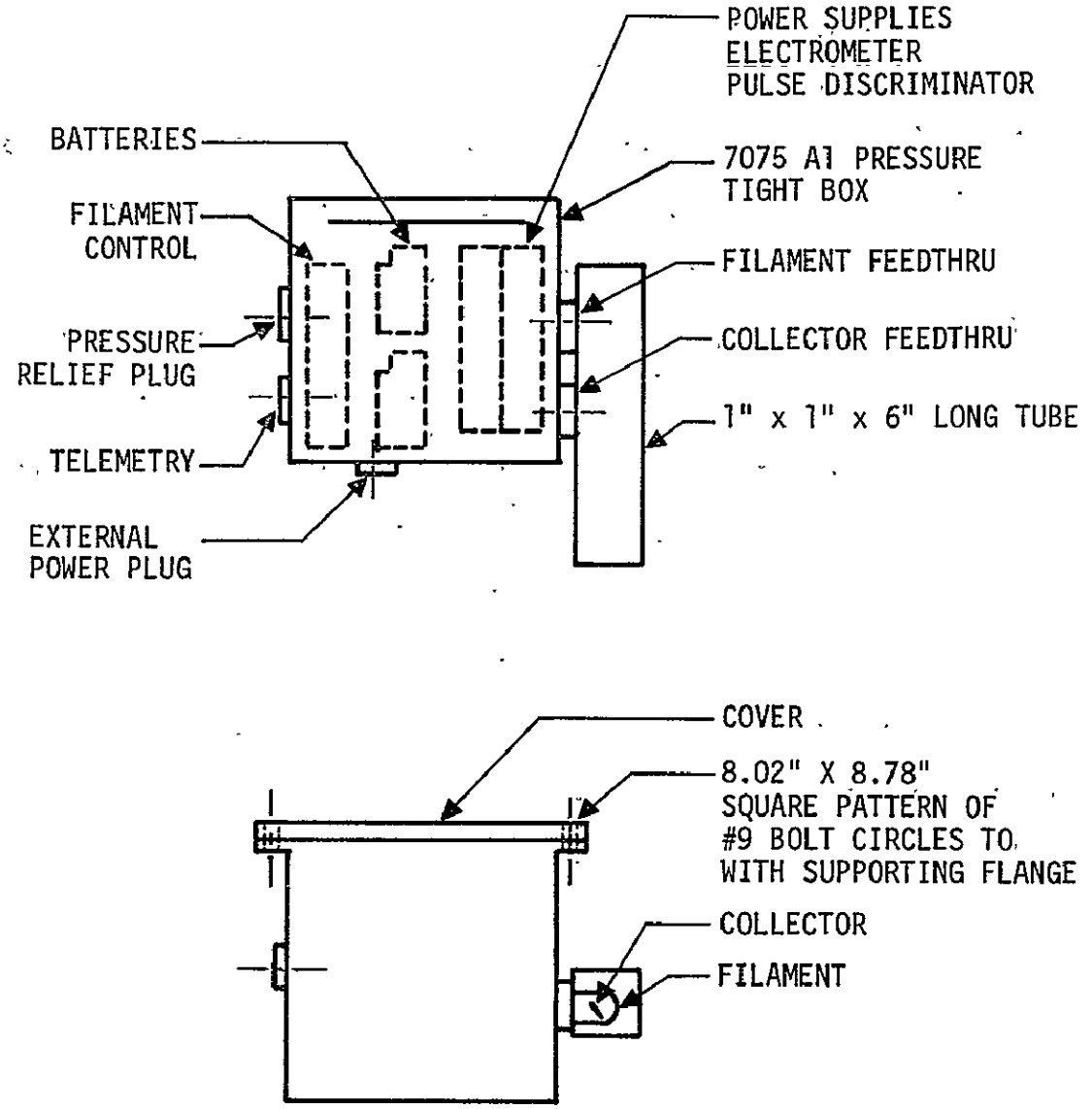

Figure 42.— Schematic diagram of the aerosol particle counter (2 views).

PAYLOAD OPERATIONS

Ascent and Float Phases

The flight profile for the Second Hydroxyl OH($X^2\pi$) Flight is illustrated in figure 43. Launch occurred at 1343:11 CDT, 19 October 1975, and was accomplished using the dynamic launch technique. The balloon system ascended at an average rate of 5.2 meters per second to a float altitude of 41.7 km. The UV absorption ozone instrument was operated during ascent and the background count rate for the resonance fluorescence instrument was monitored during the ascent and float phases of the flight by operating the experiment with the source lamp OFF. The aerosol experiment was operated at float altitude for about 30 minutes before cut-down. Thermal histories for the ozone monitor, battery and transmitter during the ascent and a portion of the float phases of the flight are given in figure 44.

Three options for the time of cut-down had been anticipated in the flight plan (1720, 1740, and 1800 CDT). The choice was to be made one hour prior to cut-down by the Science Principal Investigator depending on the background count rate from the resonance fluorescence instrument and/or the expected payload position. The 1800 CDT cut-down option was selected on the basis of Omega tracking system data (which, it turned out, to be erroneously indicating a position about 40 nm closer to the NSBF than actually was the case). While the Omega tracking system is considered the most satisfactory method for use on this payload, a procedural error occurred while plotting payload positions causing the Omega plots to be invalid. Omega tracking data was not in agreement with radar tracking

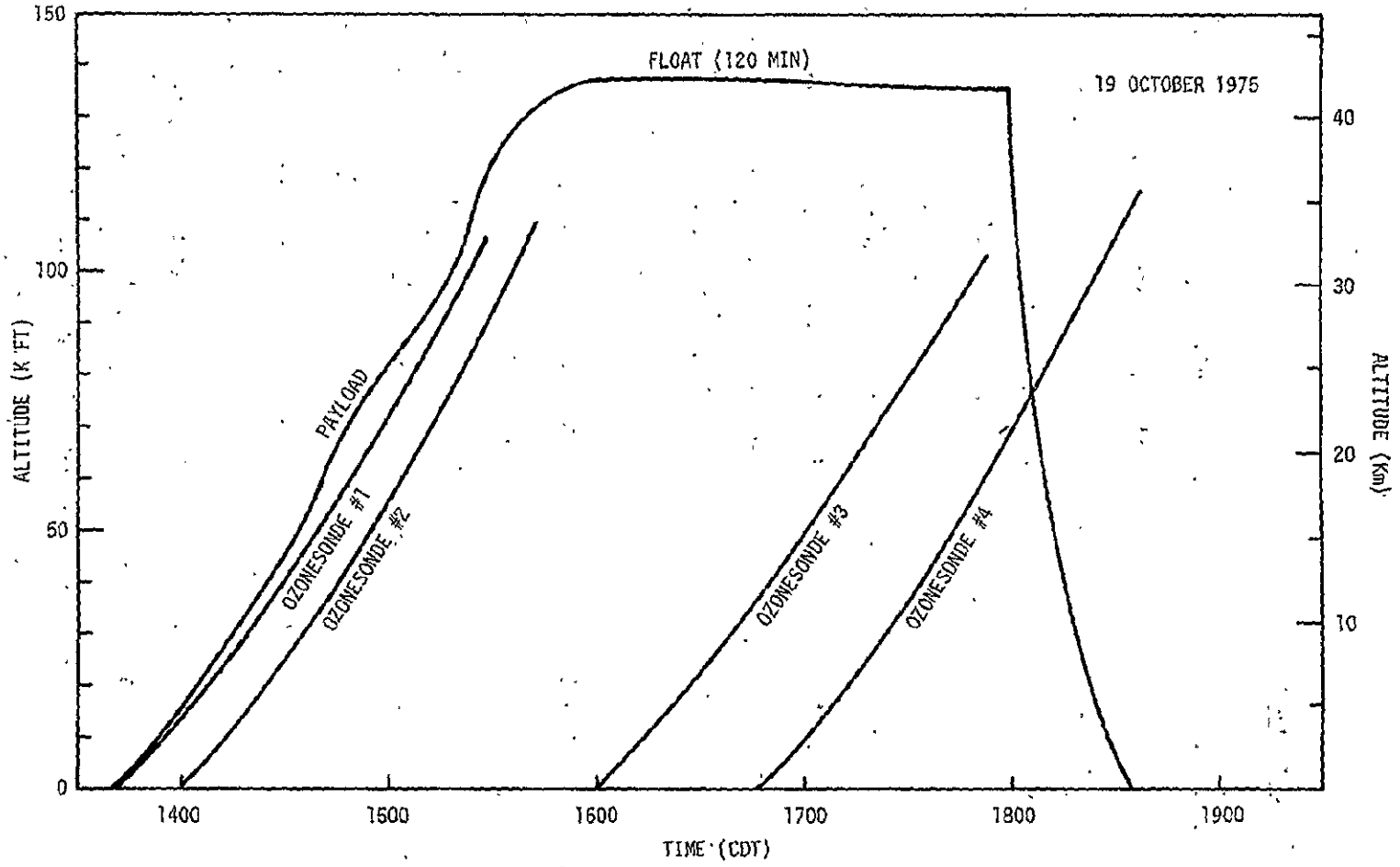

Figure 43.— Flight profile for second hydroxyl OH($X^2\pi$) flight.

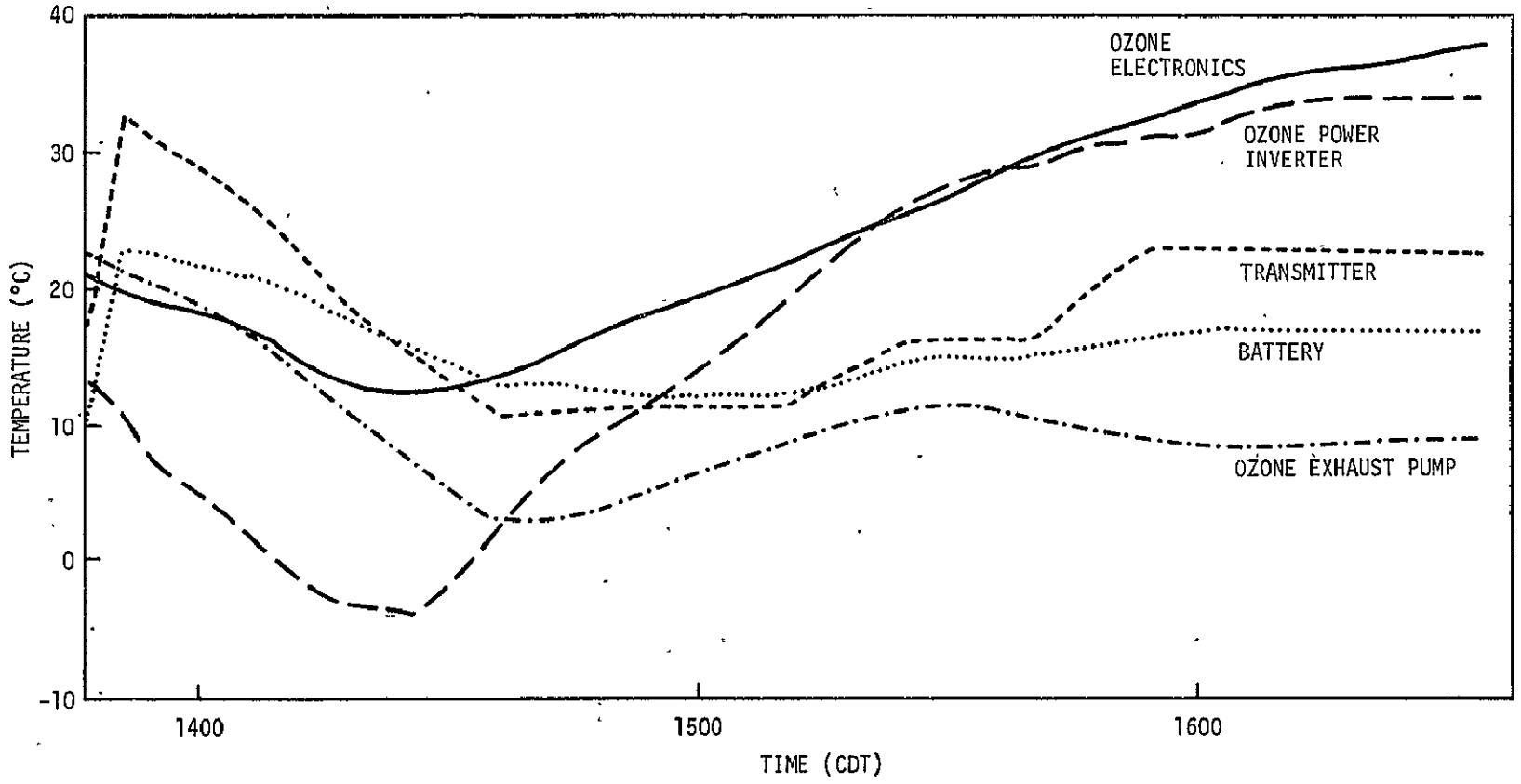

Figure 44.— Thermal histories during ascent phase of the second hydroxyl OH($X^2\pi$) flight.

data when NCAR lost radar contact with the payload at 1533 CDT (loss of radar contact was expected due to the payload range). This discrepancy was not brought to the attention of the science team. If the position information had been correct, an earlier parachute release time option would have been selected.

At 1758 CDT the "Magnetron HI voltage ON" command was sent by the tracking aircraft but was not confirmed by the payload scientist. An immediate backup command was initiated by the NCAR tower and again was not confirmed. After the unsuccessful attempts to start the magnetron lamp driver, the Principal Investigator for the resonance fluorescence instrument advised JSC operating personnel of contingency procedure commands which were sent and the magnetron lamp driver system functioned correctly at 1759:43 CDT (17 seconds before the aircraft command operator was scheduled to transmit the payload release command).

Descent Phase

The time of transmission of the payload release command was 20.5 seconds late so that the actual drop time was 1800:20.5 CDT. Both NCAR and JSC (Houston) ground stations received a severely degraded telemetry signal from the prime RF link (NCAR L-Band transmitter operating at 1483.5 MHz) within 700 milliseconds of the time of payload release. Attempts to reacquire the telemetry signal by pointing the antenna dish down met with no success. Good telemetry data was acquired 89 seconds later (at about 1801:49 CDT when the payload had reached an altitude of 32 km) by retuning the NCAR receiver to a backup telemetry transmitter frequency (JSC L-Band

transmitter operating at 1491.5 MHz) and good data were obtained for approximately 4.5 minutes with only a few minor drop-outs until the payload disappeared over the horizon, terminating all communications. Receivers at JSC (Houston) were not retuned to the backup telemetry transmitter frequency until about 8 minutes after payload release. Good telemetry signal levels on the primary frequency were not obtained at JSC during that time.

An onboard motion picture camera observed parachute deployment and showed a more violent callapse of the rigging at payload release than on previous flights. The films also showed that the parachute was cross rigged and/or wrapped. Altitude, attitude, and accelerometer data were lost due to the telemetry failure until about 89 seconds after payload release. The altitude data which exists are shown in figure 45. The payload attitude was monitored by two vertical reference gyros. Figure 46 shows the probability that the angular deviation of the payload from vertical is less than a given angle as a function of angle. This data pertains only to that portion of the drop for which data was received and cannot be considered as representative of the flight as a whole.

The brief loss of telemetered data occurred at the most critical portion of the flight. As a consequence, the primary objective of this balloon/parachute flight (to measure the vertical concentration profile of $OH(X^2\pi)$ in the altitude range from about 30 to 40 km) was not met. The sensitivity of the resonance fluorescence instrument is not sufficient to measure the concentration of hydroxyl below 32 km without the initial drop data, but an evaluation of the instrumental background could be obtained below

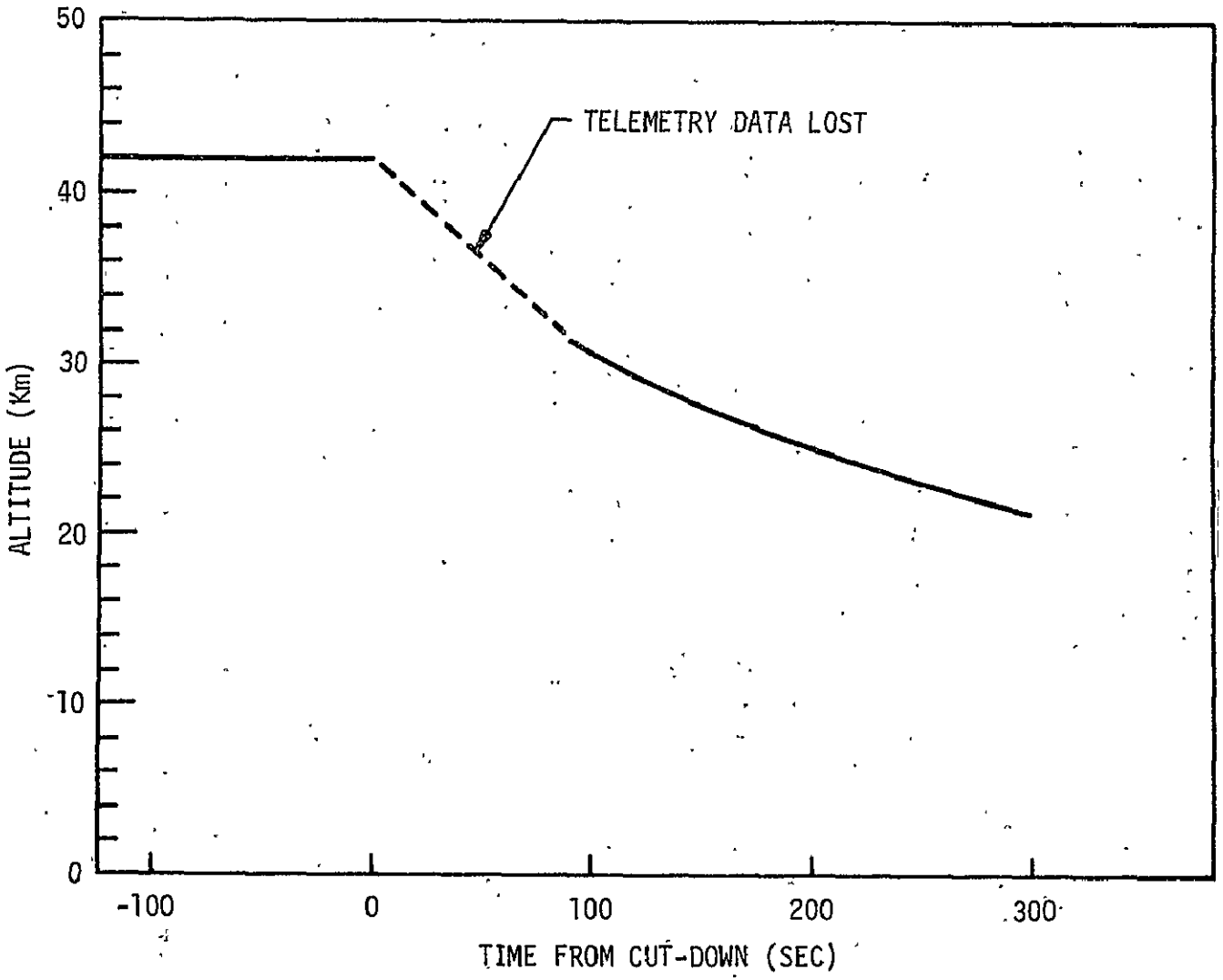

Figure 45.— Altitude/time profile of descending payload for the second hydroxyl OH($X^2\pi$) flight.

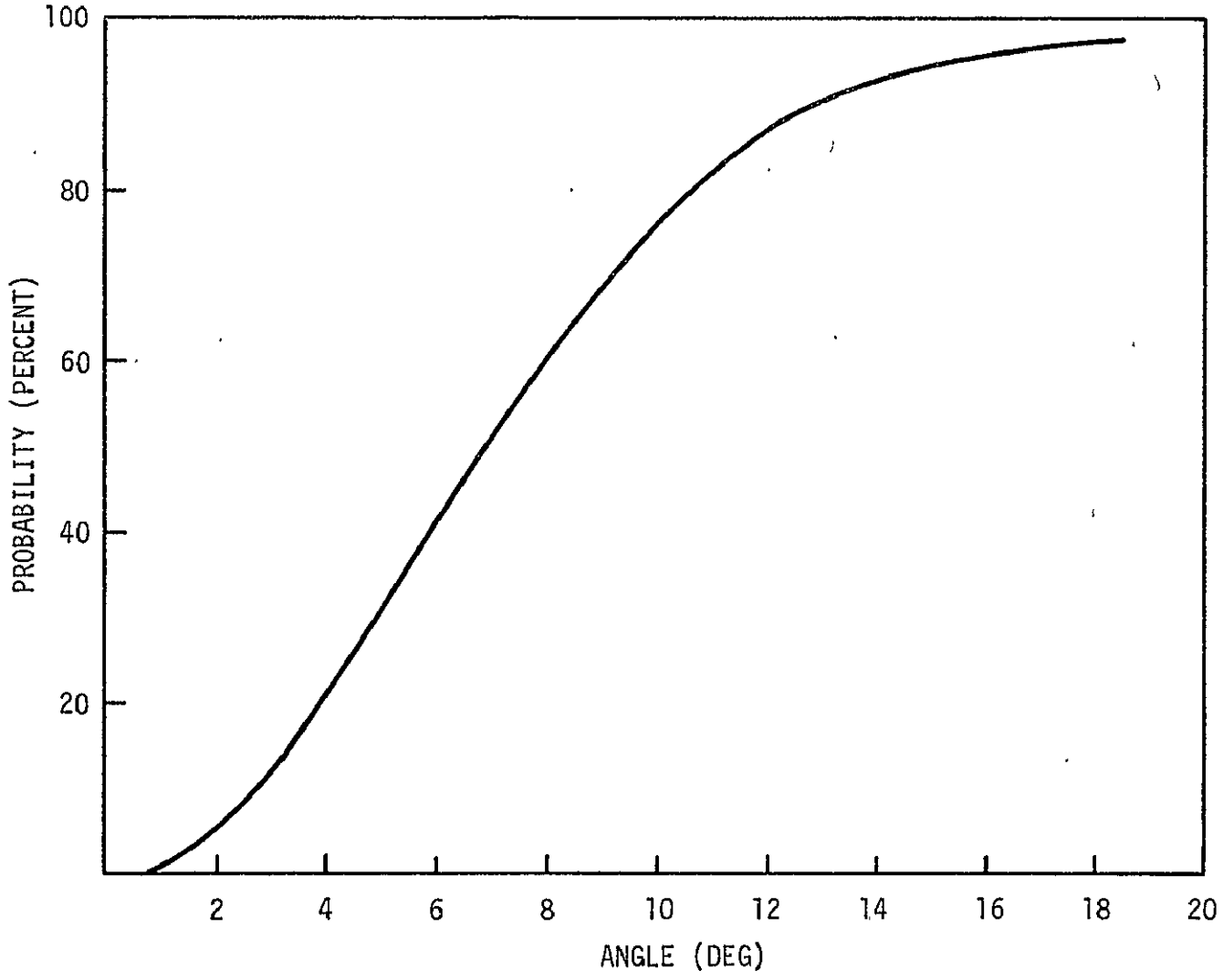

Figure 46.— Probability (percent) that the angular deviation of the payload from vertical is less than a given angle as a function of angle for the second hydroxyl CH($X^2\pi$) flight.

this altitude. The ozone monitor produced an ozone profile during that part of the descent phase for which data was obtained (from 32 to 19.8 km). Data was also obtained from the aerosol instrument in this altitude range.

DATA RESULTS

Aerosol Measurement

Data from the aerosol particle counter was received in the altitude range between 32 and 19.8 km. An emergency repair prior to launch rendered the pulse-counting circuit inoperative, so that only dc ion current information was obtained. The raw data is shown in figure 47. In the altitude range from 25 to 32 km, the signal is typical of background current resulting from surface ionizable impurities within the platinum filament, while a maximum occurs at about 22.5 km. As shown in the following section, this feature was not observed in the second flight of this prototype instrument (see fig. 65) and its reality must be viewed with caution. It is possible that the maximum was due to inadequate regulation of the filament temperature.

Ozone Measurement

The concentration profile of stratospheric ozone was measured with the ozone monitor on loan from Dr. E. Hilsenrath of GSFC. This was the second flight of this instrument in conjunction with the resonance fluorescence payload. The data which it produced was complemented by four successful ozone radiosonde flights which provided ozone reference data (taken according to accepted precepts) such that a comparison of the two techniques could be made. Figure 48 shows the ozone concentration measured by the UV absorption ozone monitor as a function of altitude for the ascent phase of the flight. The high altitude concentration does not fall off as rapidly in this profile as in the profile taken during the previous flight (see fig. 36). This is probably the result of increasing the flush time

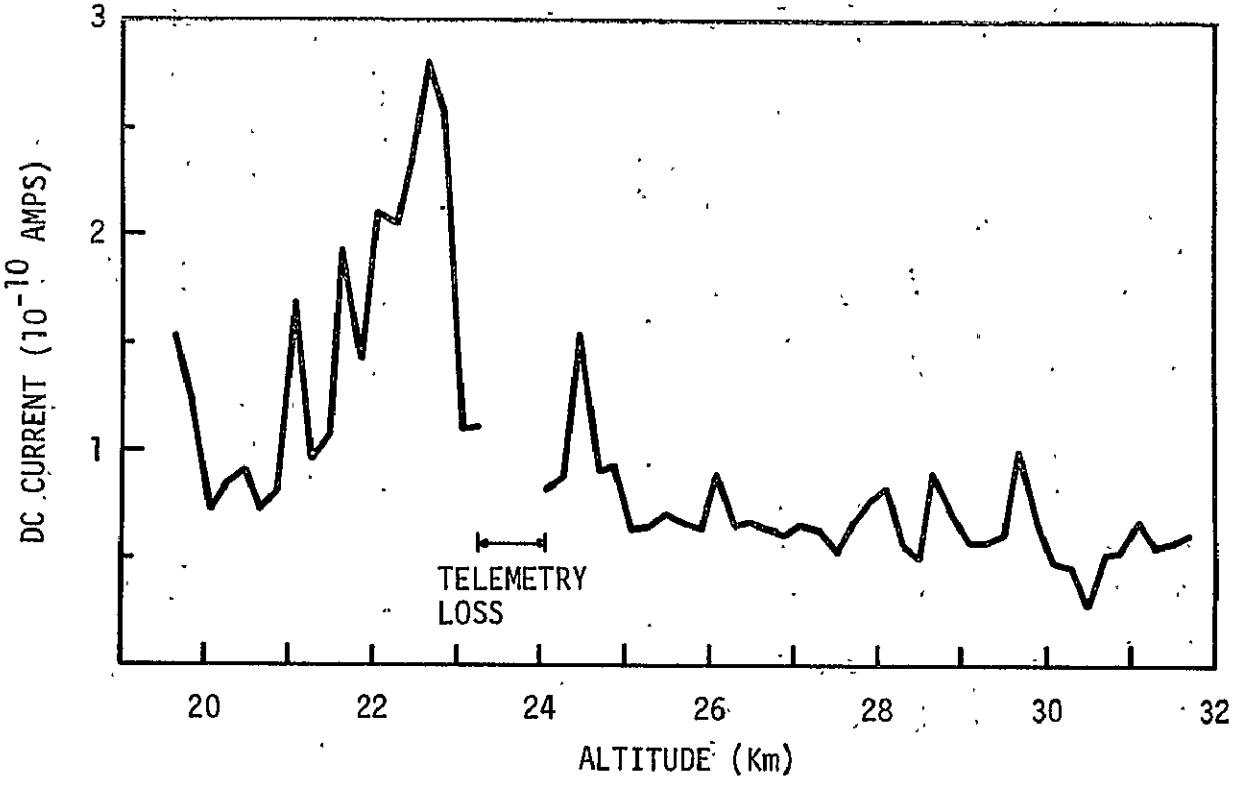

Figure 47.— DC ion current measured by the aerosol particle counter experiment during the second hydroxyl OH($X^2\pi$) flight.

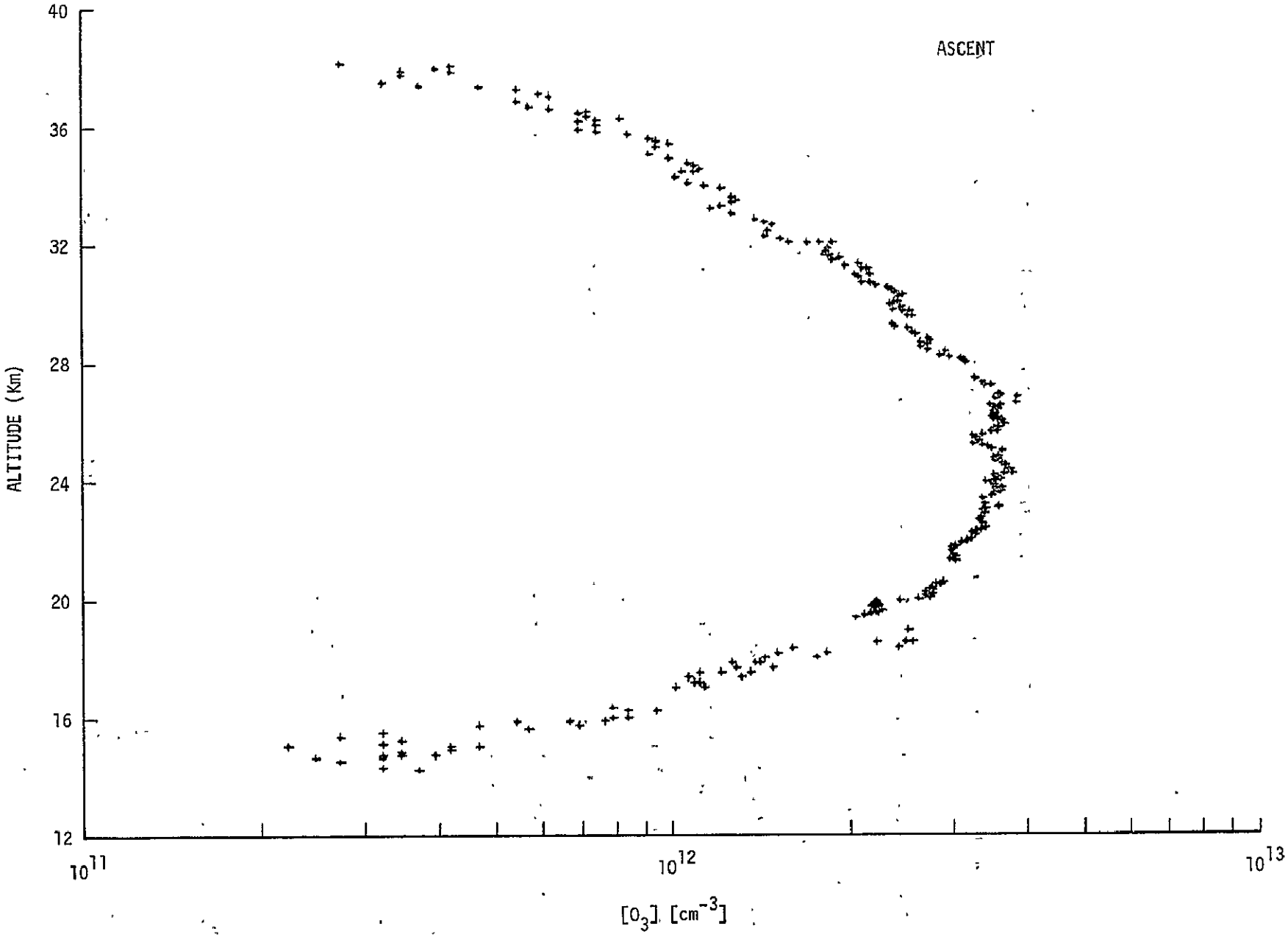

Figure 48.— Concentration of O_3 measured during ascent phase of the second Hydroxyl $OH(X^2\pi)$ flight.

from 2.2 to 3.2 seconds to provide good data up to an altitude of 36 km (data above this altitude cannot be considered valid). The ozone concentration profile measured during the descent phase of the flight is shown in figure 49. Data was obtained during descent from 32 km (the altitude of the payload when communications were reestablished) until 19.8 km when the payload dipped below the horizon.

The data taken on descent are about 30 percent lower overall than the data taken on ascent but were becoming comparable when line of sight communications were lost at lower altitude. The differential pressure transducer detected a small (5-10%) decrease in the flow of stratospheric gas through the system during descent but this is insufficient to account for the low readings.

A series of four ozonesonde launches were made in conjunction with this flight. Time of launch and termination and maximum altitude attained are given in Table II.

TABLE II

Radiosondes Launched in Conjunction with Second Hydroxyl OH($X^2\pi$) Flight

Sonde Number	Time of Launch (CDT)	Time of Terminate (CDT)	Maximum Altitude (km)
1	1342	1528	32.50
2	1400	1543	33.50
3	1600	1753	31.50
4	1647	1838	35.25

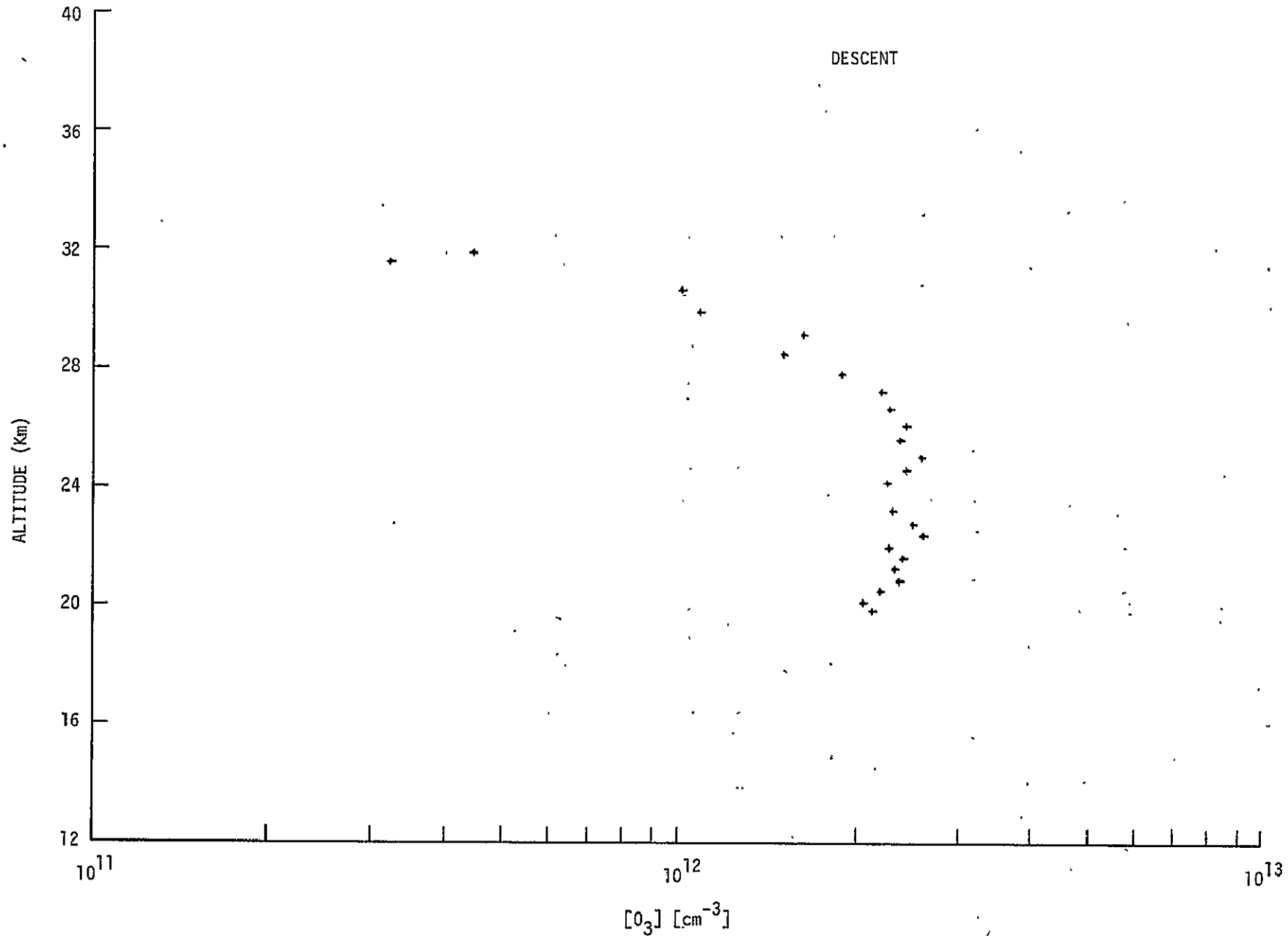

Figure 49.— Concentration of O_3 measured during descent phase of the second hydroxyl $OH(X^2\pi)$ flight.

The ozone data from these launches is shown in figure 50. The concentration levels observed are about 20 percent higher than those acquired during the ascent of the ozone monitor. Part of this difference results from the calibrations used for the two methods. The concentration data shown in figures 44 and 45 were obtained using the National Bureau of Standards calibration for the ozone monitor performed in March 1975. But they must be increased by about 6 percent to account for the difference between the ambient pressure and the pressure inside the absorption chamber. However, it is felt that the discrepancy between the ozonesonde and the in situ measurements results from the presence of a negative offset in the NBS calibration. Evidence for this explanation and a discussion of its implications may be found in JSC Internal Report JSC-11380 (Application of Dasibi Ultra-Violet Ozone Monitor to Stratospheric Measurements) dated June 1976.

In addition to the ozone concentration data, the radiosondes provided data (as a function of altitude) on temperature, dew point, humidity, and wind direction and speed.

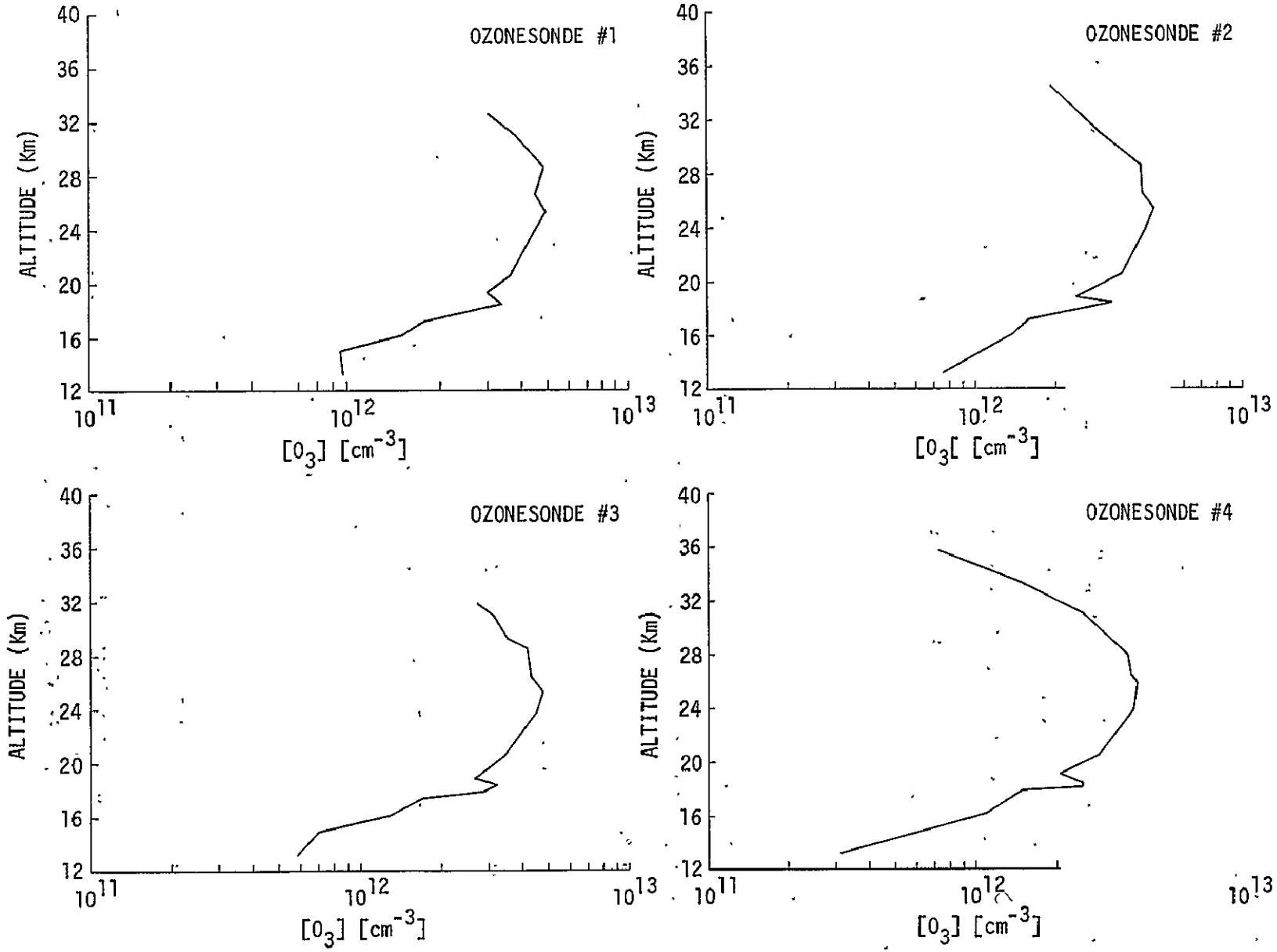

Figure 50.— Concentration of ozone determined by radiosondes released in conjunction with the second hydroxyl $OH(X^2\pi)$ flight.

POSTFLIGHT

Landing

The parachute/payload landed 5 nm SW of Vicksburg, Mississippi, at 1834 CDT in soft dry soil approximately 150 yards from the Mississippi River. The land (hunting property) was fenced and locked and access to the payload was not possible until mid-day on 20 October 1975. The payload was returned to the NSBF on 21 October 1975.

Inspection

Visual inspection showed little structural damage after impact, however, the following items relating directly to the L-band antennae used to transmit telemetry data were noted at the recovery site.

1. The dipole element of the prime antenna transmitting at 1483.5 MHz (NCAR) was bent approximately 30 degrees from vertical.

2. The support bar (see fig. 34) for both the prime NCAR antenna and the backup antenna transmitting at 1491.5 (JSC) was severly bent but still attached to the rigging cables.

3. The antenna lead for the backup antenna was loose at the transmitter end (probably pulled out on the ground).

After the payload was returned to the NSBF, the primary radiofrequency system was check (after the dipole element was rebent to proper orientation) and

found to be functional. However, the connector pin in the primary antenna base was found to be damaged.

Inspection of the film from the uplooking motion picture camera showed the parachute to be cross rigged and/or wrapped. Two of the four sets of suspension lines were wrapped together during rigging. These two sets were on opposite corners. The film also showed a more violent collapse of the rigging at cutdown than on previous flights, but it did not give any visual verification of antenna damage or misalignment.

Findings of the Independent Anomaly Review Board - Balloon Flight Telemetry Anomaly

An Independent Anomaly Review Board was formed to assemble all of the information pertinent to the telemetry anomaly and to draw an independent conclusion about the nature and cause of the telemetry data loss.

The Board concluded that the parachute rigging error did not significantly affect the performance of the parachute or contribute to the telemetry signal loss but recommended the routine use of a rigging fixture to duplicate the attachment points on the balloon payload.

The Board concluded that a procedural error in plotting payload position on the basis of Omega navigation system data did not significantly contribute to the telemetry signal degredation but recommended a review of the procedure used to determine balloon position to look for areas of possible improvement. It also recommended that operational decisions should make appropriate allowance for errors in position data.

The Board concluded that neither the lack of cognizance of a contingency magnetron start procedure by JSC or NSBF personnel nor the lack of voice communications with the operating personnel in the tracking aircraft contributed to the telemetry signal degredation. These discrepancies were pointed out as significant operational anomalies for which corrective action should be initiated.

The Board concluded that although there were some procedural errors during the flight, none of them contributed to the telemetry signal degredation. Furthermore, the Board concluded that the fact that the secondary telemetry transmitter continued to transmit good data and that channel 12 data (pressure transducer) continued to be received on the primary frequency exonerated all possible failure points except the primary telemetry transmitter, its antenna cable, and its antenna. Post recovery examination and testing demonstrated that the transmitter operated correctly. There was no visible damage to the antenna cable. However, examination of the primary telemetry antenna showed that the driven element on the antenna was bent and that the center conductor socket in the coaxial connector on the antenna was damaged. One of the "fingers" of the socket was broken off at the base and another of the "fingers" was partially broken so that it could easily bend outward to touch the shell of the connector. Either of the broken "fingers" could have produced an RF short circuit in the annulus of the connector and caused a very high standing wave ratio.

The Board concluded that the most probable cause of the degraded telemetry data was a failure of the coaxial connector on the primary telemetry antenna. A specific reason for the failure occurrence within about 700 milliseconds

of the payload release could not be identified from the film from the uplooking cameras. However, the most probable cause was the release of energy stored in the parachute harness at the time of cutdown (slingshot effect) which would drive the ballast hopper into the support bar for the primary and secondary antennae which was located directly below the ballast hopper on this flight. On previous flights the antennae were hung from booms which were attached to the four cables between the ballast hopper and the NCAR telemetry instrumentation (fig. 19 shows these cables to best advantage).

CONCLUSIONS

The effect of solar radiation backscattered from the lower atmosphere on the OH concentration measurement was evaluated during ascent and float phases of the flight and during that portion of descent for which data was obtained. The modifications made to the resonance/fluorescence instrument resulted in a reduction of instrumental background by more than an order of magnitude. However, the OH concentration profile was not obtained as the result of a failure in the telemetry system.

Good quality data on the concentration of ozone was obtained during ascent using the ultraviolet absorption ozone monitor. The instrument also produced data during descent from 32 to 19.8 km but the values appear too low when compared to the ascent profile. The cause of the low readings is likely to be the same as that which produced the six low values during the descent phase of the previous flight but is apparently not related to the exhaust pump whose performance was monitored during the current flight. A total of four ozone radiosondes were successfully launched in conjunction with the flight and provided reference data on the concentration of stratospheric ozone to allow a comparison to be made with the *in situ* measurements made aboard the payload.

The aerosol particle counter produced data from 32 to 19.8 km on descent. The data and instrumentation were sent to Dr. Myers of the University of Pittsburgh for analysis and refurbishment.

The Independent Anomaly Review Board determined that the most probable cause for the loss of data immediately after payload release was a failure of the center conductor socket in the coaxial connector on the primary telemetry antenna. Based on its recommendation, action is being taken on the following items to avoid future procedural and hardware animalies:

1. Relocate telemetry antennae to a more protected location which still gives adequate pattern coverage and/or provide non-interferring protection for antennae in their present location.

2. Provide a backup ground system to constantly monitor the backup RF link and/or provide a method for switching rapidly from primary to backup RF link monitoring.

3. Provide a complete configuration document of the NCAR hardware and a procedure for assembly and checkout of all electrical/ mechanical systems for both build-up areas and launch pad operations.

4. Work with NCAR on an acceptable aircraft communications link for all down-range activities.

THIRD HYDROXYL OH($X^2\pi$) MEASUREMENT

(NCAR FLIGHT NO. 940-P)

12 January 1976

SUMMARY

This balloon-parachute flight was the fifth flight of the laminar flow through/resonance fluorescence instrument (principal investigator: Dr. James Anderson, University of Michigan) and took place on 12 January 1976. The purposes of the flight were to measure the vertical concentration profiles of the hydroxyl radical (OH) and ozone (O_3) from about 30 to 45 km.[1] An ancillary experiment was again flown as part of the payload to perform counting measurements (as a function of altitude) of stratospheric aerosols with surface-ionizable constituents.

The flight was launched at 1256 CST from the NSBF at Palestine, Texas. The midday launch was chosen to minimize background noise (originating from solar radiation scattered from the lower atmosphere) while retaining a nominal OH density profile. Hardware consisted of a 4.3×10^5 cubic meter balloon, 9.75-meter guide surface parachute, NCAR telemetry system, JSC flight support module, the resonance fluorescence instrument tuned to the (0-0) band of the $A^2\Sigma$-$X^2\pi$ electronic transition of OH (bandhead at 306.4 nm), an ozone monitor on loan from GSFC for *in situ* measurement of ozone using the ultraviolet (UV) absorption method, and an aerosol particle counter to monitor the presence of particulates larger and/or richer in surface ionizable constituents than a pre-set discrimination level. The University of Pittsburgh, under the sponsorship of Langley Research Center, was responsible for the aerosol particle counter instrumentation

1. Anderson, J.G., "The Absolute Concentration of $OH(X^2\pi)$ in the Earths Stratosphere", Geophysical Research Letters, March 1976.

and for reduction and analysis of the aerosol data. Thus the hardware was essentially identical to that flown on the previous flight of this series. The only major differences were in the placement and support structures for antennae and the use of a voice relay system on the balloon to allow verbal communication between the NCAR tower and the tracking aircraft. The ozone monitor functioned normally only during the ascent phase of the flight above 30 km. The payload reached a float altitude of 44 km (144 k ft) at approximately 1515 CST. The surface ionization particulate detector (aerosol experiment) was turned on at float altitude for several minutes prior to cut down. The command to release the payload was sent from the NCAR tower at 1610 CST to begin the OH data gathering phase of the mission. OH concentration data was obtained from 43 km (141 k ft) to 30 km (98 k ft). This was the first time that good quality data (± 35 percent experimental uncertainty) on the concentration of hydroxyl have been obtained in this critical altitude range. The aerosol experiment was left on during descent and produced data down to approximately 4.5 km (15 k ft). No ozone radiosondes were scheduled or launched in conjunction with the present flight.

The overall performance of both JSC and NCAR telemetry systems during the flight was excellent. The JSC-Houston ground station acquired the payload approximately 19 minutes after launch when the payload was at an altitude of 6 km (20 k ft). JSC tracking continued until

the payload was below 9 km (30 k ft) on descent at a distance of approximately 210 nm from JSC. The NCAR and JSC-Palestine ground stations (being less than 80 nm away from the payload) were able to track to below 3 km (10 k ft) on descent and did not loose signal lock until the transmitters were shut down. The parachute/payload landed in damp, sandy soil in a wooded area near Avinger, Texas at 1641 CST and sustained only minor damage. Despite approaching darkness and deteriorating weather, the recovery crew was able to reach the payload and complete recovery that evening. The payload was returned to the NSBF at Palestine at 2230 CST 12 January 1976.

INTRODUCTION

This flight was essentially a reflight of the Second Hydroxyl $OH(X^2\pi)$ Flight whose primary scientific objective was not met due to a telemetry systems failure during the initial moments of the descent phase. The primary objective was to extend the altitude range of the hydroxyl concentration measurement made during the 18 July 1975 flight and to improve the signal to noise ratio of the measurement by using a resonance fluorescence instrument of modified design. The modified instrument (shown schematically in figs. 40 and 41) was expected to improve by an order of magnitude the rejection of Rayleigh-scattered radiation from the lower atmosphere as a result of extensive changes in baffling and a reduction in the reflectivities of internal surfaces. As in the two previous flights, the payload was instrumented to measure the concentration level of O_3 and OH concurrently. An ancillary experiment to perform counting measurements of stratospheric aerosols was flown for the second time on this flight.

Payload

The payload weighed approximately 263 kg, and consisted of telemetry, balloon control, descent-observation, and scientific instrumentation. As a result of the loss of telemetry data during the most crucial phase of the previous flight, the placement of antennae and the antennae support structures were modified. A sketch of the payload

which depicts these modifications is shown in figure 51. Figure 52 is a photograph of the payload taken a few minutes prior to lift-off. The JSC L-band transmitter was located on a rigid boom attached to one of the three struts which support the detection nacelle. Its location was in front of the entrance throat of the instrument but to one side so as not to effect the laminar flow of stratospheric gas through the instrument or reflect light into the detection chamber. The NCAR L-band transmitter was located just below the ballast hopper on a support bar made of PVC tubing. The omega navigational system antenna, the command receiver antenna, and voice relay antenna were attached to flexible fiberglass rods which protruded from the side of the payload. The ballast hopper was supported away from the NCAR L-band antenna in a semi-rigid fashion by PVC tubing through which the four payload suspension cables were threaded. This prevented the ballast hopper from being driven into the NCAR antenna at the time of cut-down when the energy stored in the parachute harnesses would be released.

Instrumentation

Instrumentation carried as part of the payload was functionally identical to that flown on the previous flight. It consisted of NCAR and JSC telemetry instrumentation, NCAR balloon control instrumentation, NCAR and JSC pressure transducers to measure the altitude of the payload, two vertical reference gyros to measure payload

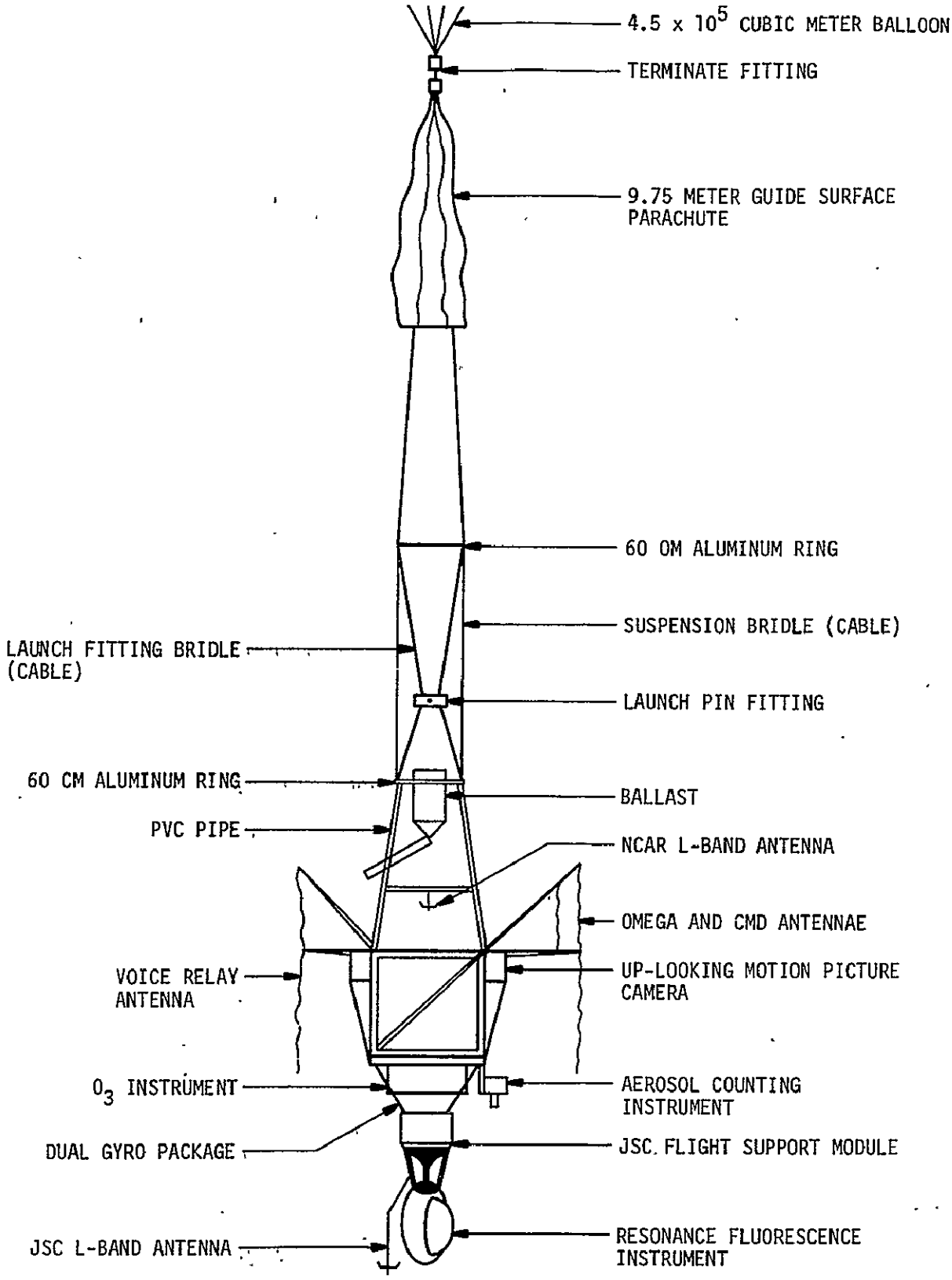

Figure 51.— Flight configuration for the third hydroxyl OH($X^2\pi$) measurement.

NASA
S- 76- 20861

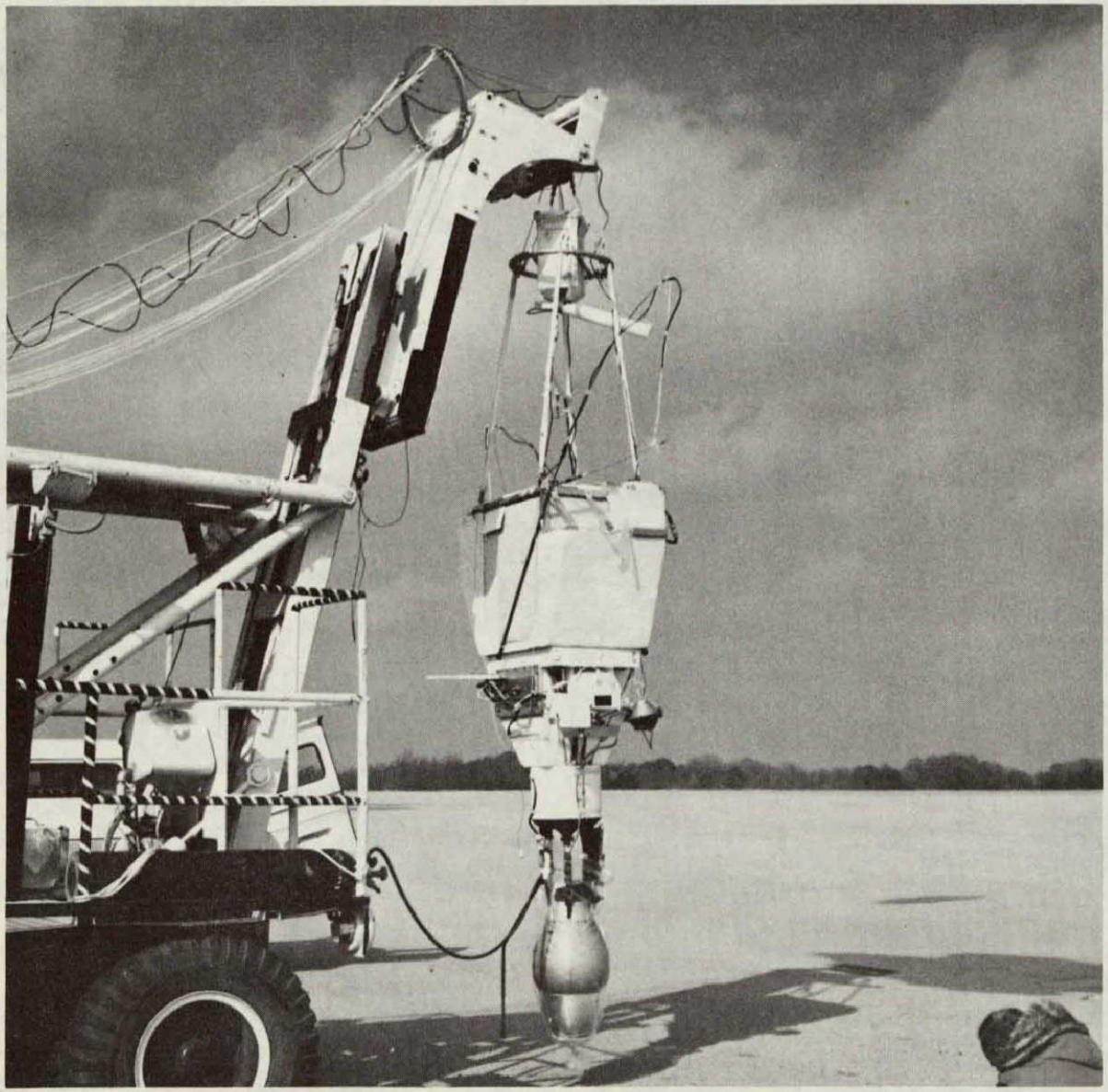

Figure 52. - Third Hydroxyl OH($X^2\pi$) Payload Several Minutes Prior to Lift-off

attitude, a z-axis accelerometer to determine the loading forces when the parachute is deployed, a single up-looking motion picture camera (64 frames/sec using a 10 mm lens) to observe parachute opening and descent characteristics, an ozone monitor (on loan from GSFC) to measure in situ the concentration of stratospheric ozone, an aerosol particle counter to monitor the presence of particulates, and the laminar flow through/resonance fluorescence instrument to measure the concentration of the hydroxyl radical. No ozone radiosondes were scheduled or launched in conjunction with the present flight.

Function, manufacturer, model, and serial numbers for support instrumentation are itemized in Appendix A. Pertinent electrical and mechanical drawings are listed in Appendix B. A description of the telemetry systems and channel allocations is given in Appendix C. Photographic documentation for the flight is itemized in Appendix D.

The only significant change in the scientific instrumentation for the present flight was to increase the flush time of the absorption chamber in the UV absorption ozone monitor from 3.2 seconds to 4.0 seconds. This change would allow accurate measurements of the concentration of ozone to be made up to an altitude of about 38 km.

PAYLOAD OPERATIONS

Ascent and Float Phases

The flight profile for the Third Hydroxyl OH($X^2\pi$) Flight is illustrated in figure 53. Launch occurred at 1256 CST, 12 January 1976, and was accomplished using the dynamic launch technique. The balloon system ascended at an average rate of 5.4 meters per second to a float altitude of 44 km. The balloon was allowed to float at altitude for approximately 55 minutes before payload release. The ozone monitor was operated during the ascent phase of the flight and the resonance fluorescence instrument was operated during the ascent and float phases (source lamp OFF) to monitor the background from Rayleigh scattering of solar radiation entering the measurement chamber from the lower atmosphere. As shown in figure 54, the modifications made since the 18 July 1975 flight of the resonance fluorescent instrument have resulted in an improvement in background level by more than an order of magnitude (see fig. 28 for comparison).

Descent Phase

The payload was released on command from the NCAR tower at 1610 CST and the OH data gathering phase of the mission began. Solar zenith angle at the time of cut down was 80 degrees and the payload latitude was 32.8 degrees North. An onboard motion picture camera and

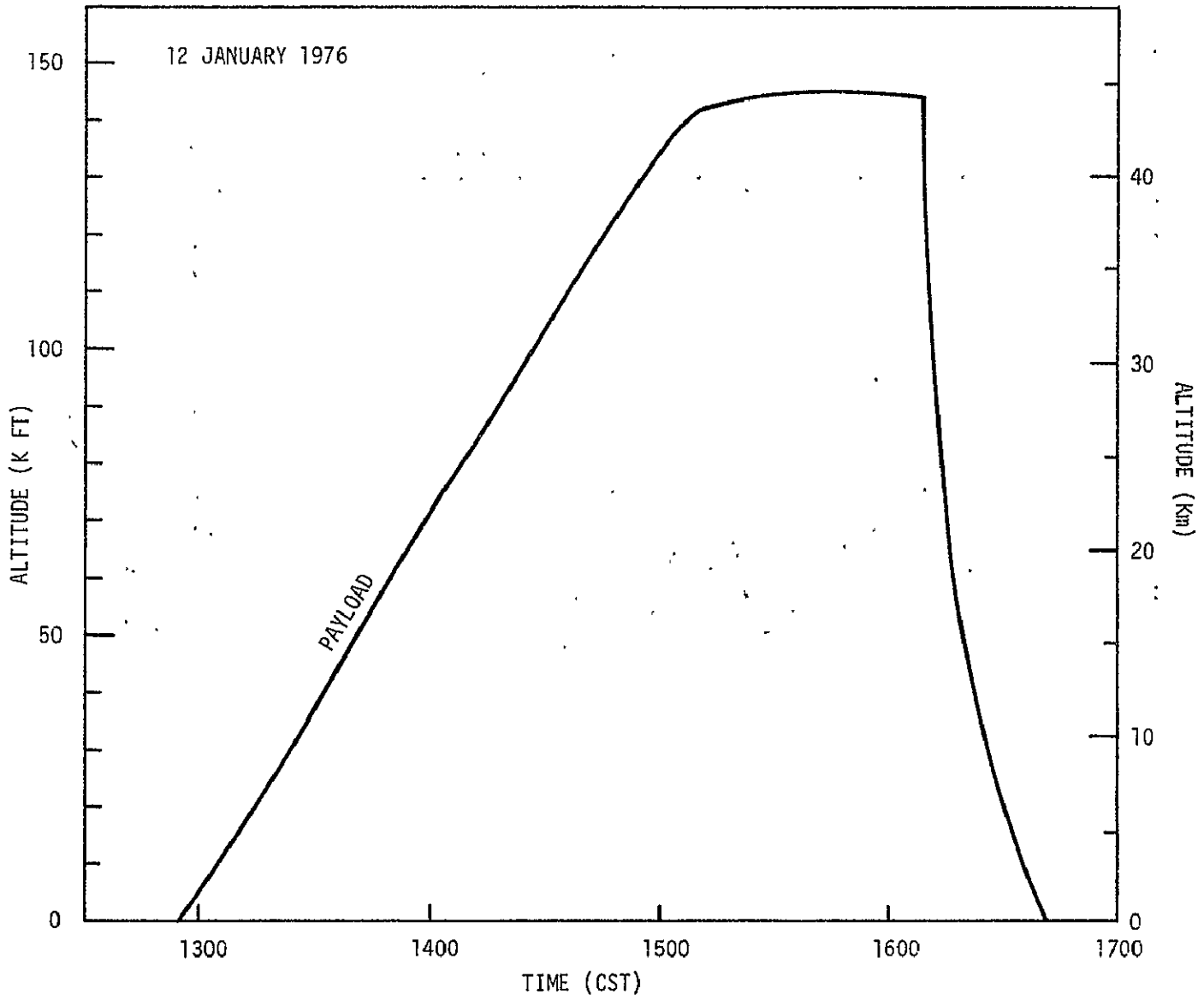

Figure 53.— Flight profile for third hydroxyl OH($X^2\pi$) flight.

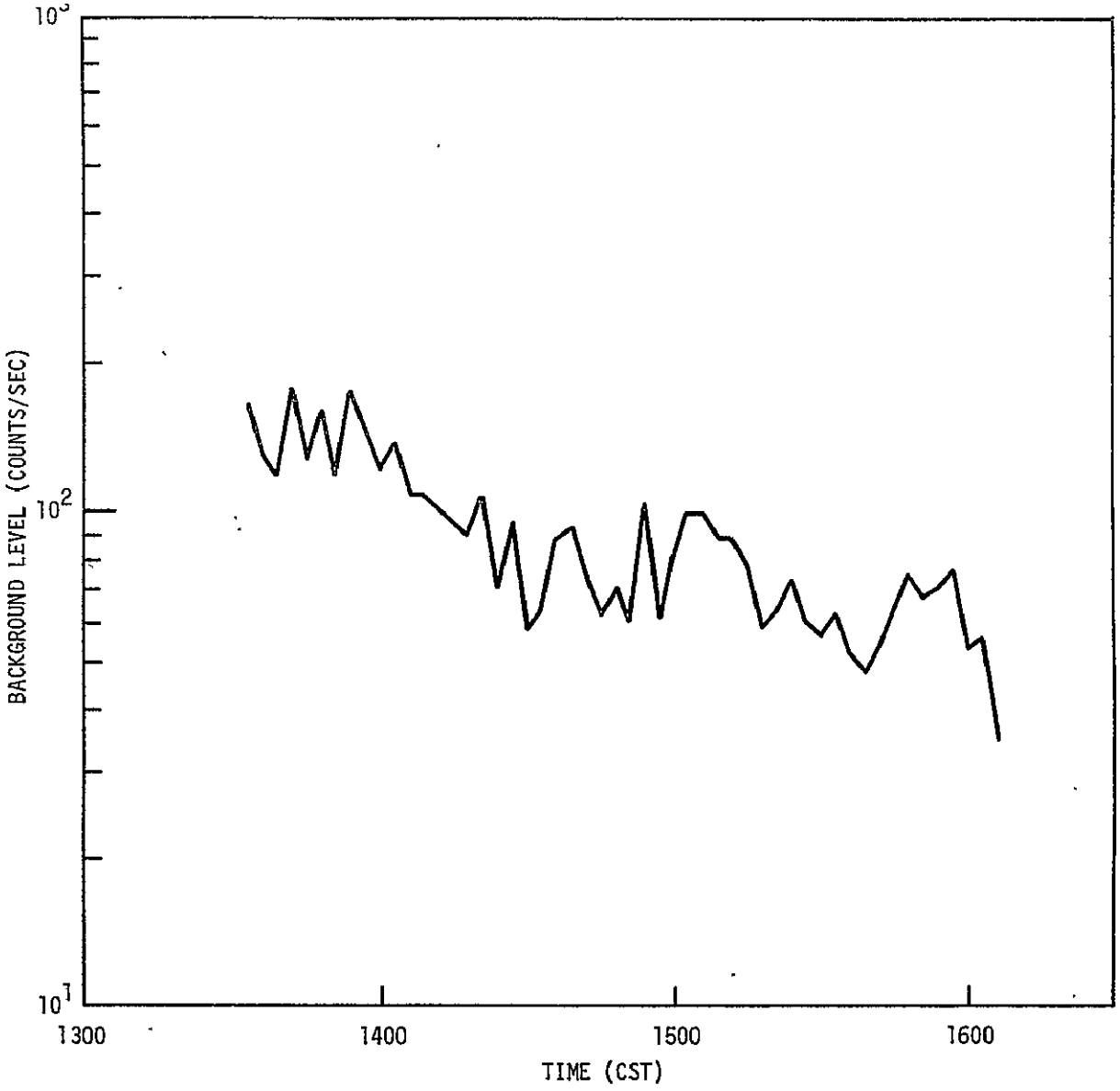

Figure 54.— Background count rate monitored during ascent and float phases of the third hydroxyl OH($X^2\pi$) flight.

accelerometer observed parachute deployment and measured the loading forces while two vertical reference gyros monitored the descent attitude of the system. Payload altitude as a function of time since cut down is shown in figure 55. The velocity/altitude profile of the descending payload is shown in figure 56. The data points represent individual determinations of the velocity made by taking the difference in altitude over 10 second intervals and calculating a velocity. The straight line is the least squares fit to the data points. The vertical force on the payload during parachute deployment is illustrated in figure 57. The payload reached terminal velocity in about 30 seconds as is normal for this parachute. Figure 58 shows the probability that the angular deviation of the payload from vertical is less than a given angle as a function of angle during the first 8 minutes of descent. The degree of stability is comparable to the stability exhibited by the parachute system in the past. The payload was within 5 degrees of vertical 14 percent of the time and within 10 degrees of vertical 46 percent of the time.

Payload Currents, Power Consumption and Temperatures

Payload currents for the resonance fluorescence instrument and for the exhaust pump and electronics of the ozone instrument are shown in figure 59. Also shown is the current level drawn from the battery. Figure 60 shows the payload power consumption as a function of time for the flight. The total power consumed after 1333 CST (when battery

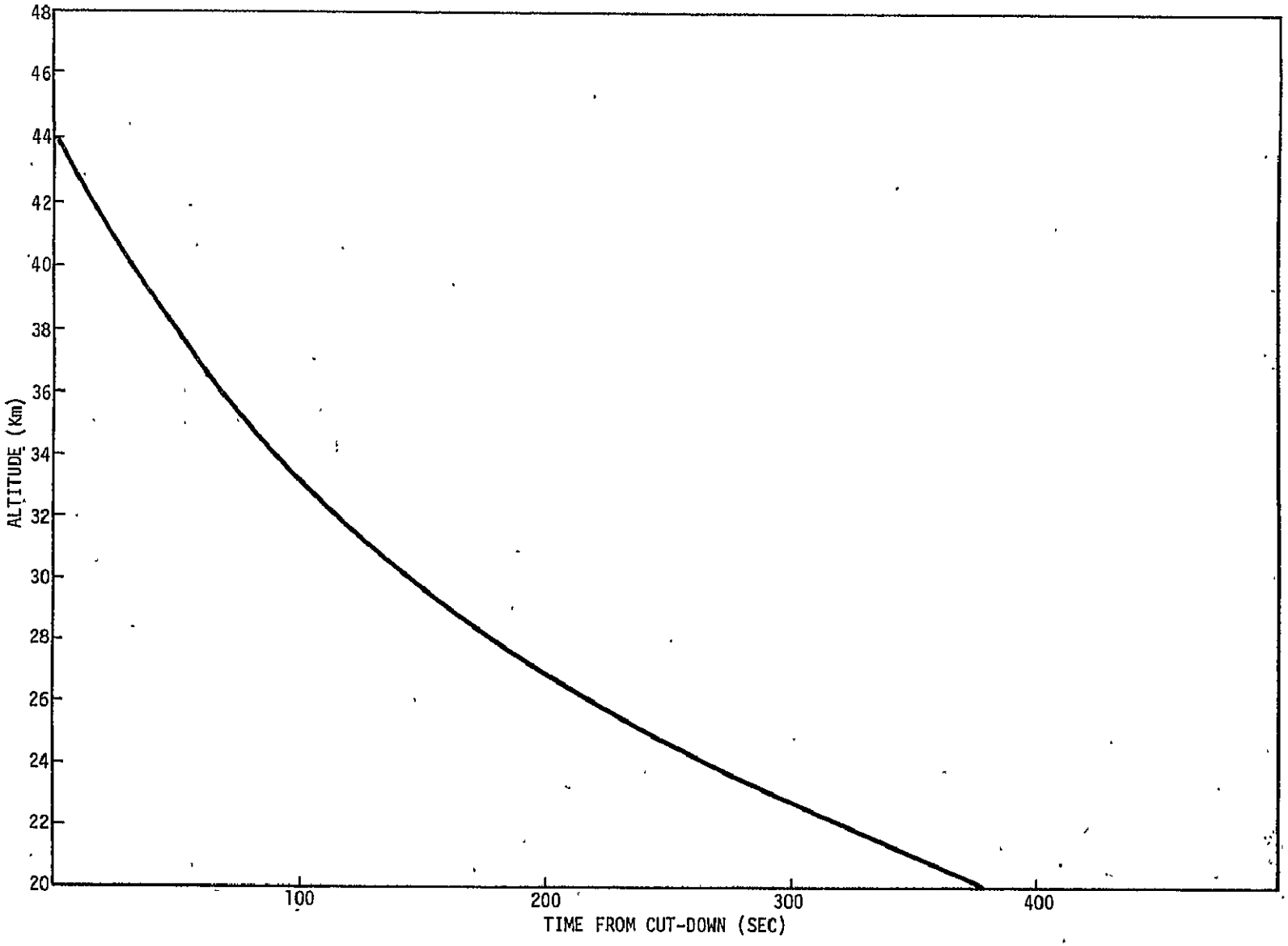

Figure 55.— Altitude/time profile of descending payload for the third hydroxyl OH($X^2\pi$) flight.

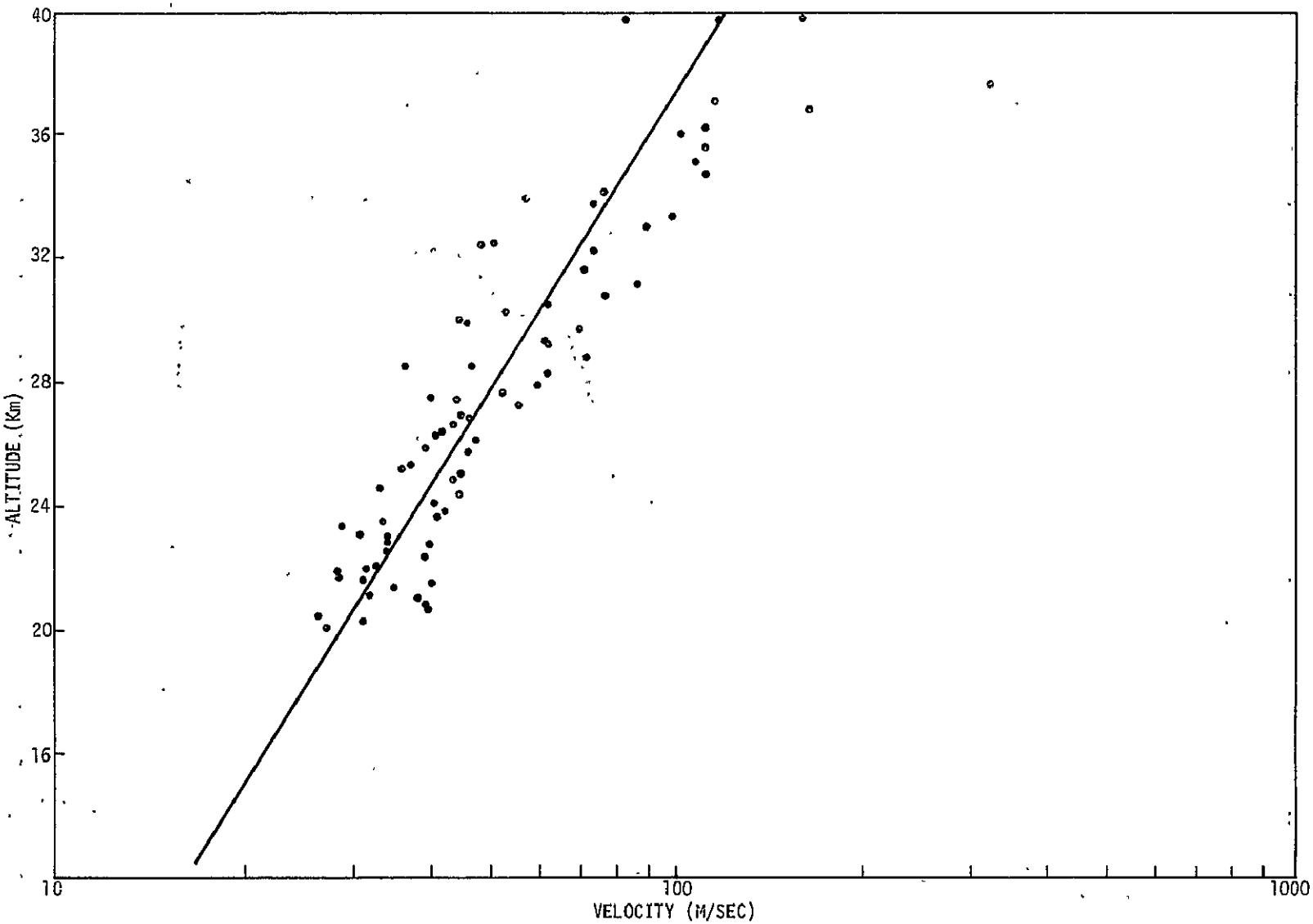

Figure 56.— Velocity/altitude profile of descending payload for the third hydroxyl OH($X^2\pi$) flight.

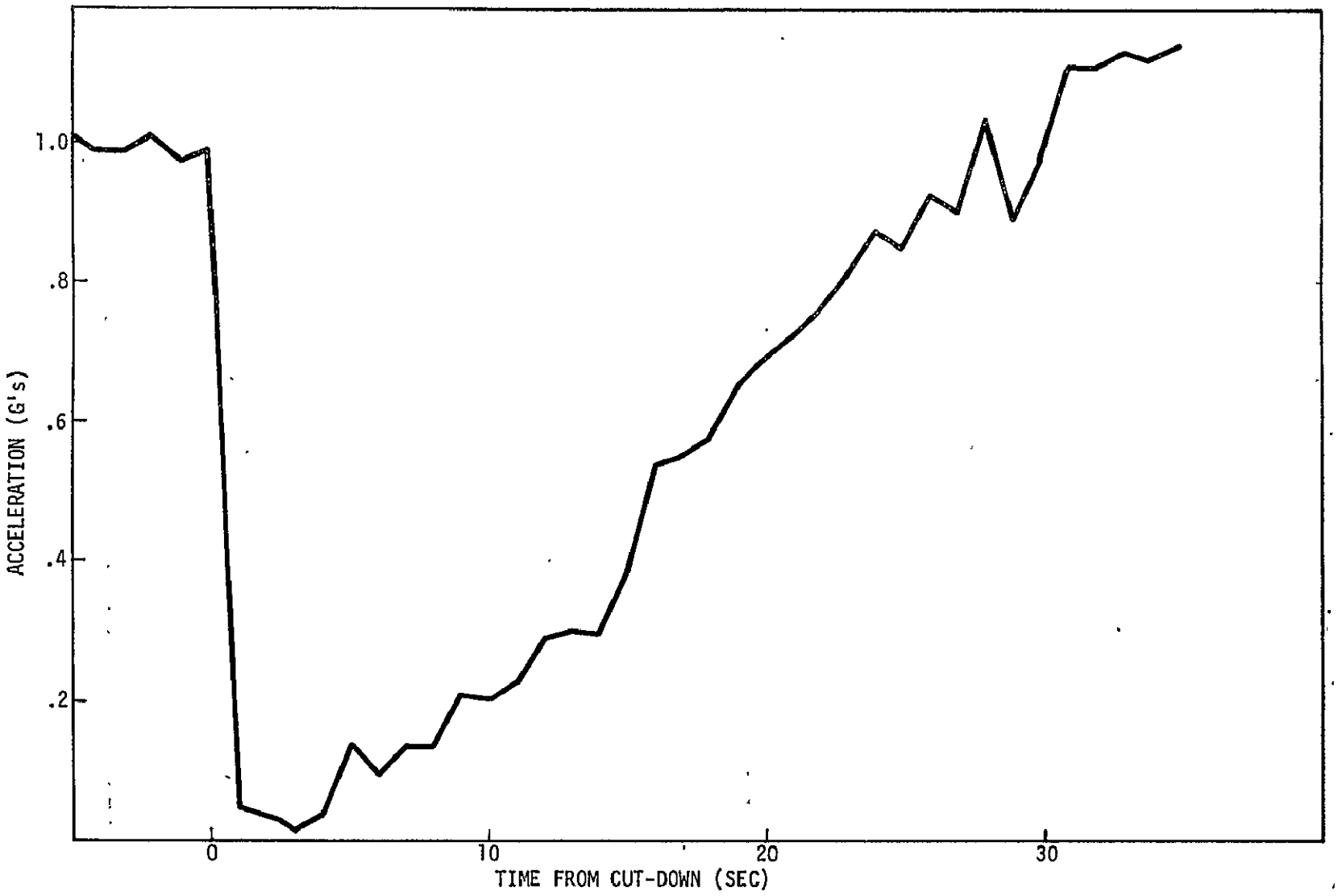

Figure 57.— Vertical force on payload during parachute deployment for the third hydroxyl OH($X^2\pi$) flight.

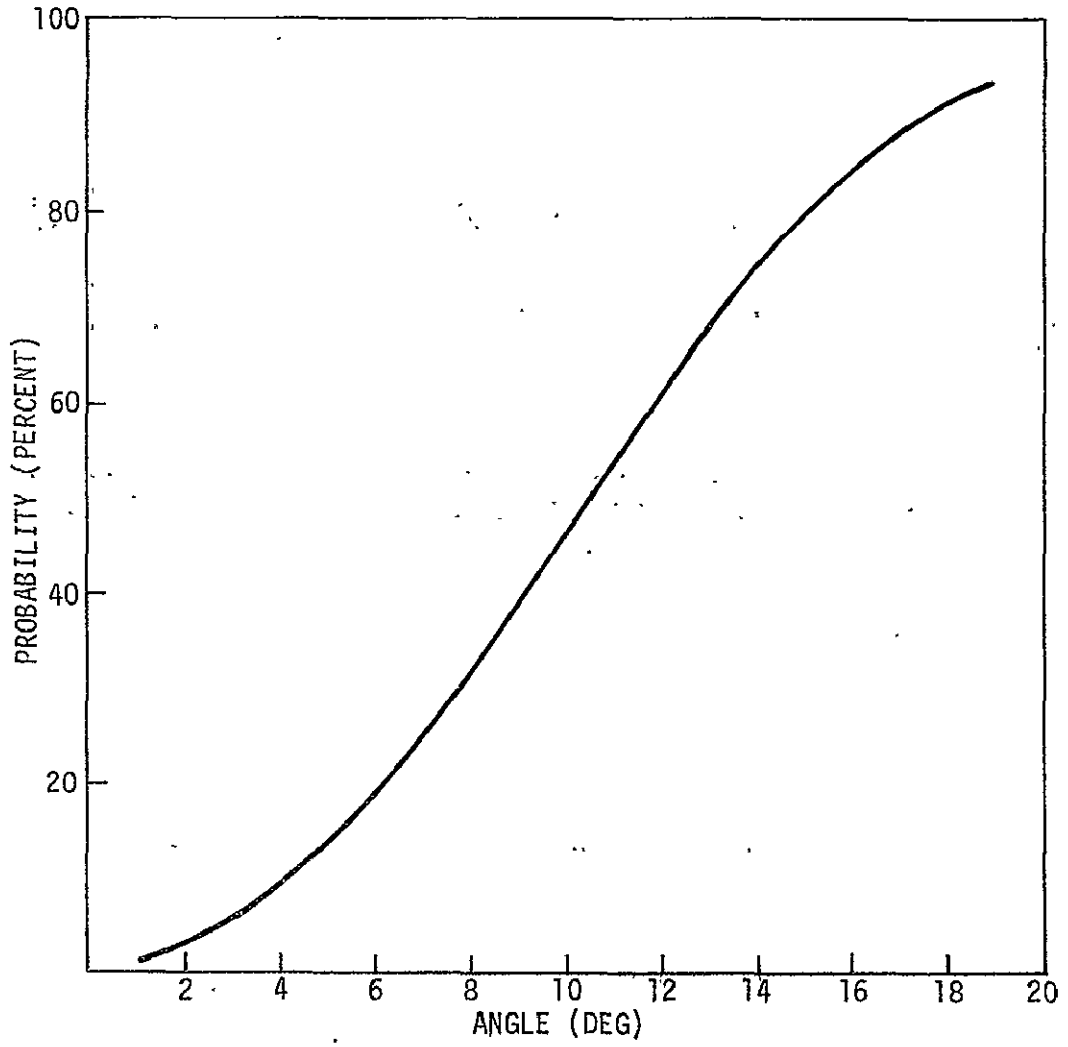

Figure 58.— Probability (percent) that the angular deviation of the payload from vertical is less than a given angle as a function of angle for the third hydroxyl $OH(X^2\pi)$ flight.

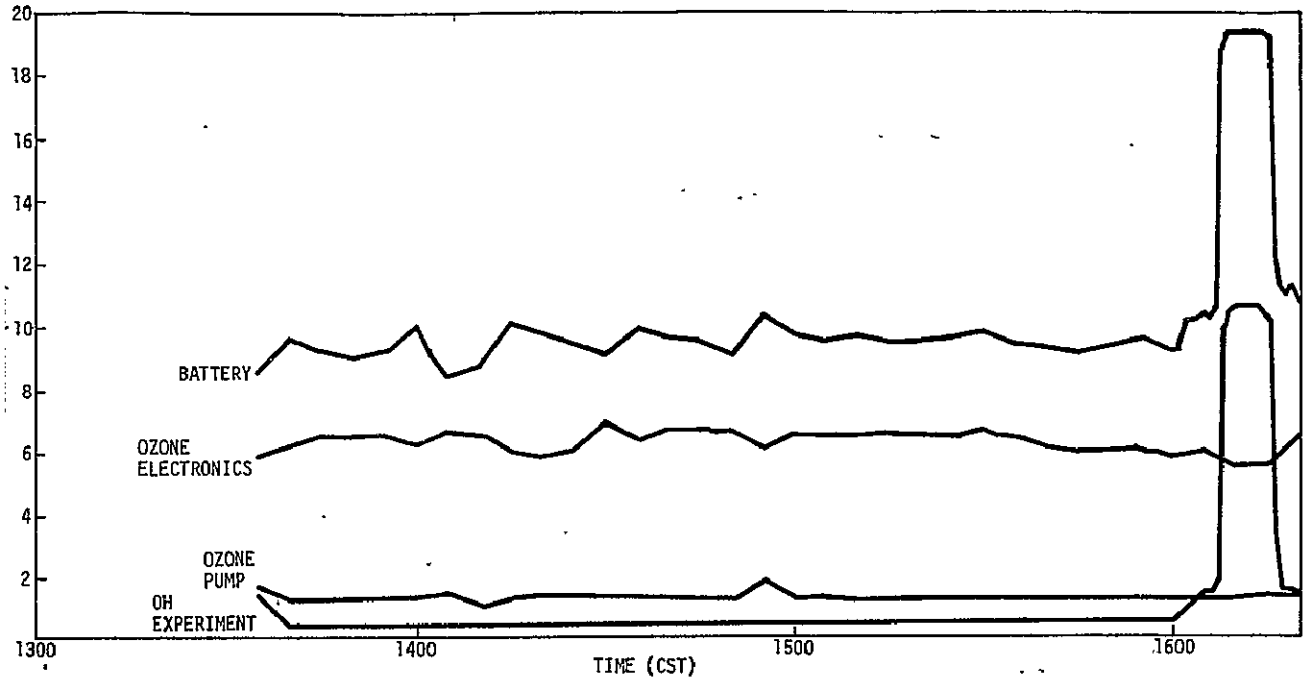

Figure 59.— Payload currents for the third hydroxyl OH($X^2\pi$) flight.

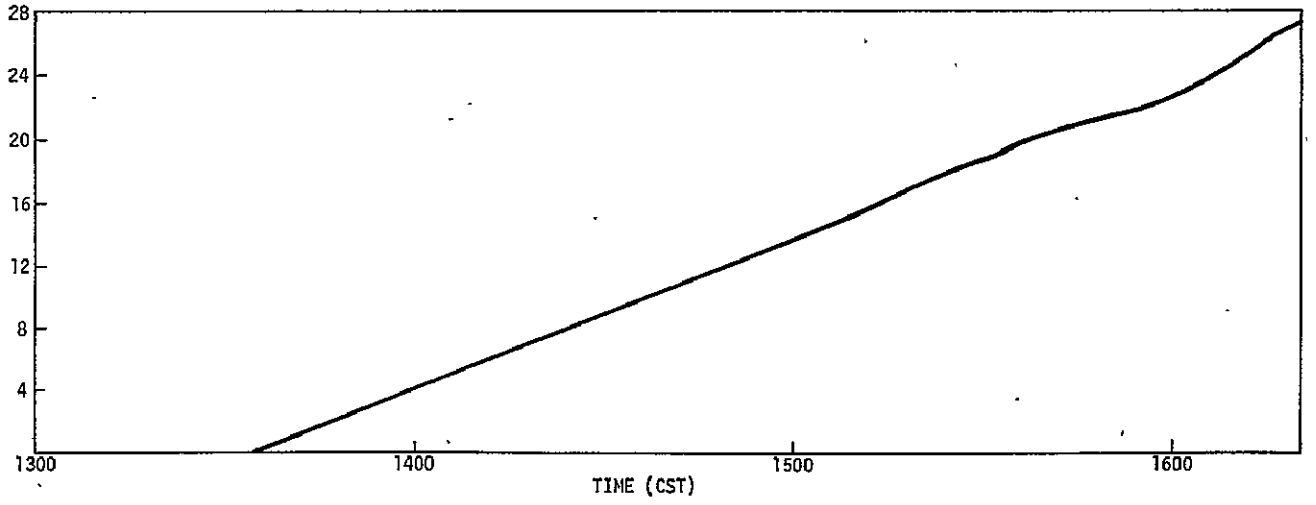

Figure 60.— Payload power consumption for the third hydroxyl OH($X^2\pi$) flight.

power was first consumed) was about 28 ampere hours. The ozone instrument used 22.3 ampere hours and the hydroxyl instrument used 3.2 ampere hours. Figure 61 is a thermal history of the battery and transmitter for the flight. Figure 62 is a thermal history of three major components of the UV absorption ozone monitor.

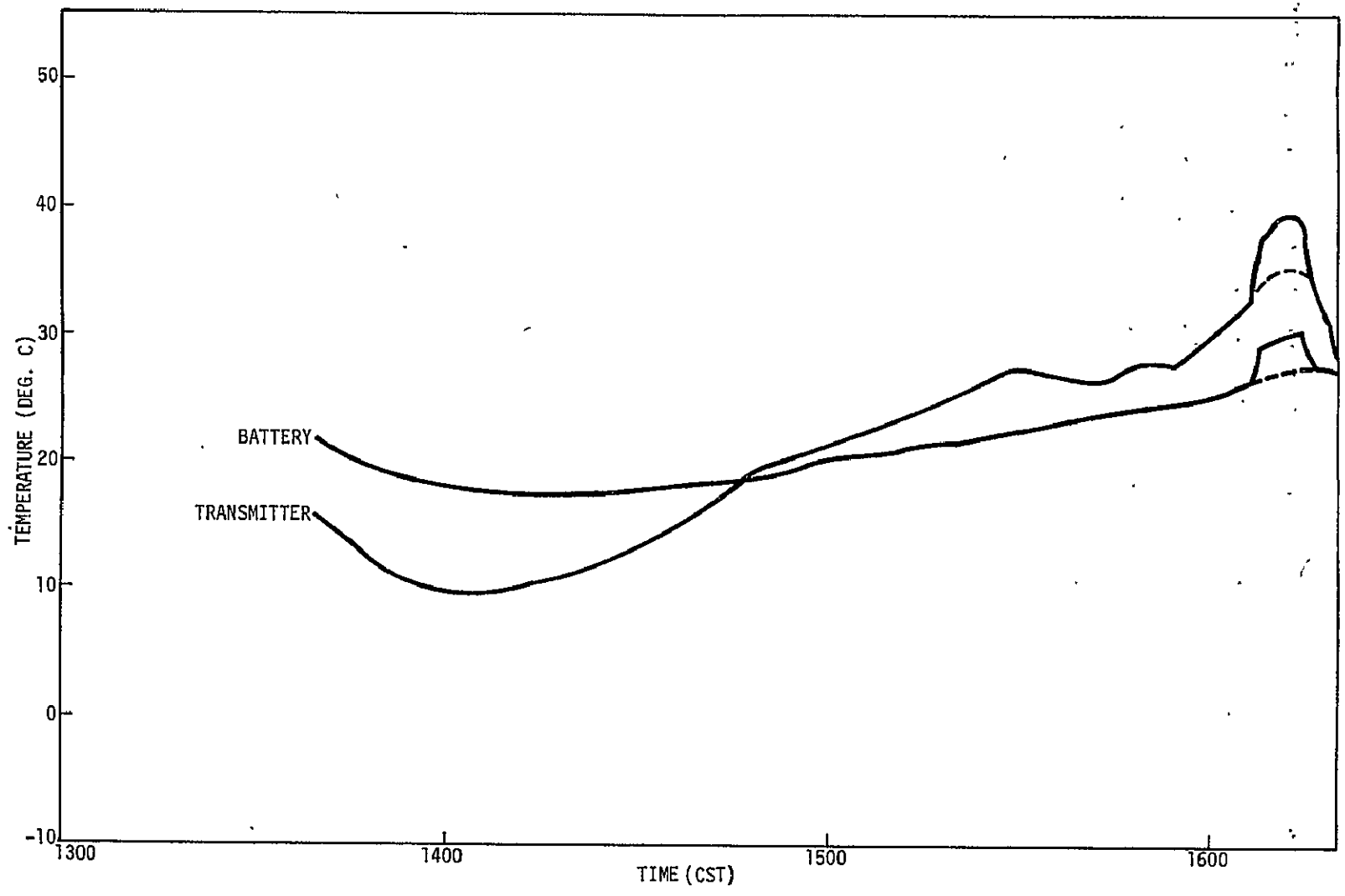

Figure 61.— Thermal history of the battery and transmitter for the third hydroxyl OH($X^2\pi$) flight.

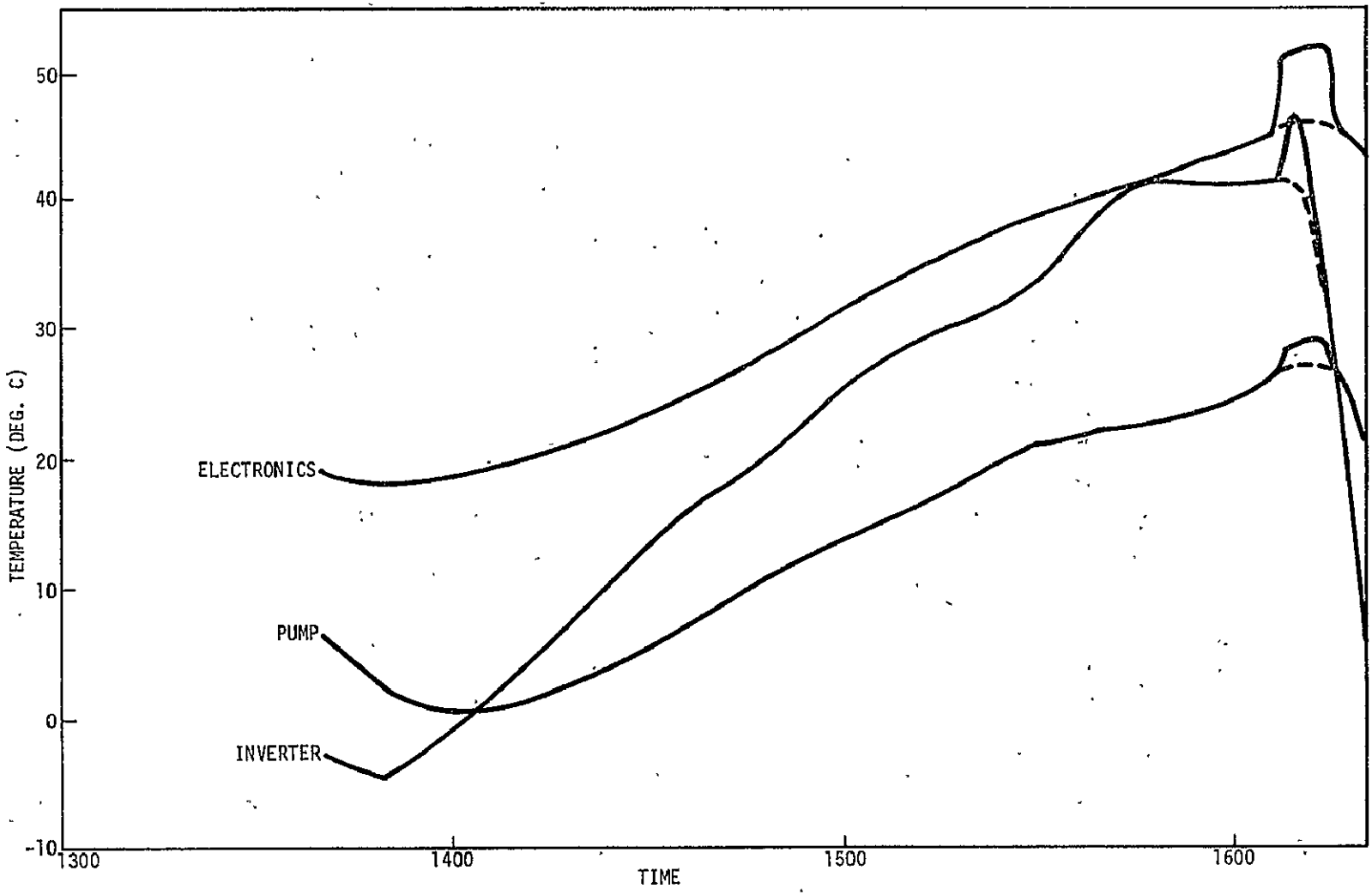

Figure 62.— Thermal history of ozone monitor components for the third hydroxyl OH($X^2\pi$) flight.

DATA RESULTS

Hydroxyl OH($X^2\pi$) Measurement

The resonance fluorescence instrument was successfully operated during the descent phase of the flight from float altitude until the payload reached an altitude of 28 km (92 k ft) when the source lamp was turned off in accordance with the flight plan. The resonance lamp, gas addition system, detector and associated electronics functioned normally throughout the flight. The flux of the source lamp was constant to within ±3 percent during the descent phase of the flight.

Hydroxyl concentration data was obtained in the altitude range from 43 to 30 km with an experimental uncertainty of about ±35 percent. This was the first profile of the vertical concentration of the hydroxyl radical in this critical altitude range. Solar zenith angle at the time of payload release was 80 degrees and the latitude of the payload was 32.8 degrees North. The results from this flight and the single measurement made during the 18 July 1975 flight are presented in figure 63. The hydroxyl concentration data obtained approached the maximum values predicted by current stratospheric photochemical theory.

Ozone Measurement

The UV absorption ozone monitor was turned on during the ascent phase of the flight at an altitude of about 6 km. The instrument did not

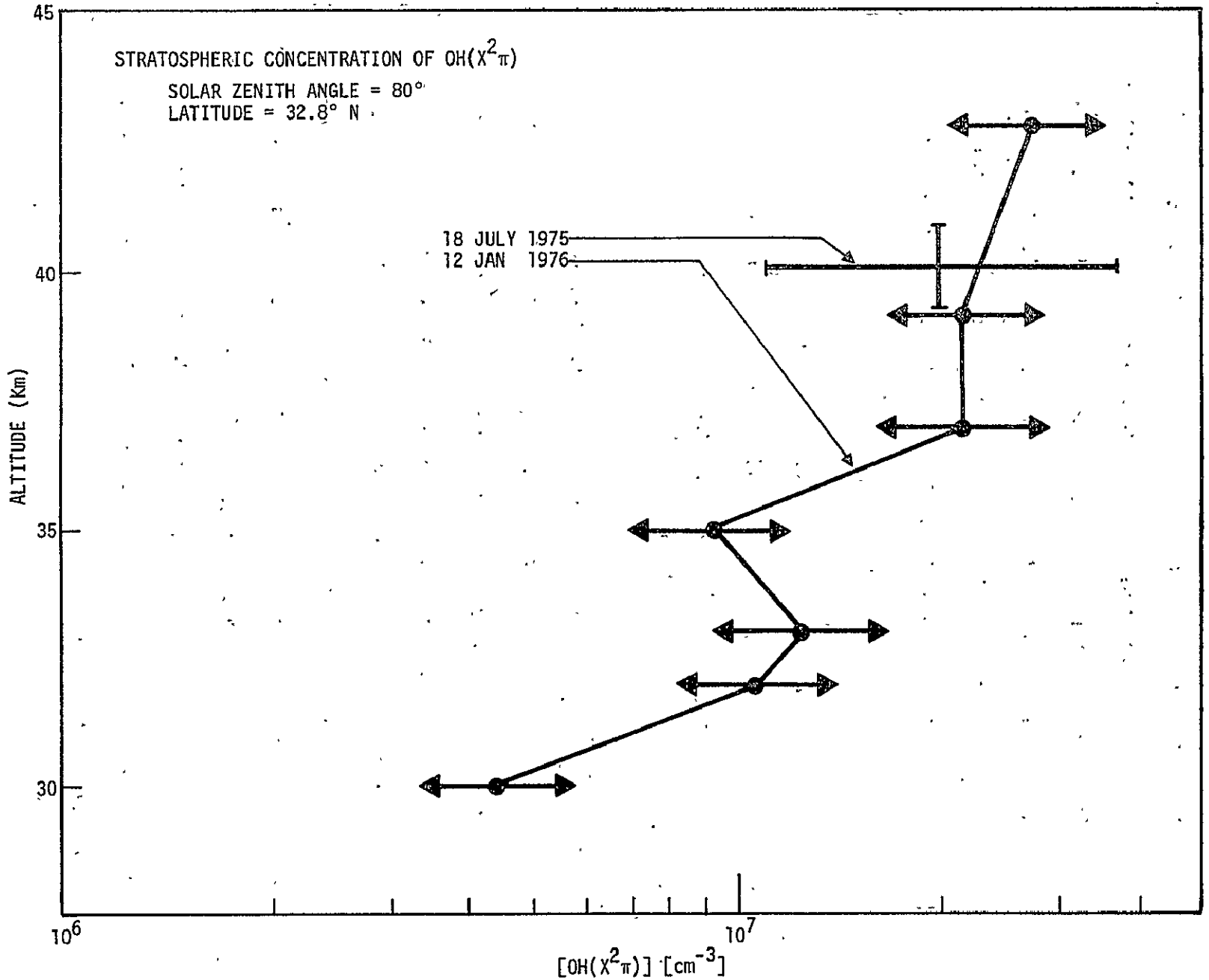

Figure 63.— Stratospheric concentration of hydroxyl measured on the first and third hydroxyl OH($X^2\pi$) flights.

function until the payload reached an altitude of 30 km. It then produced data for the remainder of the ascent. The instrument malfunctioned again after the payload reached float altitude, and no data was obtained during the descent phase of the flight. During the preflight functional, the instrument did not work properly immediately after it was turned on. After about 12 minutes, the ozone monitor produced good data.

Inspite of these problems, data was obtained in the important region between 30 and 40 km which partially overlaps the range in which hydroxyl concentration data was obtained. This data is shown in figure 64.

The flush time of the absorption chamber was increased from 3.2 to 4.0 seconds compared to the previous flight of this instrument. This change is adequate to allow accurate measurements of ozone concentration to be made to an altitude of about 38 km. Ozone data above this altitude must be considered invalid. The ozone data presented in figure 64 has been converted from the raw data using the National Bureau of Standards calibration for the instrument performed in March 1975. However, corrections for the difference between the ambient pressure and the pressure inside the absorption chamber have not been applied. These corrections will increase the concentrations shown by about 6 percent.

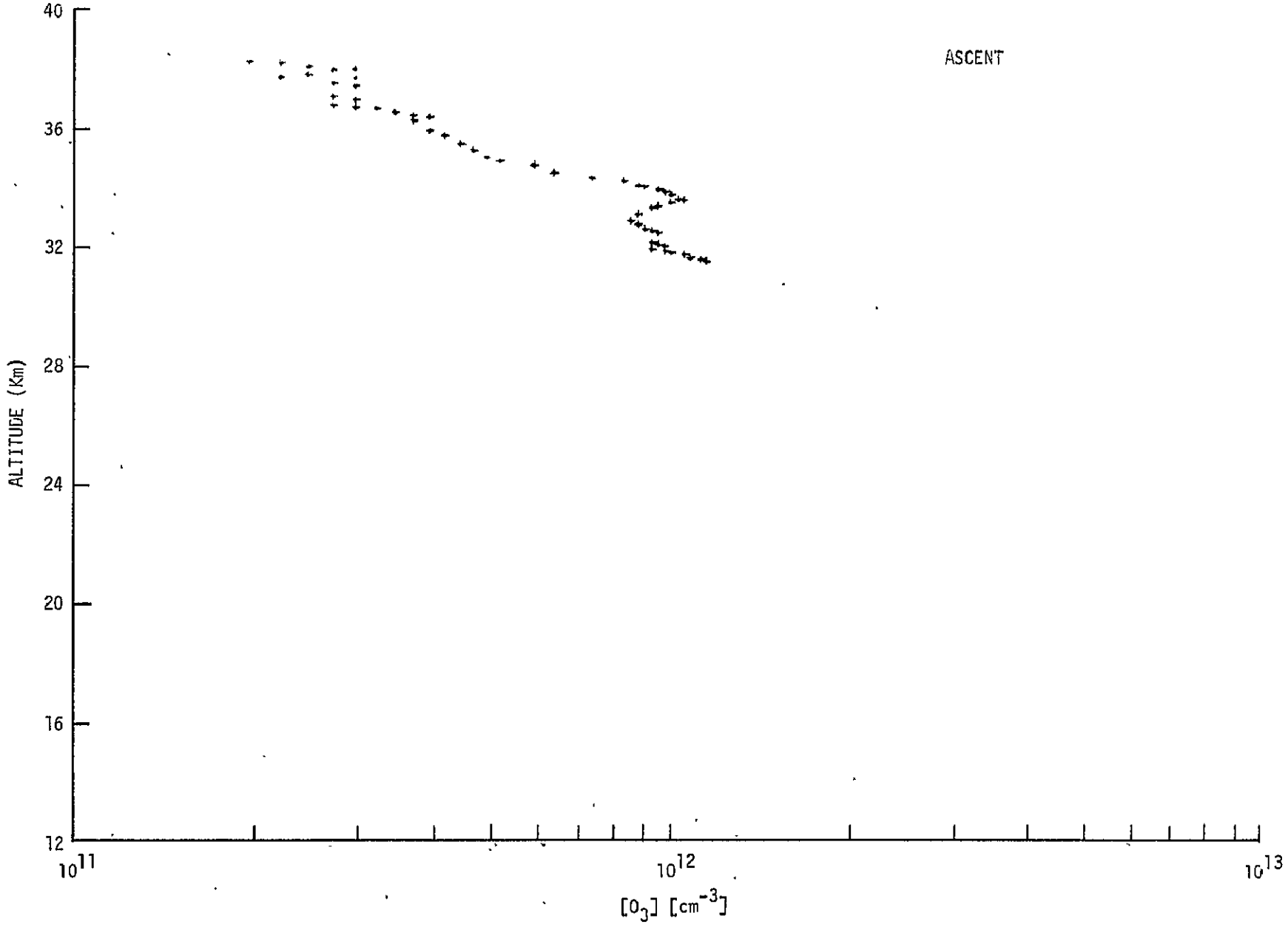

Figure 64.— Concentration of ozone measured during the ascent phase of the third hydroxyl $OH(X^2\pi)$ flight.

The concentration levels observed are considerably lower than those observed on the previous two flights. However, the stratification in the ozone concentration between 32 and 34 km is believed to be real. Stratification at these altitudes was not seen on the previous two flights of the instrument. It is interesting to note that the hydroxyl concentration data shown in figure 63 shows an apparent stratification in this same region.

Aerosol Measurement

The aerosol particle counter functioned normally during the descent phase of the flight and data was received down to approximately 4.5 km (15 k ft). The raw data are shown in figure 65. The appearance of points in pairs at the same value in the counting channel is expected, since data was taken at 5 second intervals but the flight package contained a sample-and-hold with a 10-second hold. For the purpose of plotting, the points shown at the altitudes lower than 25 km are the average of three successive readings at five second intervals, i.e., 15 second averages. The DC ion current readings are instantaneous currents sampled every five seconds.

It is doubtful that the data shown above 34 km is valid. The instrument response was tested just before lift off by blowing smoke at it. This procedure leaves a residue of contamination of the filament which must be vaporized later. The instrument was turned on at float altitude for several minutes before drop, but it is apparent from figure 65 that the final boiling off of contamination was not completed until

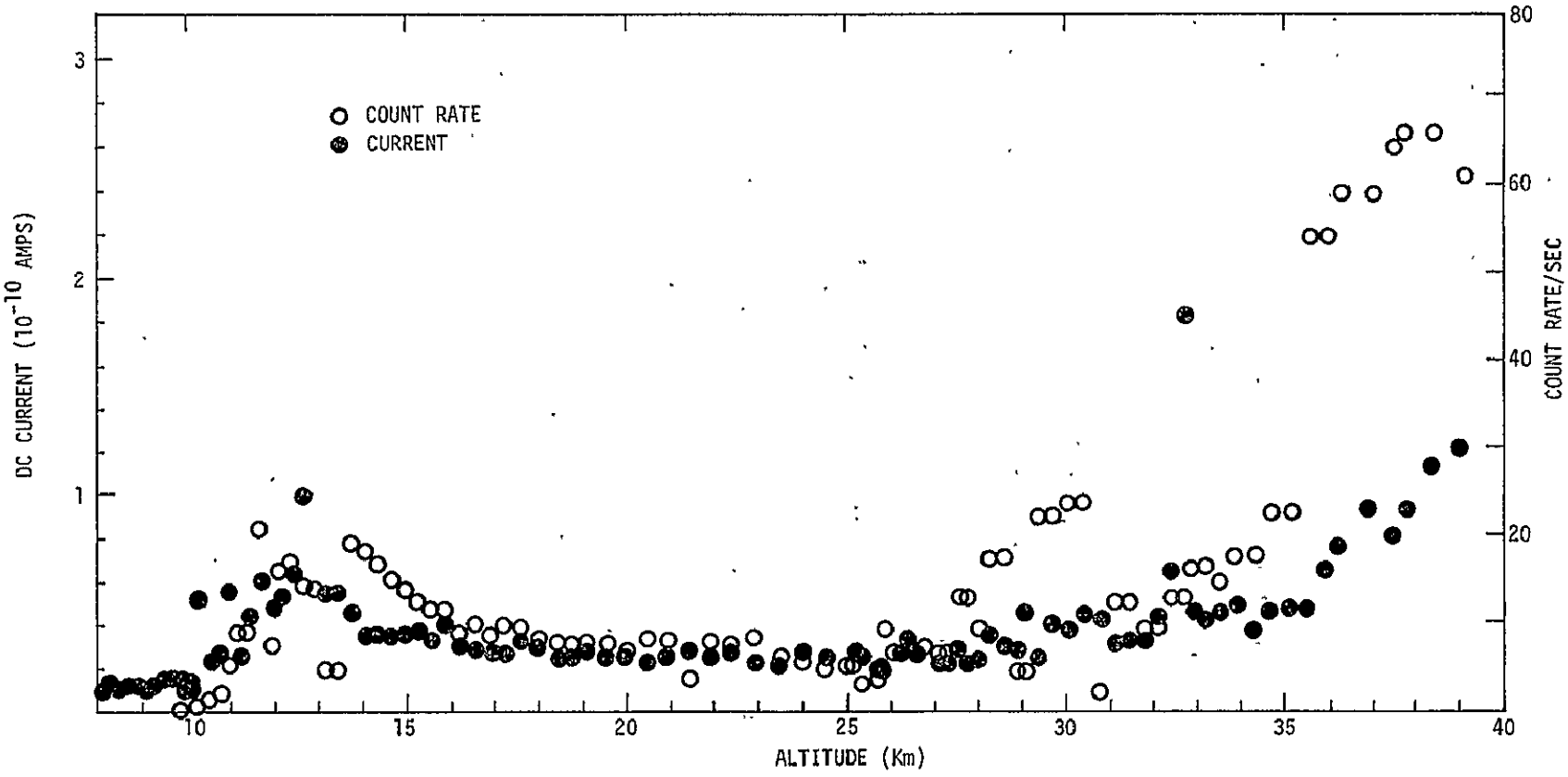

Figure 65.– Raw data from the aerosol particle counter obtained during descent on the third hydroxyl $OH(X^2\pi)$ flight.

the payload had descended to about 35 km. In future flights, electrical tests can be substituted for a smoke detection test in order to reduce contamination.

The rise in count rate, peaking at 30 km, is believed to be significant. A marked rise in count rate without an accompanying rise in dc ion current is indicative (in earth bound particulate monitoring) of an aerosol containing relatively large particles (i.e., greater than about 0.5 μm diameter of fly ash, earth dust, etc.). It is suggested that the rise in count rate observed at 30 km may be due to meteoritic dust.

The raw data shows nearly constant values between 17 and 27 km. The values observed are typical of dc background ion current levels which originate from surface ionizable impurities in the filament deposited by previous use. The dc level below 10 km is noticeably lower, which may be an indication that the batteries were becoming weak during the later stages of the flight. If this is so, the marked rise observed in the 10 to 15 km range (the Junge layer) may be much less than would have been indicated.

POSTFLIGHT

Landing

The parachute/payload landed in damp, sandy soil in a wooded area (tree farm) near Avinger, Texas, at 1641 CST. The impact recorder showed the force at impact to be 9 g. Despite approaching darkness and deteriorating weather, the recovery crew was able to reach the payload and complete recovery that evening. The payload sustained only minor damage and was returned to the NSBF at Palestine in good condition at 2230 CST 12 January 1976.

Inspection

A post-flight examination of the ozone monitor at JSC revealed the following three failure points in the electronics of the instrument: (1) an integrated circuit pin was not making contact with its socket; (2) a wire on the auto/manual switch was broken; and (3) the pins which connect the main logic board to the display board were loose. It is difficult to determine which of these failures might have caused the loss of data. However, it is felt that failure (1) is the most likely cause of the failure observed in the flight. Failure (2) may have occurred during disassembly of the instrument and failure (3) probably occurred during the 9 g force encountered at impact.

CONCLUSIONS

Hydroxyl concentration data was obtained from 43 to 30 km with an experimental uncertainty of ±35 percent. This was the first time that the OH concentration had been measured in this critical altitude range.

Ozone concentration data was obtained only during ascent between the altitudes of 30 and 40 km. Stratification between 32 and 34 km is apparently real but the concentration levels observed are considerably lower than those observed on the previous two flights of this instrument. The ozone instrument failed to produce data during descent. The most likely cause of the failure was an integrated circuit pin which was not making contact with its socket.

The aerosol particle counter functioned normally during the descent phase of the flight and data was received down to approximately 4.5 km. The data and instrumentation have been sent to Dr. Myers at the University of Pittsburgh for study.

Modifications made in the placement of antennae and antennae support were effective and the overall performance of both JSC and NCAR telemetry systems during the flight was excellent.

APPENDIX A

ITEMIZATION OF SUPPORT INSTRUMENTATION FOR BALLOON STRATOSPHERIC RESEARCH FLIGHTS CONDUCTED FROM 25 NOVEMBER 1974 TO 12 JANUARY 1976 (NCAR FLIGHT NUMBERS 868-P, 872-P, 912-P, 934-P, AND 940-P)

INSTRUMENT	MEASUREMENT FUNCTION	MANUFACTURER	MODEL NUMBER	SERIAL NUMBER
Pressure Transducers	Payload altitude	Rosemount	830A13 (0 to 15 PSIA) 830A5 (0 to 1 PSIA) 830A15 (0 to .1 PSIA)	
Vertical Reference Gyros	Payload attitude	Humphrey	VG24-0822-1	HG1 & HG2
3-axis Magnetometer	Payload attitude	Schönstedt	RAM-3	1290 1291 1285
Accelerometers	z-axis loading force during parachute deployment	Systron-Donner	Z - 4310	
Motion Picture Cameras	Monitor parachute deployment			

APPENDIX B

Itemization of Electrical and Mechanical Drawings applicable for Balloon Stratospheric Research Flights conducted from 25 November 1974 to 12 January 1976 (NCAR Flight Numbers 868-P, 872-P, 912-P, 934-P, and 940-P).

Top Drawings

Experiment Outline	SEE 39109990
Connector Layout	SHE 39109992
Battery Section	SEE 39110007
Experiment Section	SEE 39109976
Battery Box	SEE 39109999
Wiring Diagram: Flight Support Module	SIE 39112483*

BATTERY SECTION - Mechanical

Experiment Plate	SDE 39109970
Weldment	SEE 39109974
Top Plate	SDE 39109975
Side Plates	SDE 39109971
Rear Plate	SDE 39109963
Side Bar	SDE 39109967
Leg	SDE 39109968
Battery Plate	SDE 39109973
Terminal Board Plate	SDE 39110000
Covers	SDE 39109978
Bracket, Conn.	SDE 39109944
Bracket, Sensor	SDE 39110008
Lock	SDE 39109966
Block	SDE 39109965
Skin	SDE 39109972
Latch	SDE 39109964

BATTERY SECTION - Electrical

Wiring Harness	SIF 39109994
Analog Module Schematic	SIE 39110010

---

* Drawing released 6/13/75, changed for Second OH($X^2\pi$) Flight 9/17/75

EXPERIMENT SECTION - Mechanical

Telemetry Plate	SDE 39109953
Connector Bar	SDE 39109951
Connector Bar	SDE 39109979
Mounting Bar	SDE 39109952

EXPERIMENT SECTION - Electrical

Wiring Harness	SIE 39109977
Calibrator Schematic	SIE 39110005

BATTERY BOX

Weldment	SED 39109950
Rim	SDD 39109948
Wall Section	SDD 39109942
Upper Side Section	SDD 39109947
Lower Side Section	SDD 39109946
Bulkhead	SDD 39109943
Cover	SED 39109940
Cover Frame	SDD 39109944
Gasket	SDD 39109941
Heat Distributer	SDD 39109945
Battery Box Schematic	SIE 39110004

GROUND EQUIPMENT

Umbilical Cables	SIE 39110003
Handle	SDE 39109991
Flight Plug	SDE 39109955
Control Console Patching	SIE 39110011
Tripod	SEE 39109956

APPENDIX C

TELEMETRY SIGNAL LIST FOR FIRST HYDROXYL OH($X^2\pi$) MEASUREMENT (OH/O_3-1, NCAR FLIGHT 912-P)

	Function	PCM Telemetry (word/frame)
Hydroxyl Instrument	Gas Fiducial	(9)
	Visible Monitor 1A	(12/1)
	Visible Monitor 1B	(12/2)
	Magnetron HV Current	(12/9)
	Magnetron HV Voltage	(12/10)
	PMT #1 HV (S_{DATA})	(12/17)
	PMT #2 HV (S_{UV})	(12/18)
	Gas Pressure	(12/25)
	Frame Temp. 1 (TANK)	(12/27)
	Frame Temp. 2 (PMT #1)	(12/28)
	Frame Temp. 3 (LAMP)	(12/29)
	Furnace Temp.	(28/1)
	OH Experiment Current	(28/29)
	Lamp Cavity Temp.	(28/2)
	Magnetron Tube Temp.	(28/3)
Ozone Instrument	O_3 Digital Data	(29)
	O_3 Control Electrometer	(26)
	O_3 Sample Electrometer	(27)
	O_3 Electronics Temp.	(28/21)
	O_3 Pump Temp.	(28/22)
	O_3 Inverter Temp.	(28/23)
	O_3 Monitor Current	(28/27)
	O_3 Pump Current	(28/28)
Support Module	Rosemount (Low)	(13)
	Rosemount (Med)	(14)
	Rosemount (High)	(25)
	Gyro 1 Pitch	(15)
	Gyro 1 Roll	(16)
	Gyro 2 Pitch	(12/30)
	Gyro 2 Roll	(12/31)
	Battery Temp.	(28/20)
	Battery Voltage	(28/26)
	Battery Current	(28/30)
	Battery Heater Monitor	(28/25)
	Z-Axis Accelerometer	(28/31)
	0 VDC Calibrate Level	(28/17)
	2.5 VDC Calibrate Level	(28/18)
	5 VDC Calibrate Level	(28/19)

APPENDIX C (Cont.)

TELEMETRY SIGNAL LIST FOR SECOND AND THIRD HYDROXYL OH($X^2\pi$) MEASUREMENTS
(OH/O_3/Aerosol-2 and OH/O_3/Aerosol-3, NCAR FLIGHTS 934-P and 940-P)

	Function	PCM Telemetry (word/frame)
Hydroxyl Instrument	Gas Fiducial	(9)
	Visible Monitor 1A	(12/1)
	Visible Monitor 1B	(12/2)
	Magnetron HV Current	(12/9)
	Magnetron HV Voltage	(12/10)
	PMT #1 HV (S_{DATA})	(12/17)
	PMT #2 HV (S_{UV})	(12/18)
	Gas Pressure	(12/25)
	Frame Temp. 1 (TANK)	(12/27)
	Frame Temp. 2 (LAMP)	(12/28)
	Frame Temp. 3 (PMT #1)	(12/29)
	Furnace Temp.	(28/1)
	OH Experiment Current	(28/29)
	Lamp Cavity Temp.	(28/2)
	Magnetron Tube Temp.	(28/3)
Ozone Instrument	O_3 Digital Data	(29)
	O_3 Control Electrometer	(26)
	O_3 Sample Electrometer	(27)
	O_3 Electronics Temp.	(28/21)
	O_3 Pump Temp.	(28/22)
	O_3 Inverter Temp.	(28/23)
	O_3 Monitor Current	(28/27)
	O_3 Pump Current	(28/28)
	O_3 Differential Pressure	(12/19)
Aerosol Instrument	Aerosol Digital Data	(12/32)
	Aerosol Electrometer	(12/20)
	Aerosol LED Decoupler	(12/21)
	Aerosol HV Monitor	(12/22)
Support Module	Rosemount (Low)	(13)
	Rosemount (Med)	(14)
	Rosemount (High)	(25)
	Gyro 1 Pitch	(15)
	Gyro 1 Roll	(16)
	Gyro 2 Pitch	(12/30)
	Gyro 2 Roll	(12/31)
	Battery Voltage	(28/26)
	Battery Current	(28/30)
	Z-Axis Accelerometer	(28/31)
	0 VDC Calibrate Level	(28/17
	2.5 VDC Calibrate Level	(28/18)
	5 VDC Calibrate Level	(28/19)
	Xmit Temp.	(28/24)

APPENDIX C (Cont.)

DIGITAL TAPES (PCM TELEMETRY DATA) FOR BALLOON STRATOSPHERIC RESEARCH FLIGHTS CONDUCTED FROM NOVEMBER 1974 TO JANUARY 1976

Flight	NCAR Flight Number and Launch Date	Type of Experiment	Manufacturer's Tape Number	Phase	Time Interval	Density (BPI)
1	867-P 11-12-74	Parachute Test Flight	64929 17	Descent		556
2	868-P 11-25-74	1st Atomic Oxygen $O(^3P)$ Measurement	6086811	Descent		556
3	872-P 2-7-75	2nd Atomic Oxygen $O(^3P)$ Measurement	10662407	Descent		800
4	912-P 7-18-75	1st Hydroxyl $OH(X^2\pi)$ Measurement (OH/O_3-1)	110885057	Descent		800
5	934-P 10-19-75	2nd Hydroxyl $OH(X^2\pi)$ Measurement OH/O_3/Aerosol-2)	111492 135	Descent		800
6	940-P 1-12-76	3rd Hydroxyl $OH(X^2\pi)$ Measurement (OH/O_3/Aerosol-3)	111754024	Ascent	Start: 1332:40 Stop: 1444:15	800
			7298836	Ascent	Start: 1444:30 Stop: 1548:25	800
			7298840	Descent	Start: 1551:09 Stop: 1632:17	800

*All digital tapes are 7 track odd parity and are in the custody of Dr. Jess G. Carnes, Building 36, Room 3030, NASA-JSC.

APPENDIX D

Photographic Documentation for Balloon Stratospheric Research Flights Conducted from November 1974 to January 1976

Flight	NCAR Flight Number and Launch Date	Type of Experiment	Still Frame Numbers	NASA-JSC Motion Picture File Roll Numbers and Footage
1	867-P 11-12-74	Parachute Test Flight	S74-32949 to S74-32970	S74-184 S74-185 (1120')
2	868-P 11-25-74	1st Atomic Oxygen $O(^3P)$ Measurement	S74-33808 to S74-33811 and S74-33948 to S74-33982	S75-015 (735')*
3	872-P 2-7-75	2nd Atomic Oxygen $O(^3P)$ Measurement	S75-21687 to S75-21709	S75-009 (756') S75-010 (?') S75-016 (610')*
4	912-P 7-18-75	1st Hydroxyl $OH(X^2\pi)$ Measurement (OH/O_3-1)	S75-30229 to S75-30242	
5	934-P 10-19-75	2nd Hydroxyl $OH(X^2\pi)$ Measurement (OH/O_3/Aerosol-2)	S75-32699 to S75-32712 and S76-21170 to S76-21175	S75-137 (695')
6	940-P 1-12-76	3rd Hydroxyl $OH(X^2\pi)$ Measurement (OH/O_3/Aerosol-3)	S76-20810 to S76-20862	S76-004 (840')

* Edited motion picture flim

Distribution List for JSC 11846

NASA Headquarters
MHQ/P.F. Wetzel
W. Land
SU/L. R. Greenwood (5)
RPS/R. A. Wasel

Ames Research Center
SA/I. G. Poppoff (3)

Jet Propulsion Laboratory
180-404/Dr. D. P. Burcham (3)

Kennedy Space Center
AA-STA-1/J. P. Claybourne (3)
J. Perris
MD/P. Buchanan, M.D.

Langley Research Center
217K/H. Scott Wagner (3)

Johnson Space Center
AC/H. E. Clements
AP/J. E. McLeaish
DD7/D. S. Nachtwey
JM61/Documentation Management Office (3)
LA5/D. C. Cheatham
NA/E. M. Fields
LM/C. C. Gay
TA/O. K. Garriott
P. J. Armitage
TC/V. R. Wilmarth

Dr. James Anderson
University of Michigan
Space Research Building
2455 Hayward
Ann Arbor, MI 48105

NOTE: Additional copies may be obtained by calling the JSC Environmental Effects Office at (713) 483-2576.